FULLEROL BASED ENZYME MIMICS AND SYNTHESIS EFFORT OF TETRA ARYL PYRANONE

A THESIS SUBMITTED TO
THE GRADUATE SCHOOL OF NATURAL AND APPLIED SCIENCES
OF
MIDDLE EAST TECHNICAL UNIVERSITY

BY

MEDİNE SOYDAN

IN PARTIAL FULFILLMENT OF THE REQUIREMENTS
FOR
THE DEGREE OF MASTER OF SCIENCE
IN
CHEMISTRY

FEBRUARY 2021

Approval of the thesis:

FULLEROL BASED ENZYME MIMICS AND SYNTHESIS EFFORT OF TETRA ARYL PYRANONE

submitted by **MEDİNE SOYDAN** in partial fulfillment of the requirements for the degree of **Master of Science** i**n Chemistry, Middle East Technical University** by,

Prof. Dr. Halil Kalıpçılar
Dean, Graduate School of **Natural and Applied Sciences** _____

Prof. Dr. Özdemir Doğan
Head of the Department, **Chemistry** _____

Assoc. Prof. Dr. Salih Özçubukçu
Supervisor, **Chemistry, METU** _____

Examining Committee Members:

Prof. Dr. Cihangir Tanyeli
Chemistry, METU _____

Assoc. Prof. Dr. Salih Özçubukçu
Chemistry, METU _____

Assoc. Prof. Dr. E. Görkem Günbaş
Chemistry, METU _____

Assist. Prof. Dr. Gülcihan Gülseren
Molecular Biology and Genetics, Konya Food and Agriculture University _____

Assoc. Prof. Dr. Yunus Emre Türkmen
Chemistry, İhsan Doğramacı Bilkent University _____

Date: 12.02.2021

I hereby declare that all information in this document has been obtained and presented in accordance with academic rules and ethical conduct. I also declare that, as required by these rules and conduct, I have fully cited and referenced all material and results that are not original to this work.

Name Last name: Medine, Soydan

Signature:

ABSTRACT

FULLEROL BASED ENZYME MIMICS AND SYNTHESIS EFFORT OF TETRA ARYL PYRANONE

Soydan, Medine
Master of Science, Chemistry
Supervisor: Assoc. Prof. Dr. Salih Özçubukçu

February 2021, 93 pages

Although, natural enzymes have high catalytic activity and specificity, they are fragile and costly due to long purification processes. Therefore, scientists started to design and synthesize structures with enzyme-like activity called nanozymes to overcome the limitations of the natural enzymes. In the first part of this project, amino acids of catalytic site of three enzymes were conjugated into fullerol. The names of three enzymes are lactate dehydrogenase, protease and nitrilase. Then, the catalytic activity of fullerol amino acid derivatives was tested with the model reactions.

Luminescence was observed and attracted attention throughout the history. Accordingly, understanding of the luminescence made great progress. Aggregation caused quenching and the aggregation induced emission processes are the relatively new concept in the comprehension of luminescence. Moreover, new molecules which show ACQ or AIE property are designed and synthesized for various applications like imaging. In the second part of this project, it was aimed to synthesize 2,3,4,5-tetraphenyl-4H-pyran-4-one by a new synthesis route. Moreover, it was planned to investigate whether it has aggregation caused quenching or the aggregation induced emission property with fluorescence spectroscopy.

Keywords: Fullerol, nanozymes, luminescence, aggregation caused quenching, aggregation induced emission

ÖZ

FULLEROL BAZLI ENZİM MİMİKLERİ VE TETRA ARİL PİRANONUNUN SENTEZ ÇALIŞMALARI

Soydan, Medine
Yüksek Lisans, Kimya
Tez Yöneticisi: Doç. Dr. Salih Özçubukçu

Şubat 2021, 93 sayfa

Doğal enzimler yüksek katalitik aktivite ve seçicilik göstermelerine rağmen, bu enzimler hassas ve uzun saflaştırma işlemlerinden dolayı pahalıdır. Bu yüzden, bilim insanları doğal enzimlerin sınırlamalarının üstesinden gelmek için enzim benzeri aktivite gösteren ve nanozimler olarak adlandırılan yapılar tasarlamaya ve sentezlemeye başladılar. Bu projenin birinci kısmında, üç enzimin aktif kısımlarında bulunan aminoasitler fullerole konjuge edildi. Bu üç enzimin isimleri laktat dehidrogenaz, proteaz ve nitrilaz. Daha sonra, fullerol amino asit türevlerinin enzim aktivitesi model reaksiyonlar ile test edildi.

Lüminesans tarih boyunca gözlemlenmiş ve dikkat çekmiştir. Bu doğrultuda, lüminesansın kavranması konusunda büyük ilerleme katedilmiştir. Kümeleşme kaynaklı sönümlenme ve kümeleşme indüklenmesiyle emisyon süreçleri lüminesansın kavranmasında kısmen yeni kavramlardır. Ek olarak, kümeleşme kaynaklı sönümlenme veya kümeleşme indüklenmesiyle emisyon özelliği gösteren yeni moleküller görüntüleme gibi farklı uygulamalar için dizayn ediliyor ve sentezleniyor. Bu projenin ikinci kısmında, 2,3,4,5-tetrafenil-4H-piran-4-on molekülünün yeni bir yol üzerinden sentezlenmesi amaçlanmıştır. Buna ek olarak, bu molekülün kümeleşme kaynaklı sönümlenme özelliği mi kümeleşme

indüklenmesiyle emisyon özelliği mi gösterdiğinin floresan spektroskopisiyle incelenmesi planlanmıştır.

Anahtar Kelimeler: Fullerol, nanoenzimler, lüminesans, kümeleşme kaynaklı sönümlenme, kümeleşme indüklenmesiyle emisyon

To my aunt

ACKNOWLEDGMENTS

I would like to state my appreciation to my supervisor Assoc. Prof. Salih Özçubukçu for his guidance and encouragement. This thesis was completed with his valuable advices and perspectives.

I also would like to thank each member of Özçubukçu Research Group, including previous members, Burcu Okyar, Dr. Melek Parlak, Muzaffer Gökçe, Tuğçe Yılmaz, Dr. Aytül Saylam, Güzide Aykent, Mehmet Seçkin Kesici, Şafak Tekir, Pakizan Tasman and Volkan Dolgun for their supportive attitude and friendship. Moreover, I want to specially thank Güzide Aykent and Şafak Tekir for their contribution in NMR analysis.

I also would like to thank Assoc. Prof. Özgül Persil Çetinkol for enabling to use UV-Vis spectrometer and Fluorimeter instruments. Also, I appreciate Dr. Mehrdad Forough from Çetinkol's Research Group for his help on how to use these instruments.

I have had a productive undergraduate and graduate education in Department of Chemistry at METU. Moreover, I took advantage of the departmental facilities during this project, which are the collective yield of the studies of the faculty members. Therefore, I want to thank all faculty members.

I would also like to thank ODTU-BAP for the financial support.

Finally, I would like to thank my family for their endless support.

TABLE OF CONTENTS

LIST OF TABLES

TABLES

LIST OF FIGURES

FIGURES

LIST OF SCHEMES

SCHEMES

LIST OF ABBREVIATIONS

ABBREVIATIONS

ACQ	Aggregation Caused Quenching
AIE	Aggregation Induced Emission
Arg	Arginine
Asp	Aspartic acid
BASF	Badische Anilin und Soda Fabrik
Bn-Br	Benzyl bromide
Cys	Cysteine
DCC	N, N'-Dicyclohexylcarbodiimide
DMAP	N, N-dimethyl aminopyridine
DMF	Dimethylformamide
DMSO	Dimethyl sulfoxide
F-AA	Fullerol-amino acids derivatives
GFP	Green fluorescent protein
Glu	Glutamic acid
Gly	Glycine
His	Histidine

HRMS	High resolution mass spectrometer
LDA	Lithium diisopropylamide
Lys	Lysine
mAU	Mini Arbitrary Unit
MOF	Metal organic framework
MPPS	1-methyl-1,2,3,4,5-pentaphenylsilole
NAD^+	Nicotinamide-adenine dinucleotide
NADH	Nicotinamide adenine dinucleotide hydride
$NADP^+$	Nicotinamide-adenine dinucleotide phosphate
NADPH	Nicotinamide Adenine Dinucleotide Phosphate Hydrogen
PBS	Phosphate-buffered saline
PCC	Pyridinium chlorochromate
PDC	Pyridinium dichromate
PPP	1,2,3,4,5-pentaphenylpyrrole
PPPO	1,2,3,4,5-pentaphenylphosphole oxide
RIM	Restriction of intramolecular motions
RIR	Restriction of Intramolecular Rotation
RIV	Restriction of Intramolecular Vibration
Ser	Serine
TBAH	Tetrabutylammonium hydroxide
TCEP	Tris (2-carboxyethyl) phosphine

TCPP	Tetrakis (4-carboxyphenyl) porphyrin
TEMPO	(2,2,6,6-Tetramethylpiperidin-1-yl) oxyl
TFA	Trifluoroacetic acid
TGA	Thermogravimetric analysis
TMS	Tetramethyl silane
TPBD	1,1,4,4-tetraphenylbutadiene
TPC	1,2,3,4-tetraphenyl-1,3-cyclopentadiene
TPS	1,1-dimethyl-2,3,4,5-tetraphenylsilole
Tris-HCI	Tris (hydroxyethyl) amino methane-hydrogen chloride

CHAPTER 1

FULLEROL BASED ENZYME MIMICS

1.1 Introduction

1.1.1 Carbon

Carbon is located in 4A group of the periodic table and it is the first element in this group with 6 atomic number. The name of the element stems from Latin word "carbo" which has a meaning of coal and charcoal.[1]

Carbon is essential component of the life on Earth. Since it can form plenty of molecules with relatively few number of atoms such as hydrogen and nitrogen, the diversity of life on Earth is carbon based.[2] Moreover, carbon chemistry is studied intensively as organic chemistry which is the subfield of the chemistry.

1.1.2 Allotropes of the carbon

There are several approaches for the categorization of the carbon allotropes. They can be grouped by considering material properties, hybridization or whether the allotropes are obtained naturally or synthetically. Figure 1.1 indicates the main allotropes of carbon classified based on the hybridization of carbons in the chains.[3] Among them, diamond and graphite are the natural allotropes of carbon. Various additional allotropes can be obtained by arranging carbon atoms with sp^3 and sp^2 hybridization in different ordering.[4]

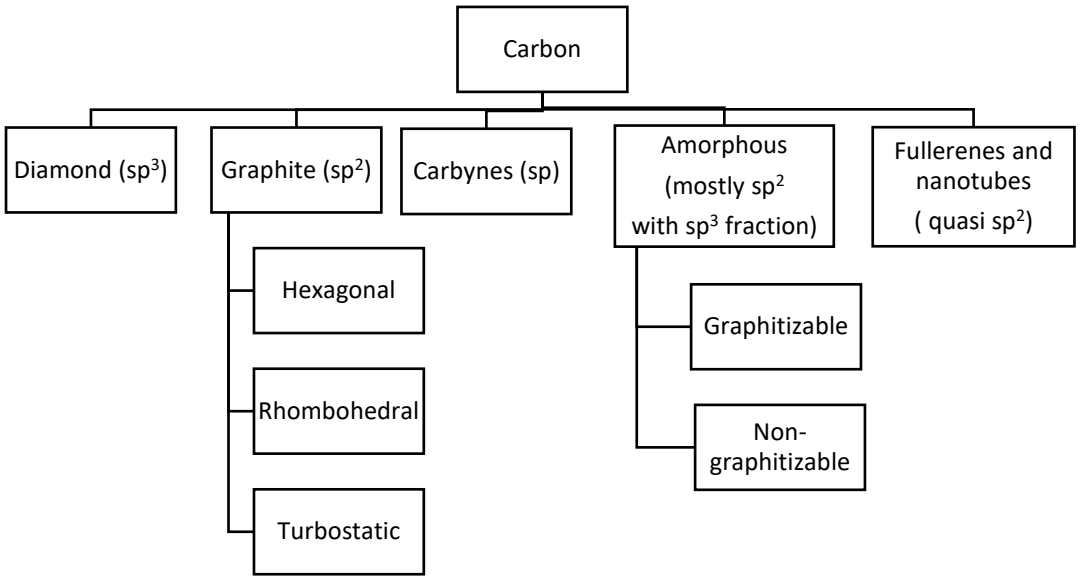

Figure 1.1 Allotropes of the carbon.

1.1.2.1 Diamond

Diamond is the hardest material with 10 in Mohs scale at which the hardness of the other materials is listed with respect to diamond. It can also be found in hexagonal form which is known as Lonsdaleite. Lonsdaleite was the first noticed in the Diable Canyon meteorite in 1967.[5] It was also observed cubic dimond can be transformed into the hexagonal diamond.[6]

1.1.2.2 Graphite

Graphite means "writing stone" in Greek and this name was given by German mineralogist Abraham Gotlob Werner in 1789.[7] In this structure, carbon atoms form planar hexagonal layers and single layer of graphite is called graphene. When the

layers stack in ABAB fashion, commonly observed hexagonal graphite is formed. When the layers come together with ABCABC fashion, rhombohedral graphite can be formed.[3] In turbostatic graphite, interlayer spacing and shape of atomic layers are distorted due to the translation and rotation of the layers.[8]

1.1.2.3 Carbynes

Carbynes are formed with sp-hybridized carbon atoms. This kind of carbon chains are possible to construct with consecutive arrangement of triple and single bond or accumulated double bonds. In any case, they are quite reactive and thus unstable. It is known that this kind of structures are available in space.[9]Also, carbynes attract interest due to their possible applications like molecular wires.[3]

1.1.2.4 Amorphous Carbon

Although amorphous carbon structures mainly contain sp^2 hybridized carbon, they have some sp^3 hybridized portions which can form crosslinks between layers and prevent the long-range order. There are two types of amorphous carbons. The first one is the graphitizable amorphous carbons. Amorphous carbons are converted to graphitic structure upon heating between 1500 °C to 3000 °C. Pyrolytic graphite can be given as an example. The second one is the non- graphitizable amorphous carbons. These structures do not form graphitic structure with the heat treatment, because their structures are heavily cross-linked. Activated carbons, chars, glassy carbons are non-graphitizable amorphous carbons.

1.1.2.5 Fullerenes and Nanotubes

Fullerenes are a kind of molecules with ellipsoid, spherical or tubular structure. They were discovered in 1985 by Robert F. Curl, Harold W. Kroto and Richard E. Smalley in their joint project at which they studied the ways how the carbon chains are formed

in red giant stars. Curl, Kroto and Smalley were awarded with Nobel Prize in 1996. Although, C_{60} and C_{70} attracted interest more for practical applications, C_{76}, C_{82}, and C_{84} were also synthesized.[10]

Carbon nanotubes were synthesized first by Sumio Iijima in 1991 by arc-discharge evaporation of graphite.[11]Since then, plenty of multilayer carbon nanotubes, double-walled carbon nanotubes and single walled carbon nanotubes were constructed for various applications with the desired properties.[5]

1.1.3 Fullerol

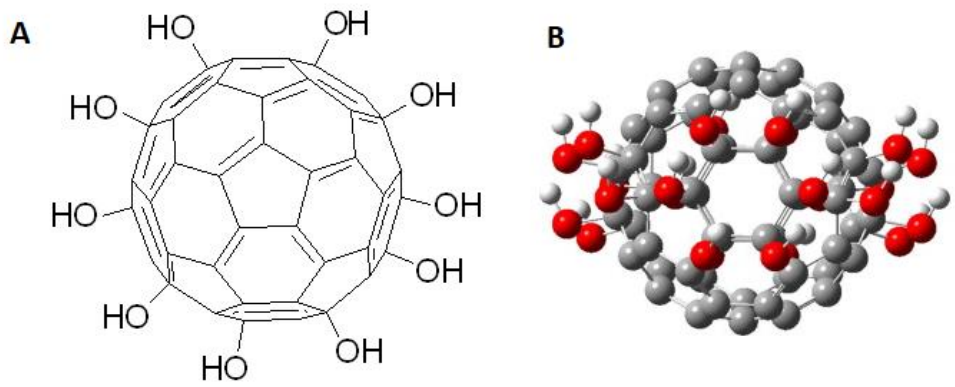

Figure 1.2 Structure of fullerol (A) and hydroxyl groups located on equatorial region (B). Reprinted with permission from (He, H., Zheng, L., Jin, P. & Yang, M. The structural stability of polyhydroxylated C60(OH)24: Density functional theory characterizations. *Computational and Theoretical Chemistry* **974**, 16–20 (2011).). Copyright © 2011 Elsevier B.V.

Fullerenol is the polyhydroxylated form of the fullerene as shown in Figure 1.2. Due to the hydroxyl groups, they are water soluble, but degree of solubility based on the number of the hydroxyl groups. They can be functionalized easily and employed in various applications.[12] Number of hydroxyl groups for C_{60} can vary between 2 to 44.[13] Moreover, stability studies were performed with different number of hydroxyl groups and isomers. To illustrate, stability studies of $C_{60}(OH)_{24}$ isomers based on

Density Functional Theory (DFT) were done. It was found that as the number of hydroxyl groups occupying the equator of C_{60} fullerene, then the molecules show lower energy, which imply higher stability of the corresponding molecules. Figure 1.2 B indicates the egg-shaped $C_{60}(OH)_{24}$.[14]

However, there is one disadvantage with the fullerols, which is low reproducibility of characterization that brings about some challenges in studies.[15]

1.1.4 Enzyme Mimics

1.1.4.1 Natural Enzymes

Natural enzymes are proteins catalyzing reactions. Natural enzymes differ from chemical enzymes in reaction rates, reaction conditions, reaction specificity, and control mechanisms. They have high reaction rates which can be as higher as 10^6 to 10^{12} compared uncatalyzed reactions and specificity to their substrate. They need milder reaction conditions to act. For example, operating temperature is generally lower than 100 °C. Also, control mechanisms of natural enzymes can be covalent modification of the enzyme and allosteric control which is intervention of a small molecule at the allosteric site of the enzyme.[16] Although these advantages of natural enzymes, they have some limitations. Natural enzymes are large biomolecules with several subunits, which make them fragile and open to denaturation and digestion. They are generally extracted from an organism and purification processes are long and tedious, so that increases their cost. These limitations directed scientist to construct structures which indicate enzyme-like activity.[17]

1.1.4.2 Classification of Natural Enzymes

Natural enzymes are divided into six main classes as tabulated in Table 1.1. The categorization is based on the type of the reaction catalyzed. There are variety of subclasses and sub-subclasses of enzymes under this main classes.[16]

Table 1.1 Enzyme classes based on reaction type.[16]

Classification	Catalyzed reaction type	Examples
1.Oxidoreductases	Oxidation-reduction reactions	Lactate dehydrogenase, peroxidases
2.Transferases	Transfer of functional groups	Kinases
3.Hydrolases	Hydrolysis reactions	Esterase, protease
4.Lyases	Group elimination to form double bonds	Tryptophan decarboxylase
5.Isomerases	Isomerization	Racemase
6.Ligases	Bond formation with need for ATP energy	DNA ligase

1.1.4.3 Nanozymes

Nanozyme as a term was first proposed by Pasquato, Scrimin, Manea, and Houillon in 2004. They are inspired from synzymes which is the abbreviated version of "synthetic enzymes". Synzyme term is used to define polymers indicating catalytic activity.[18] In this context, nanozymes are materials in 1-100 nm size with the enzyme-like activity.[19] Size, shape, morphology, composition, surface modification, pH, temperature and promoters or inhibitors are important parameters in the design of nanozymes.[20]

1.1.4.3.1 Classification of Nanozymes

Nanozymes can be classified in two ways. The first way is that it can be based on the enzyme class catalyzed.[19] The other way depends on the material type.[21] Here, the second way is considered. Thus, nanozymes are classified into three kinds based on material types. These are metal-based, metal-oxide or metal-sulfide-based and carbon-based nanomaterials.

Metal-based enzymes can be prepared with platinum, gold, vanadium, silver, palladium and their nanoparticles.[20]

Metal oxide or metal-sulfide-based nanozymes can be employed with manganese (IV) oxide, iron (II, III) oxide (Fe_3O_4), molybdenum disulfide (MoS_2), copper sulfide (CuS), copper oxide (CuO) and cerium (IV) oxide (CeO_2). There are more than listed here. Moreover, new materials are still prepared.[19]

Carbon-based nanozymes can be designed with carbon nanotubes[22], graphene oxide[23], graphitic carbon nitride[24], fullerene[25] and carbon dots.

It was investigated that nanozymes with various material types have effective enzyme-like activity of peroxidase, oxidase, catalase, superoxide dismutase, and hydrolase.[26]

Although, nanozymes are considered as an alternative to natural enzymes, they indicate lower specificity and reaction rate. Also, variety of the enzymes mimicked with nanozymes are limited mainly to oxidase, peroxidase, catalase and hydrolase.[17,19]

1.1.4.3.2 Application areas of nanozymes

Nanozymes are employed as tool in *in vitro* sensing for detection of H_2O_2, glucose and other oxidase substrates, nucleic acids, protein, cancer cell, ions etc., in *vivo* sensing, imaging, therapeutics as neuroprotection, cytoprotection and anti-

inflammatory agents and environmental protection.[17,18] Although, numerous examples to the each of these applications are provided in the literature, some of them are considered in the following paragraphs.

As an example, to *in vitro* detection application, Liu et al. prepared a cerium oxide (CeO_2) nanozymes with the peroxidase activity. They utilized a fluorescent DNA probe which is normally attached to the nanoparticle. When hydrogen peroxide is added, displacement of DNA probe with the hydrogen peroxide takes place. They also tested nanozyme cerium oxide coupling with glucose oxidase enzyme to detect glucose. In that case, *in situ* hydrogen peroxide generation occurs and they can detect the amount of glucose indirectly.[27]

Cheng et al. constructed a metal organic framework (MOF) nano sheet to detect the heparin amount *in vivo*. They utilized an AG73 which is heparin specific peptide to catch the heparin. As catalytic site, they produced iron bound tetrakis (4-carboxyphenyl) porphyrin (TCPP) nano sheets to obtain peroxidase activity. Also, they used micro dialysis probe to discharge the heparin from the live rat blood. Figure 1.3 is the graphical abstract of this process. Ampliflu red is fluorescent substance to quantify hydrogen peroxide or peroxidase activity and it is oxidized to rezorufin.[28]

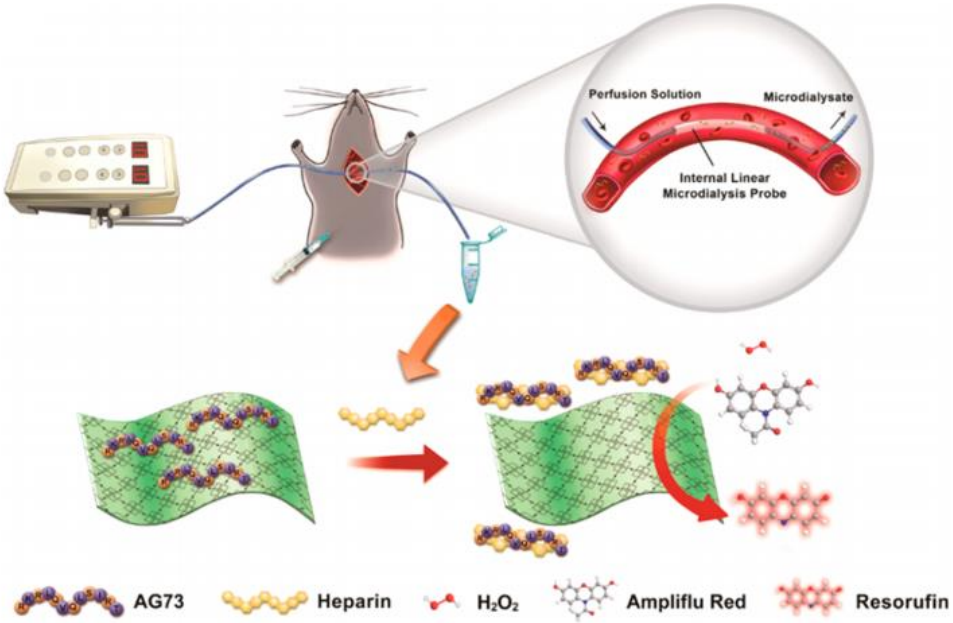

Figure 1.3 Heparin elimination process in live rats using 2D MOF nanozymes. Reprinted with permission from (Cheng, H. *et al.* Monitoring of Heparin Activity in Live Rats Using Metal–Organic Framework Nanosheets as Peroxidase Mimics. *Anal. Chem.* **89**, 11552–11559 (2017)). Copyright (2017) American Chemical Society.

1.1.5 Studied Enzymes

In this thesis project, active sites of three enzymes were conjugated to fullerol and examined for their activity.

Table 1.2 Enzyme classes of studied enzymes.

Enzymes classes	**Studied Enzymes**
Oxidoreductases	Lactate dehydrogenase
Hydrolases	Protease and nitrilase

1.1.5.1 Lactate dehydrogenase

Lactate dehydrogenase (LDH) which takes role in non-aerobic glycolysis is an enzyme in oxidoreductase class. Since glycolysis is common to all organisms, it functions in cytoplasm of cells. There are five isozymes which define the enzymes with different amino acid composition, but they catalyze the same reaction. Additionally, LDH is formed by four subunits which is a combination of H and M polypeptide chains. The possible combinations for LDH isozymes are H_4, M_4, HM_3, H_2M_2, H_3M. Moreover, any one form of the enzyme is present in almost all animals, in microorganisms and in plants.[29] It catalyzes the conversion of L-lactic acid to pyruvic acid or pyruvic acid to L-lactic acid in the defined conditions in Scheme 1.1. Moreover, its molecular weight is around 14,000 Daltons.[30] It has histidine and arginine amino acids in its catalytic site.[31]

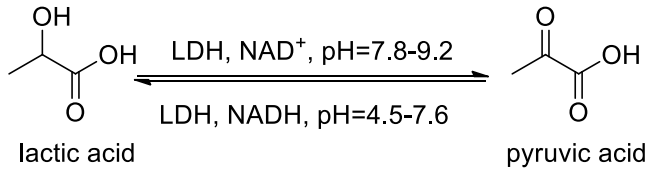

Scheme 1.1 Reaction catalyzed by Lactate dehydrogenase.

1.1.5.1.1 Coenzymes of Lactate dehydrogenase

LDH needs a coenzyme which can be nicotinamide-adenine dinucleotide (NAD^+) or nicotinamide-adenine dinucleotide phosphate ($NADP^+$) while the lactic acid is oxidized to pyruvic acid.[29] The structure of NAD^+ and reduced form were presented in Scheme 1.2. Also, $NADP^+$ and reduced form are coenzyme of LDH and it has one additional phosphate group in the position indicated in bold black.

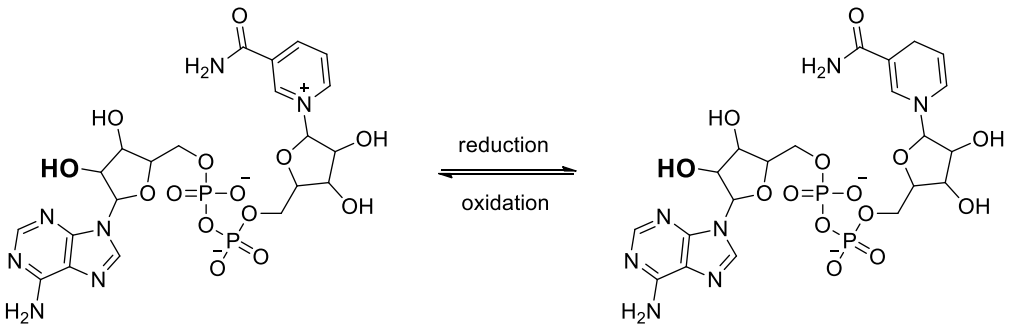

Scheme 1.2 Structure of coenzyme NAD^+ and its reduced form.

1.1.5.1.2 Proposed Mechanism

The amino acids in the active site of LDH are known in the literature and plausible mechanism for LDH catalytic action is available in the literature.[31] In this reduction mechanism, a hydride transfer takes place first from the coenzyme NADH to the carbonyl carbon of the substrate, then a proton transfer from the histidine residue of the enzyme to the carbonyl oxygen of the substrate. The arginine residues stabilize the intermediate. Scheme 1.3 indicates this transformation.

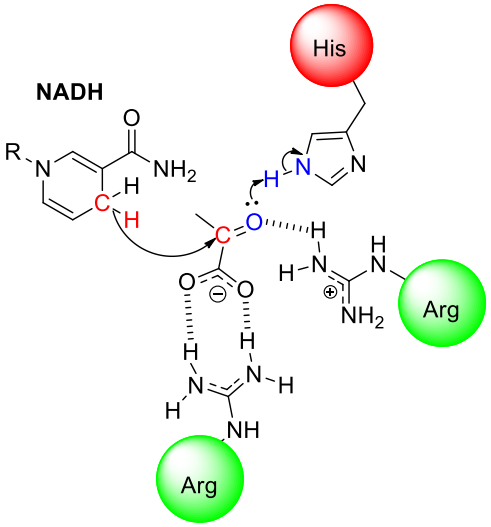

Scheme 1.3 Proposed mechanism of LDH for the reduction of pyruvic acid.

1.1.5.2 Serine Protease

Its name comes from the nucleophile residue serine which attacks to the carbonyl of the peptide bond in the substrate sequence. Serine protease is a kind of hydrolase enzyme which cuts peptides into smaller pieces. Serine protease family is ubiquitous in organisms, so they constitute one third of all proteolytic enzymes. Also, aspartic acid-histidine-serine catalytic triad is conserved in this enzyme family.[32] Moreover, serine proteases can be observed in all the kingdoms of organisms such as eukaryotes, prokaryotes, archaea, and viruses. They basically break the amide bond which is one of the most stable bonds in chemistry or in biology. If its reactivity is compared to an ordinary alkyl ester, the alkyl ester bond is 3000 times more reactive than an amide bond.[33]

1.1.5.2.1 Proposed Mechanism

Serine protease was studied intensively and its active site amino acids and how they act to realize the reaction is known in the literature. The mechanism starts with protonation of basic nitrogen of imidazole group as presented in Scheme 1.4 and the deprotonation forms Ser-O^-. Then, Ser-O^- attacks to the carbonyl of amide bond and first transition state occurs. After that, peptide bond is broken, and amine component departs from the reaction site. Water enters to the active site, ionizes and form the second transition state. At the final stage, carboxylic acid is formed and the enzyme is regenerated.[34]

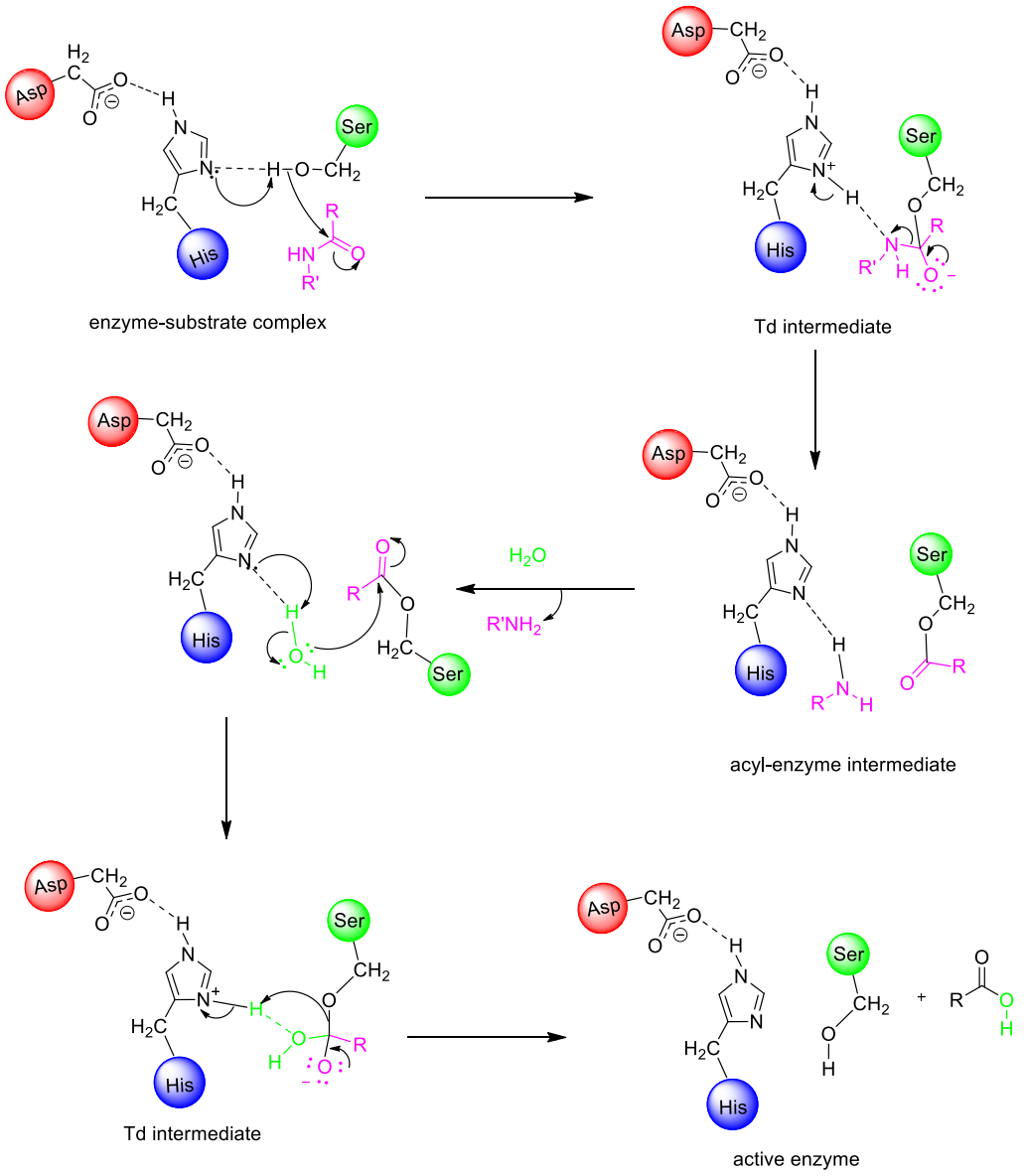

Scheme 1.4 Proposed mechanism of serine protease.[34]

1.1.5.3 Nitrilase

First known nitrilase was discovered by Thimann and Mahadevan in 1964.This enzyme catalyzes indole acetonitrile to indole acetic acid. In general, nitrilases are cyanide dihydratase which performs hydrolysis of the nitriles to the corresponding carboxylic acids and cyanide hydratase which makes one step hydrolysis of nitriles

to the corresponding amides. They are group of enzymes with the similar structures whose differences are mainly observed in optimum pH, amino acid sequence and substrate specificity.[35] Since they can convert a nitrile group to an amide or carboxylic acid, they are commercially significant. To illustrate, nicotinic acid by Lonza in China and R-mandelic acid by Mitsubishi in Japan and by BASF in Germany are massively produced by employing the nitrilases. Also, they can be assigned in waste treatment and surface modification. Thus, the nitrilases for commercial use can be extracted from the organisms they are present such as bacteria, filamentous fungi, yeasts, and plants. Depending on the organisms, their optimum pH can be between 5.5-9.5 and temperature can vary between 30-65 °C. The conserved catalytic triad for nitrilase family is glutamic acid-lysine-cysteine.[34,35]

1.1.5.3.1 Proposed Mechanism

The mechanism of action of the enzyme is proposed as follows in the literature shown in Scheme 1.5. Nucleophilic thiol group of cysteine residue attacks to the nitrile carbon which has a partial positive charge. The resulting imine can be hydrolyzed to corresponding amide or acyl enzyme complex can be further exposed to the hydrolysis at which ammonia is released as a by-product accompanied with the regeneration of the enzyme.[36]

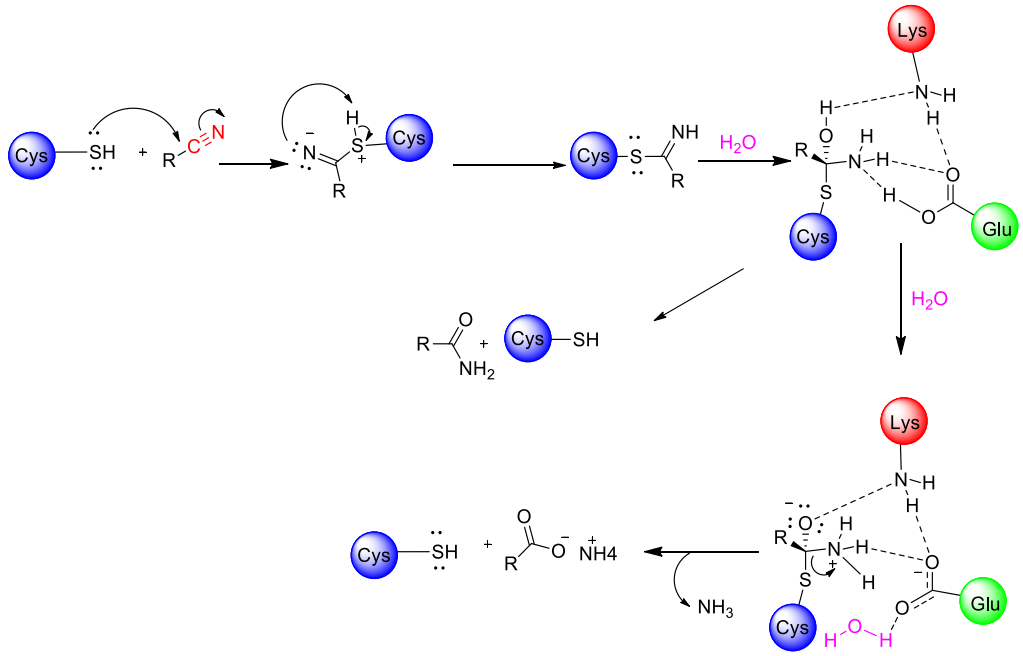

Scheme 1.5 Proposed mechanism for the nitrilase.[38]

1.1.6 Motivation of the Study

Previously in our research group, fullerol conjugated amino acids of catalytic triad Ser-Gly-His was synthesized to study enzymatic activity of esterase with 4-nitrophenyl acetate. Ser-Gly-His catalytic triad is the active site amino acids which reside on the catalytic site of esterase. It was observed that fullerol conjugated amino acids mimics the enzyme activity and catalyze the ester hydrolysis reaction. When it was compared to the activity of single, unprotected amino acids, fullerol conjugated amino acids derivatives shows significantly higher enzymatic activity. Then, it was hypothesized that this strategy which is the conjugation of active site amino acids to the fullerol can be applied to other enzyme or reaction types to mimic. Accordingly, lactate dehydrogenase, protease and nitrilase enzymes were determined to apply the approach and investigate the enzyme-like activity.

1.2 Results and Discussion

1.2.1 Synthesis of Fullerol and Activated Fullerol

Firstly, fullerol was synthesized starting with fullerene as described in Scheme 1.6.[39] The synthesis was performed in basic medium. Moreover, tetrabutylammonium hydroxide (TBAH) was employed as phase transfer catalyst hydrogen peroxide as the oxidant. TBAH transfers fullerene which is soluble normally in toluene into water phase. The reaction mixture was mixed for five days at room temperature. At the end of the reaction, toluene was removed, and the product was collected on filter paper. Then, the product was washed repeatedly with ethanol to remove the TBAH and other impurities.

Moreover, it was expected that number of hydroxyl groups on fullerene with this procedure would be from 24 to 26.

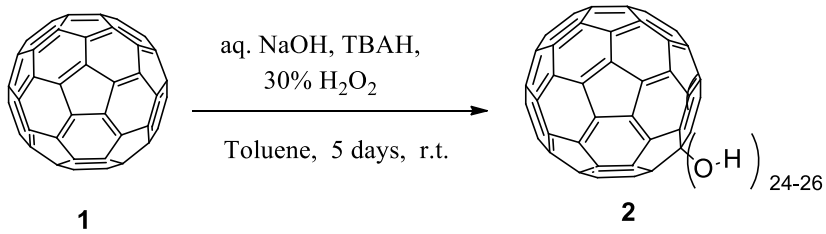

Scheme 1.6 Synthesis of fullerol.

After synthesis of fullerol, it was kind of activated as seen in Scheme 1.7.[39] The reagent providing activation is *p*-nitrophenyl chloroformate. Pyridine was a base utilized to take the hydrogen of hydroxyl groups on the fullerol. 4-Dimethylaminopyridine (DMAP) which is a common organic catalyst for esterification reactions was used as catalyst.[40] The obtained product is activated fullerol. Since the conjugated group forms 4-nitrophenol and carbon dioxide, it is more susceptible to a nucleophilic attack.

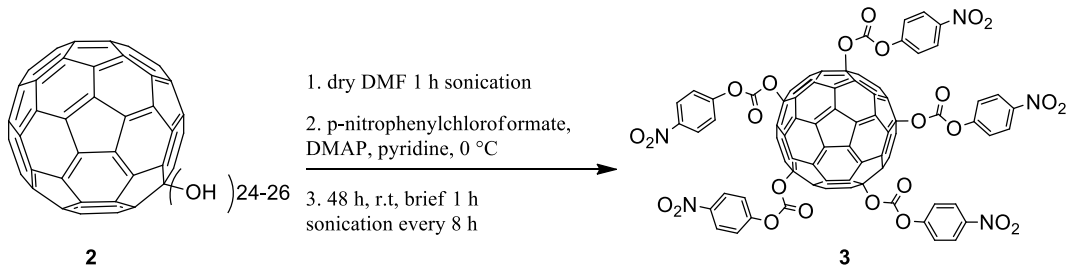

Scheme 1.7 Activation reaction of fullerol.

After fullerol and activated fullerol were synthesized, their characterization was performed. Fullerol characterization was done via IR spectroscopy and Thermogravimetric Analysis (TGA). Figure 1.4 indicates the IR spectrum of fullerol. Broad peak around 3500 cm^{-1} indicates the existence of hydroxyl groups on the structure. There can be quite small peaks around 3000 cm^{-1} and 2100 cm^{-1}, which is due to TBAH residue coming from the synthesis.[41] Also, If the peak around 2500 cm^{-1} is observed, it can be attributed to the epoxide groups on fullerol.

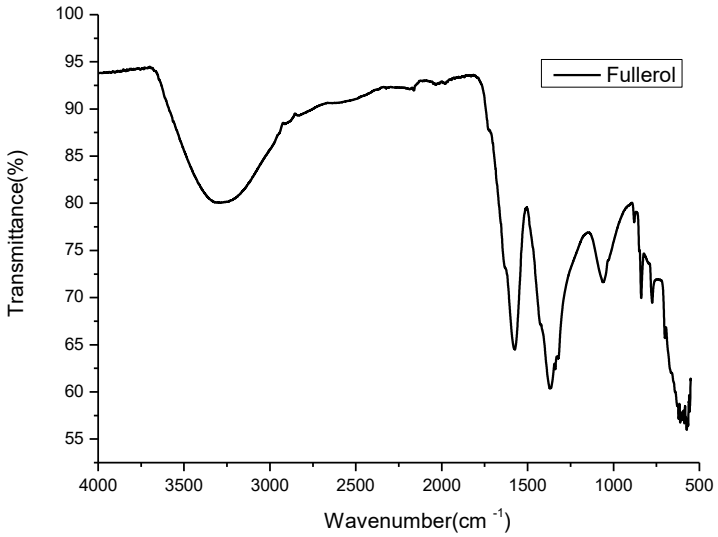

Figure 1.4 IR spectrum of fullerol.

Figure 1.5 indicates the TGA thermogram. TGA measurement was performed in order to determine the number of hydroxyl groups on fullerene. An empirical formula was utilized.[12] It was formulated as number of hydroxyl groups= (720/y)

(x/m). It was assumed in this formulation that y is percentage of weight loss above 570 °C due to structural degradation of char and fullerene, x is percentage of weight loss between 150-570 °C and m is the weight of each attached group which is 17 for hydroxyl group. Weight loss up to up to 150 °C was not considered, because removal of solvents and absorbed water occurs up to 150 °C.

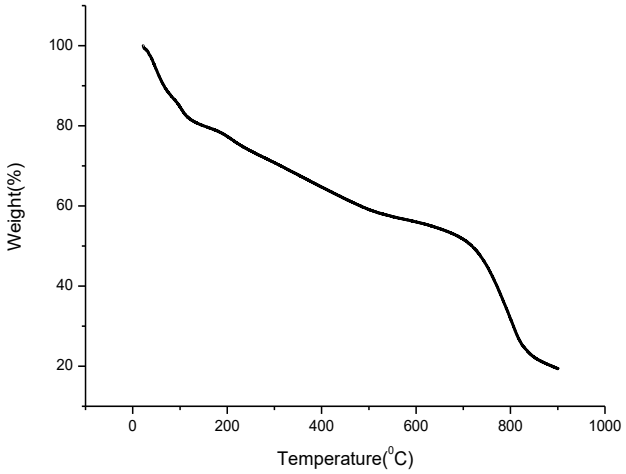

Figure 1.5 TGA thermogram of fullerol.

When the values are inserted into the formula, it was found that number of hydroxyl groups is 26 as expected. However, this number varies between batches to batch. Therefore, TGA measurements should be performed for each different batch. Also, number of hydroxyl groups affect the subsequent reactions, since the functionalization is done from the hydroxyl groups.

Moreover, characterization of activated fullerol was done with ^{1}H NMR. Figure 1.6 indicates ^{1}H NMR spectrum of the activated fullerol in deuterated DMSO Doublets of 4-nitrophenyl group in 6.9 ppm and 8.2 ppm indicates the activation of the fullerol.

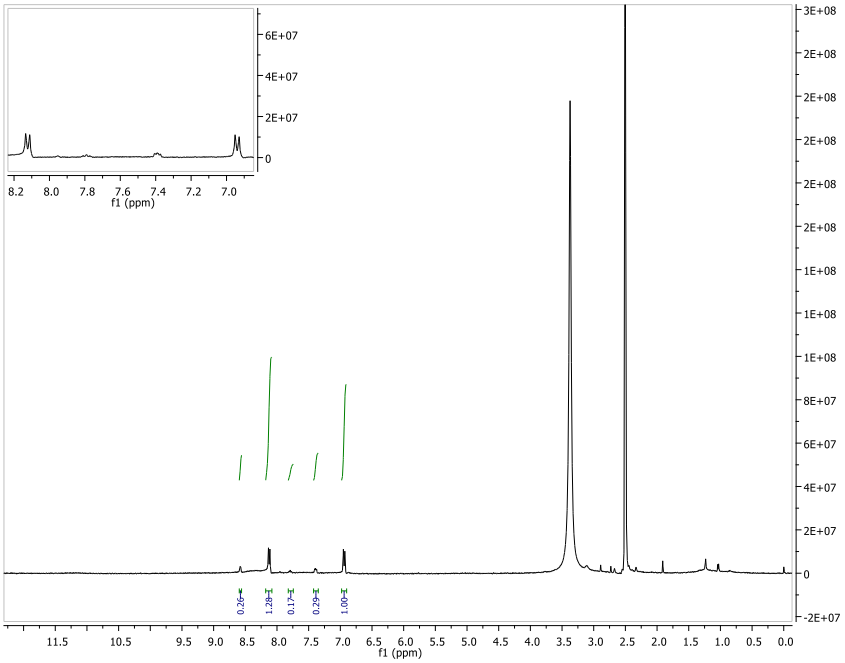

Figure 1.6 ^{1}H NMR spectrum of activated fullerol.

1.2.2 **S**ynthesis of Fullerol-amino acid derivatives

After the activation of fullerol, amino acid conjugated fullerol derivatives were synthesized as in the literature.[39] Scheme 1.8 indicates the synthesis of these molecules. Once it was seen that the conjugation of the unprotected amino acid to the fullerol derivative takes place, the rest of fullerol amino acid derivatives was synthesized based on the same procedure.

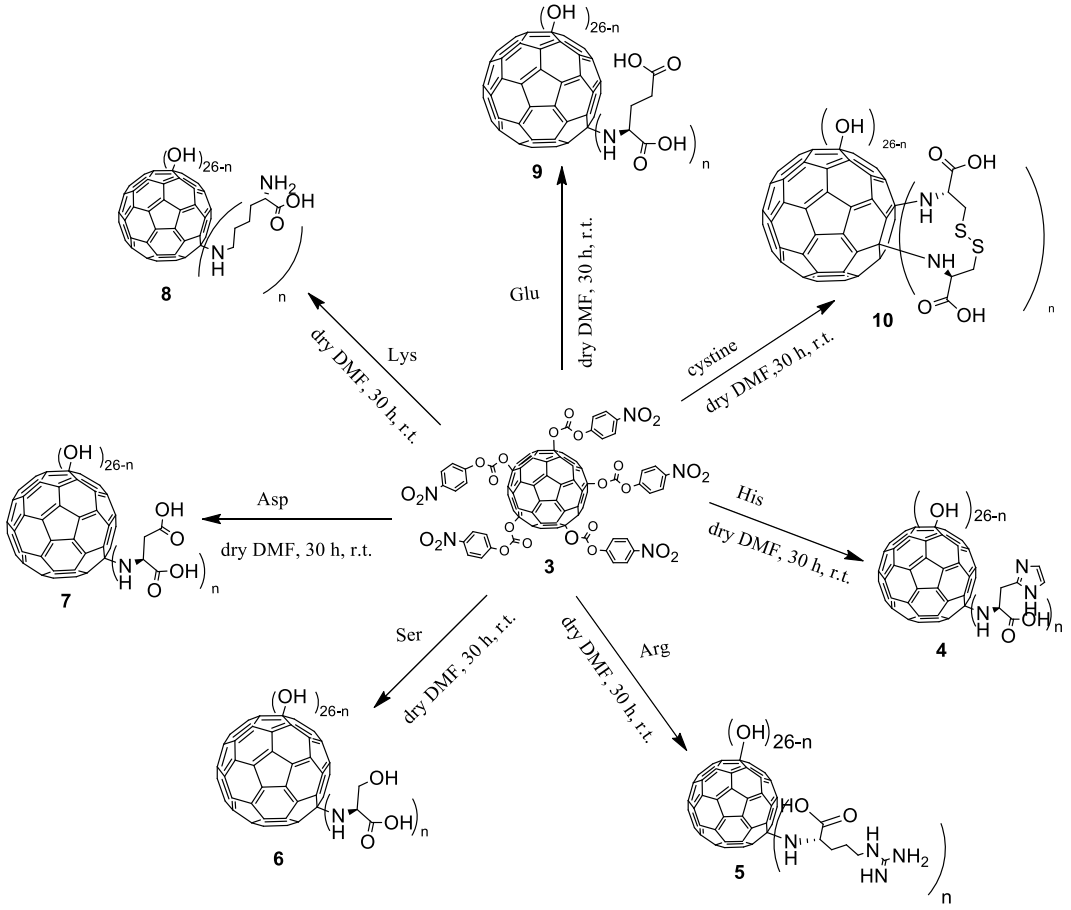

Scheme 1.8 Synthesis of fullerol-amino acid derivatives.

In the synthesis of fullerol lysine (F-Lys), when pKas of amino groups are considered, pKas of alpha amino group and side chain amino group are 10.5 and 9.0, respectively. Therefore, basicity of side chain amino group is more than ten times higher. Also, It is a well-known fact that there is a direct proportionality between nucleophilicity and basicity, although it is not always true.[42] Therefore, it was thought that side chain amino group attacks to the activated fullerol, because it is less hindered and has higher nucleophilicity.

After the synthesis of the fullerol amino acid derivatives they are characterized via ^{1}H NMR. ^{13}C NMR spectrum was not presented. As amino acid attached carbons are different and thus gives peaks in different frequencies in NMR, their intensity decreases. As a result, a bands of carbon peaks were observed. This observation is

valid for both solid and solution phase NMR results. Thus, ^{13}C NMR results do not give any additional information regarding the structure of fullerol amino acid derivatives.

Figure 1.7 indicates the fullerol histidine (F-His) derivative as representative example.

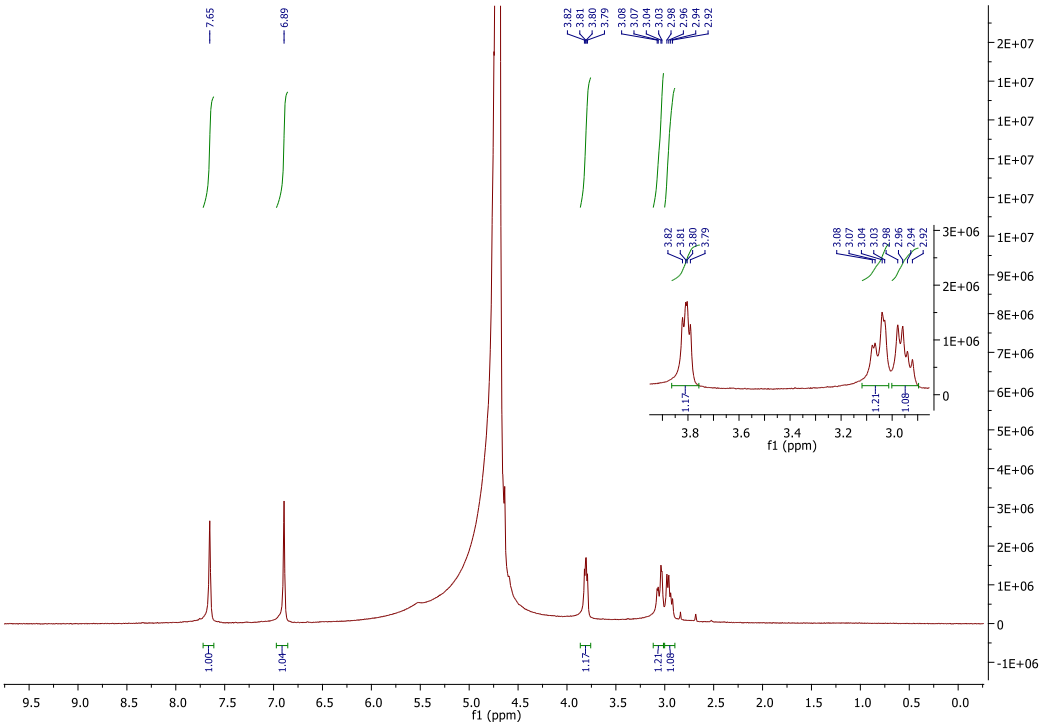

Figure 1.7 ^{1}H NMR spectrum of F-His derivative.

After it was observed that amino acids can be conjugated to the activated fullerol, the number of conjugated amino acids was determined via internal standard method. Since the peaks of dimethyl formamide (DMF) and fullerol amino acids derivatives do not interfere, DMF was chosen as internal standard. As representative example, Figure 1.8 shows ^{1}H NMR spectrum of F-His derivative with internal standard DMF. In internal standard method, amount of internal standard and sample is known, and the ratio of peaks in NMR spectrum can be utilized to calculate the number of conjugated amino acids on fullerol.

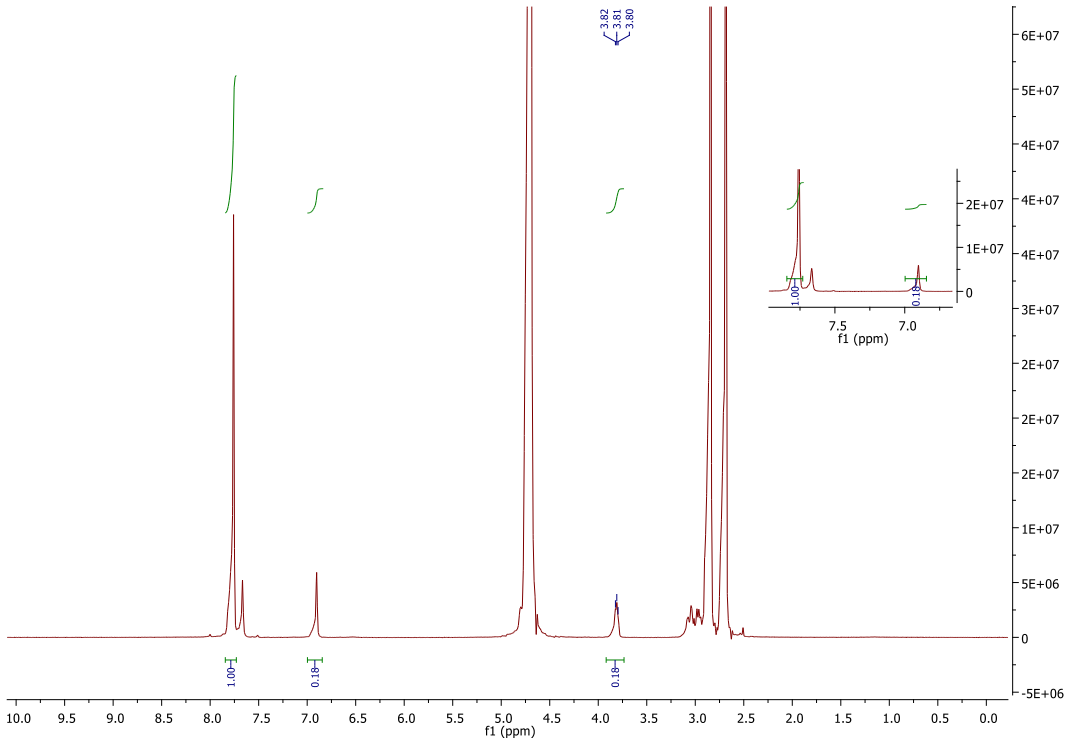

Figure 1.8 ^{1}H NMR spectrum of F-His derivative with internal standard DMF.

Internal standard method was supported with elemental analysis results. Since the carbon and hydrogen percentage results in the elemental analysis did not give consistent values, only nitrogen percentage was considered to calculate the number of amino acids on fullerol. Also, since the doublets of nitro phenyl group in activated fullerol were not observed in NMR spectrum of fullerol-amino acid (F-AA) derivatives, it was assumed that F-AAs contain hydroxyl groups other than amino acid residues. Figure 1.9 indicates the simple formulation to compute the number of amino acids on fullerol. Table 1.3 tabulates the results of elemental analysis and internal standard method. The average of these values was inserted to calculate the molecular weights of fullerol amino acid derivatives.

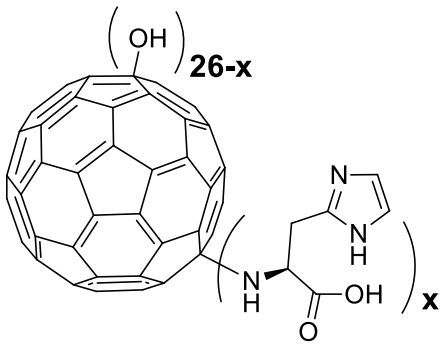

3x*14.00/[(720+26*17.00)+154.15*x-17.00*x]=N%

Figure 1.9 Formulation in consideration of elemental analysis results.

Table 1.3 The results of elemental analysis and internal standard method.

F-AA	**%N in Elemental analysis**	**Average number of amino acids by elemental analysis**	**Number of amino acids by internal standard method**
F-His	15.03	8.16	9.21
F-Arg	20.05	9.44	9.27
F-Asp	-	-	3.01
F-Lys	-	-	5.46
F-Glu	-	-	4.64
F-Ser	-	-	11.77

1.2.3 Lactate Dehydrogenase Mimics

Lactate dehydrogenase (LDH) has histidine and arginine on its active site. It also needs NADP nicotinamide-adenine dinucleotide (NAD^+) or nicotinamide-adenine

dinucleotide phosphate ($NADP^+$) while the lactic acid is oxidized to pyruvic acid. Since NAD^+ was not available in the lab and it was too expensive, its analog was synthesized as in the literature.[42,43] Moreover, Scheme 1.9 illustrates the synthesis. These analogs were used to mimic the LDH.

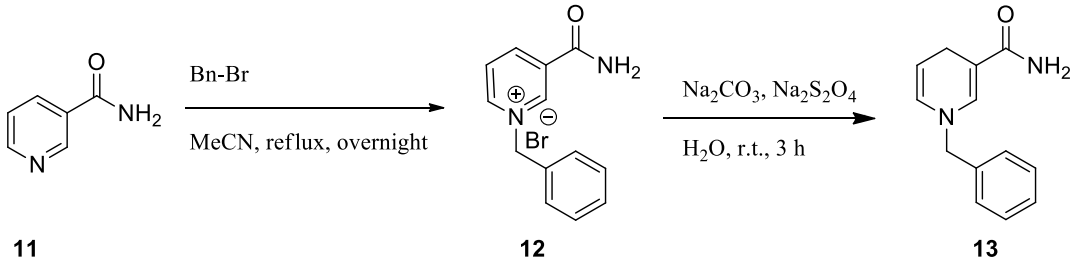

Scheme 1.9 Synthesis scheme of NAD^+ and NADH coenzyme analogs.

1.2.3.1 Oxidation reaction with LDH mimics

LDH was chosen as first enzyme to mimic, because the course of the reaction can be followed in decrease or increase in 340 nm at which NADH gives absorption peak. However, the absorption maximum is shifted to 360 nm with the above NADH analog. Firstly, UV-Vis spectrum was obtained to follow the reaction, but the spectrum data were not meaningful, it was the collection of fluctuated data. Then, High Pressure Liquid Chromatography (HPLC) was employed as a sensitive instrument to trace the reaction. In order to follow the reaction, the marker molecule should have a different retention time. For this reason, phenyl lactic acid was selected as the reactant in the oxidation mimic of LDH. Scheme 1.10 indicates the reaction conditions. As enzyme mimic, F-His and F-Arg with 5 mol% of reactants was added.

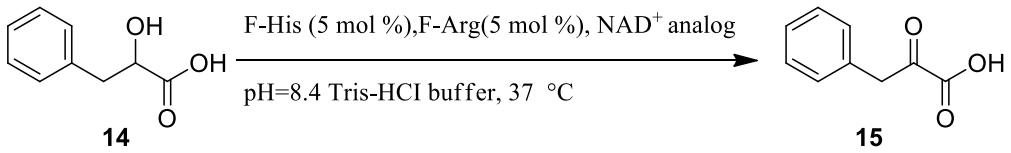

Scheme 1.10 Oxidation reaction with LDH mimics.

Figure 1.10 indicates the retention times of phenyl lactic acid, phenyl pyruvic acid and NAD^+ analog.

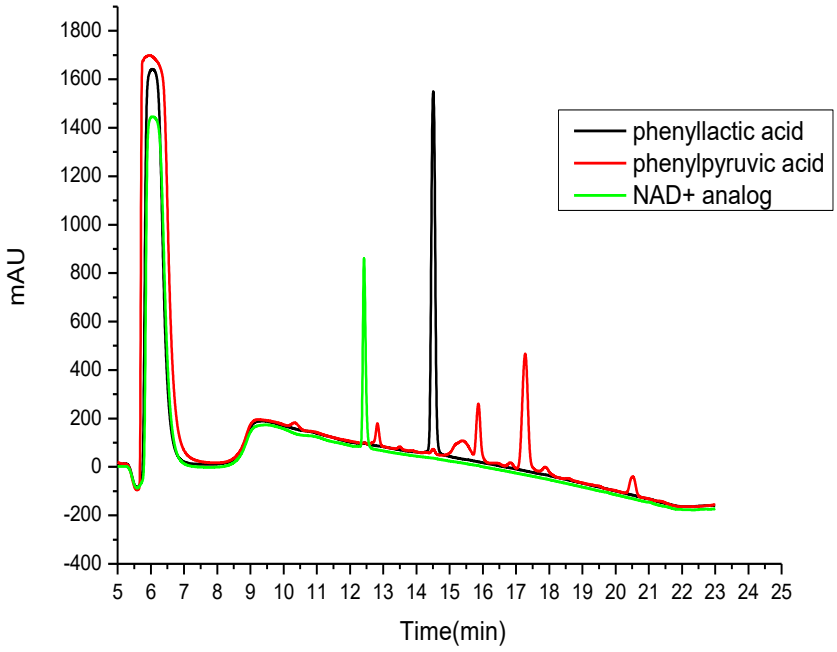

Figure 1.10 HPLC chromatogram of reactant, expected product and NAD^+ analog.

Figure 1.11 shows HPLC chromatogram of oxidation reaction with LDH mimics. If LDH mimics indicated the enzyme activity, the intensity of NAD^+ peak would decrease or there would be a new peak around 17.5 minutes as time passes. However, there is no such change in the chromatogram, which means that LDH mimic does not have enzyme activity.

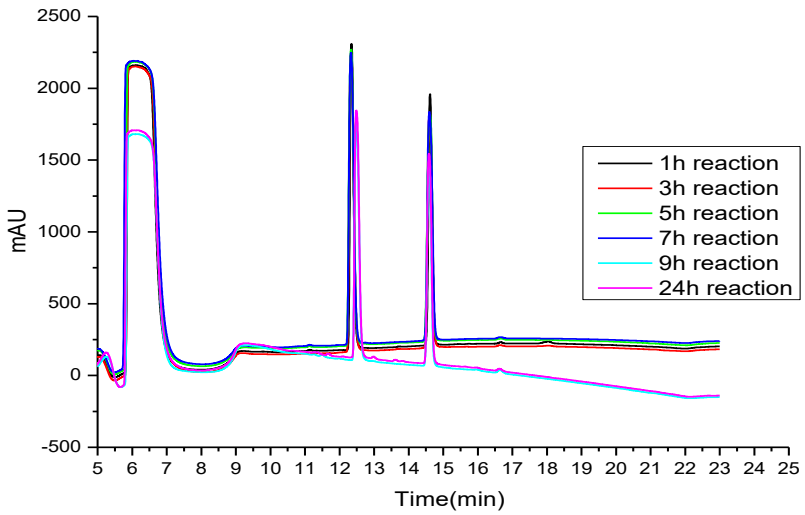

Figure 1.11 HPLC chromatogram of the oxidation reaction with LDH mimics.

1.2.3.2 Reduction reaction with LDH mimics

When the negative result was considered for the oxidation reaction with LDH mimic, it was thought that it may be due to the requirement of NAD^+ to NADH conversion at which aromaticity of NAD^+ is broken and this is not desirable for the molecule. Therefore, reduction reaction as seen in Scheme 1.11 would be performed, after purification of NADH analog.

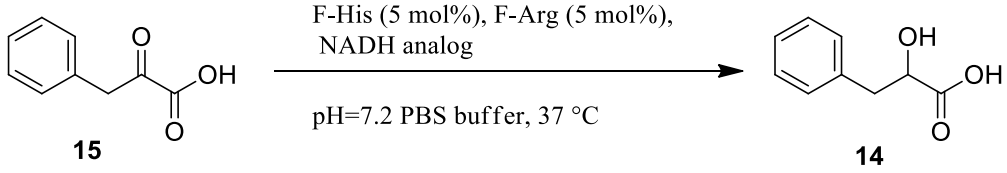

Scheme 1.11 Reduction reaction with LDH mimics.

1.2.4 Serine Protease mimics

Serine proteases have conserved Asp-His-Ser catalytic triad in the active site. To mimic this enzyme, active site amino acids are conjugated to the fullerol, then they were added to the reaction vessel.

First of all, para-nitro acetamide was synthesized as in the literature.[45] Then, it was added to the reaction as reactant with the ser protease mimic elements. Scheme 1.12 indicates the synthesis of reactant and the reaction conditions. Also, the reaction was traced with HPLC instrument.

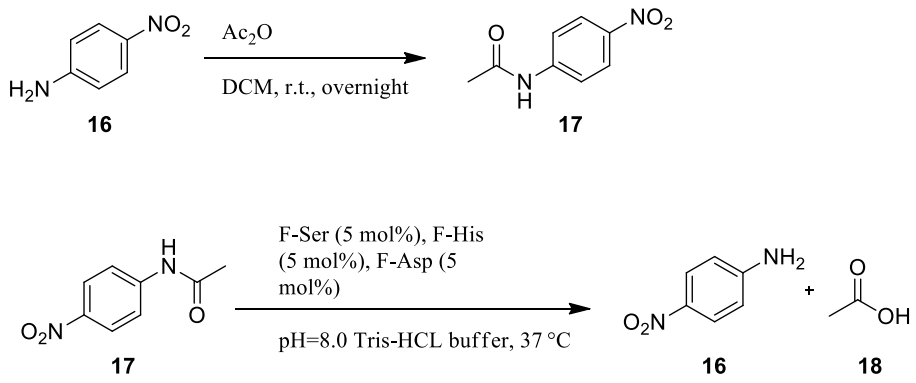

Scheme 1.12 Synthesis of the reactant (above), reaction with ser protease mimic (below).

Figure 1.12 indicates HPLC chromatogram of the reactant, expected product and time-based reaction graph. The expected product is para-nitro aniline and its retention time about 17 minutes. If the ser protease mimic elements indicated enzyme activity, then a new peak would appear around 17 minutes and intensity of the peak

would increase with the time. As seen in the Figure 1.12, there is no such change with time, thus it can be interpreted that there is no ser protease activity.

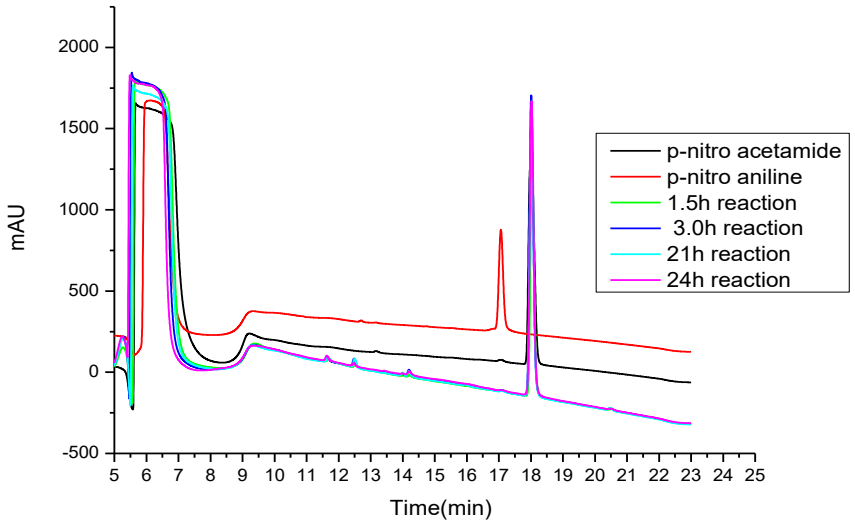

Figure 1.12 HPLC chromatogram of the reaction with ser protease mimic elements.

As a second reactant, L-alanine anilide was synthesized based on the literature.[46] Then it was used as the reactant with the ser protease mimic molecules. Scheme 1.13 indicates the synthesis and reaction with the ser protease mimic elements. The course of the reaction was traced with HPLC.

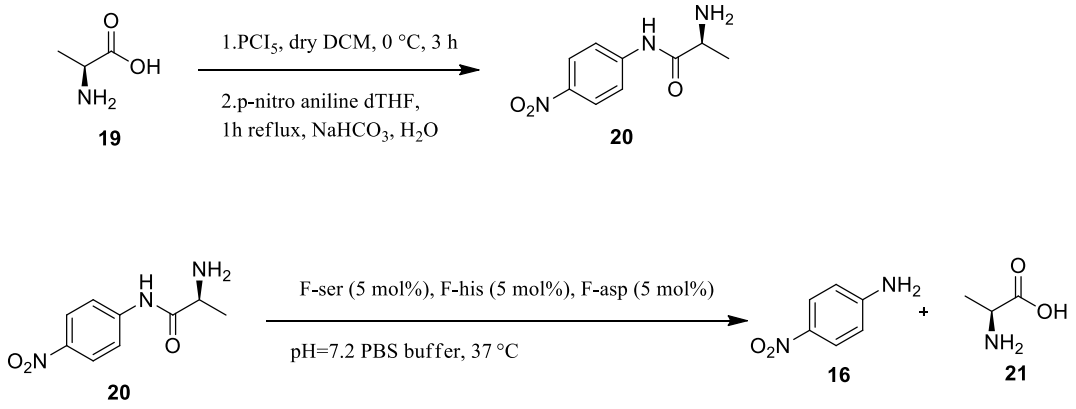

Scheme 1.13 Synthesis of the reactant L-alanine anilide (above), reaction with ser protease mimic (below).

Figure 1.13 indicates the HPLC chromatogram of reactant, expected product and time-based graphs of the reaction. The expected product is *p*-nitroaniline and its retention time is around 17 minutes. When the reaction is performed, the intensity of the peak around 17 minutes would increase. Simultaneously, there would be a decrease in the L-alanine anilide peak intensity. However, this trend was not observed. There is a small peak around 17 minutes due to *p*-nitroaniline residue which was employed in the synthesis of L-alanine anilide. Since its intensity stays constant with time, it cannot be attributed to the product formation.

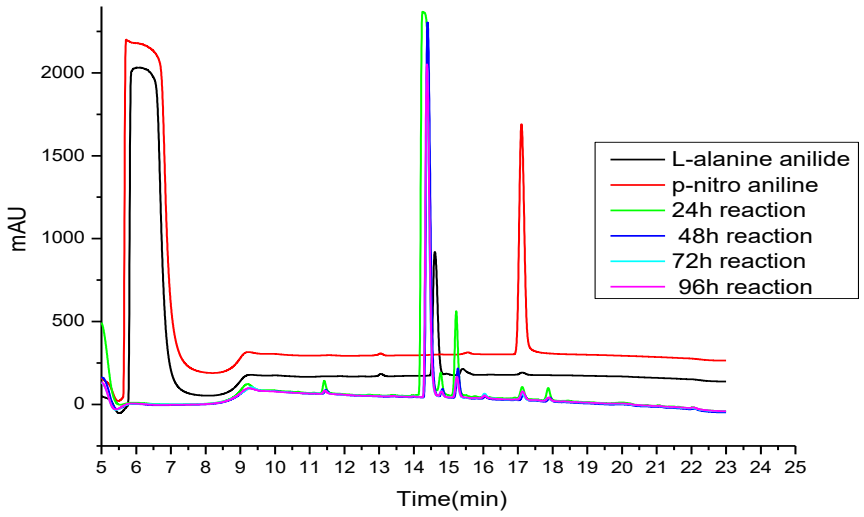

Figure 1.13 HPLC chromatogram of the reaction with ser protease mimic elements.

1.2.5 Nitrilase Mimics

Nitrilases are enzymes hydrolyzing nitriles to corresponding amides or carboxylic acids. They have Glu-Lys-Cys catalytic triad in the active site. These active site amino acids are conjugated to the fullerol as described in previous section, then used as enzyme-like molecules.

Benzonitrile as substrate was utilized to mimic the nitrilase. The preliminary studies were performed.

Since benzonitrile can be converted into benzamide and benzoic acid. Retention times of both of the expected products were obtained. This kind of blank was performed to check whether benzonitrile is hydrolyzed into benzamide and benzonitrile or stay the same in the reaction conditions. It can be seen that as time passes, there is no conversion to other molecules as indicated in Figure 1.14, thus benzonitrile stays the same in the buffer at reaction temperature.

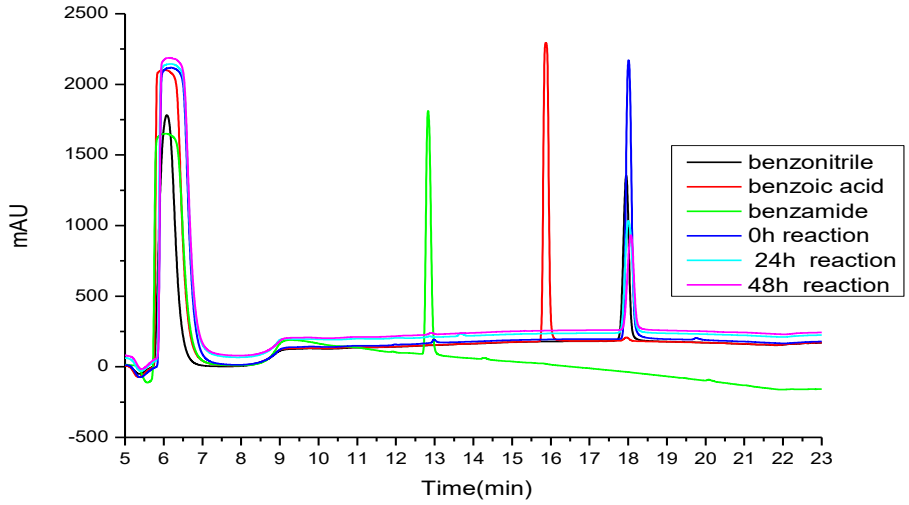

Figure 1.14 HPLC chromatogram of benzonitrile in sodium carbonate-sodium bicarbonate buffer at 50 °C.

Scheme 1.14 shows the reaction of benzonitrile with the active site amino acids at the described reaction conditions. This reaction is also kind of blank reactions to check the activity of the non-conjugated amino acids. Also, tris(2-carboxyethyl) phosphine (TCEP) was added to prevent S-S bond formation.

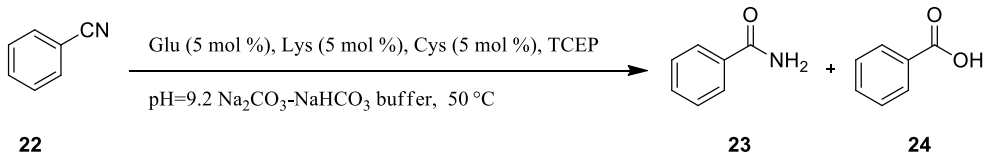

Scheme 1.14 Reaction of benzonitrile with active site amino acids.

Figure 1.15 shows the time-based graph of the reaction of benzonitrile with active site amino acids. As it can be seen, there is no conversion of benzonitrile into benzamide or benzoic acid. The small peaks around 12 minutes and 15 minutes are due to the cysteine and TCEP.

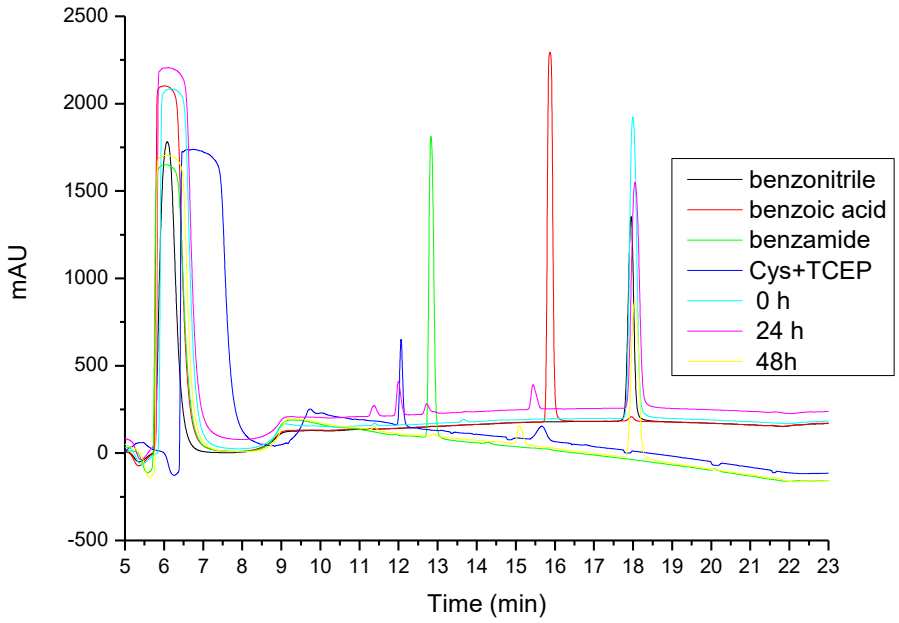

Figure 1.15 HPLC chromatogram of reaction of benzonitrile with active site amino acids.

Scheme 1.15 indicates the reaction of benzonitrile with Cys, F-Glu and F-Lys in the defined reaction conditions. This reaction was performed to observe the effect of glutamic acid and lysine conjugated fullerol on the course of the reaction.

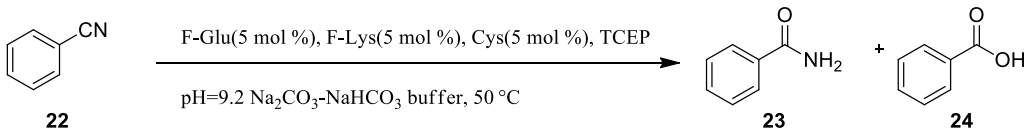

Scheme 1.15 Reaction of benzonitrile with Cys, F-Glu and F-Lys.

Figure 1.16 shows the retention times of substrate, expected product and the time-based course of the reaction of benzonitrile with Cys, F-Glu and F-Lys. Based on this chromatogram, existence of F-Glu and F-Lys does not make any change in the reaction progress.

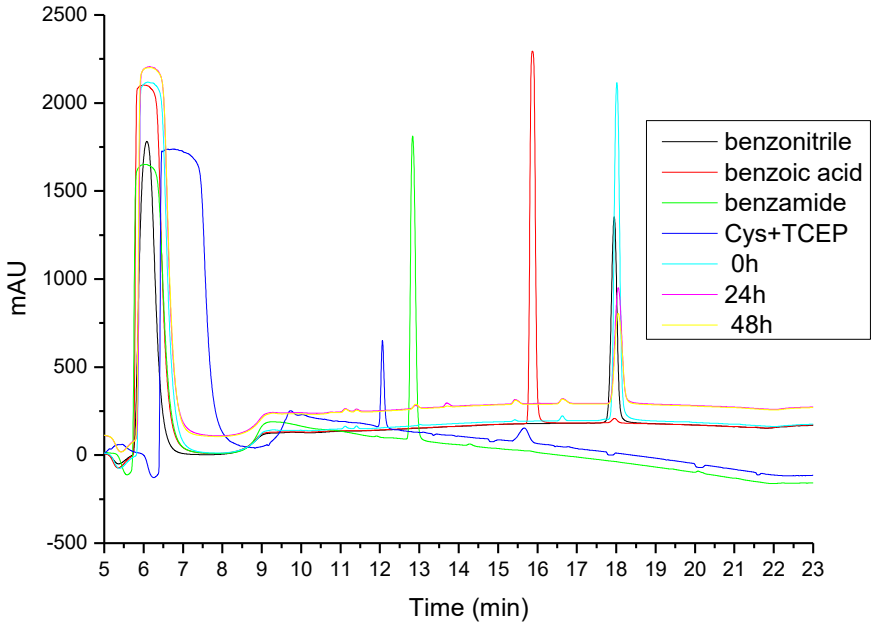

Figure 1.16 HPLC chromatogram of reaction of benzonitrile with Cys, F-Glu and F-Lys.

For the conjugation of cysteine to the fullerol, both alpha amine of cysteine and thiol of cysteine can attack to the activated fullerol. Therefore, cystine was preferred to be conjugated, but the characterization of cystine fullerol derivative was difficult. Although, the attack of second amino group of cystine to the activated fullerol after conjugation of first amino group is feasible due to the close interaction with the

activated fullerol, singly attach of cystine is also possible. The ratio of doubly attached and singly attached cystine molecules can be detected by ^{1}H NMR, but determination of number of cystine on fullerol is still vague. It may be determined by internal standard method by using this ratio. For the moment, cystine conjugated fullerol was not used in activity studies.

1.2.6 Conclusion

In this part of the study, active site amino acids of lactate dehydrogenase, protease and nitrilase were conjugated to the fullerol and then fullerol amino acid derivatives were tested for enzymatic activity. The progress of the corresponding reactions was followed via HPLC chromatogram. It was observed that there is no enzymatic activity of fullerol amino acid derivatives on the reactions.

The reason for the negative results can be that all the studied reactions are catalyzed by the large biomolecules with several subunits in biological systems. Therefore, conjugation of only active site amino acids to fullerol was obviously not sufficient to mimic the corresponding enzymes. Conjugation of active site amino acids to the fullerol and enzymatic activity studies can work for simpler reactions, but it did not for the ones studied in this project. Also, although nanozymes are good candidate as the alternatives of natural enzymes, variety of enzymes is quite limited, although the material variety is wide.

In brief, risky but promising enzymes were chosen and studied, but the realization of the reactions did not take place.

1.3 Experimental

1.3.1 Materials and Methods

Commercial amino acids were supplied from Chem-Impex International Inc. Commonly used solvents such as DCM, MeCN, THF, Et_2O, DMF, ethanol and methanol were obtained from Merck. Solvents such as EtOAc, hexane and DCM employed to perform column chromatography were technical grade and they were dried with calcium chloride in distillation system.

Deuterated solvents were provided by Merck.

In the preparation of HPLC solvents, HPLC grade solvents were supplied by Sigma Aldrich.

Column chromatography purifications were performed with Merck Silica gel 60 (0.063-0.20 mm)

Nuclear Magnetic Spectrum of molecules obtained on Bruker Spectrospin Advance DPX 400 spectrometer. Chemical shifts were presented in parts per million (ppm) and TMS was utilized as internal standard. NMR spectrums were given partly in the text and the rest of the spectrums in Appendix A.

The progress of the reactions was traced with TLC plates which were purchased from Merck. TLC plates were coated with silica gel and contain F254 fluorescent indicator which enables the visualization at 254 nm.

The course of the reactions of studied enzymes was followed by using Dionex Ultimate 3000 Series instrument with 4 different wavelengths. The eluents are Milli Q-0.1%TFA and MeCN-0.08%TFA and flow rate is 0.5 mL/min.

The HPLC chromatograms are presented based on 210 nm data.

Telstar Cryodos instrument for lyophilization was employed for the removal of water and dioxane solvents in the samples.

FT-IR measurements were performed in Thermo Scientific Nicolet is 10 instruments.

1.3.2 Synthesis of fullerol (2)

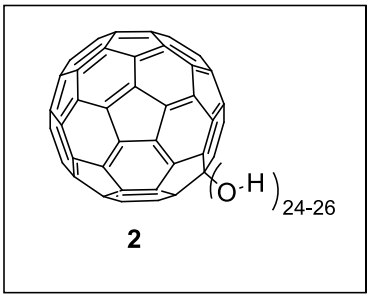

2

To the fullerene (80 mg) solution in toluene (50 mL), 2 mL NaOH solution (1 g/ml) was prepared and added, then 5-6 drops of 30% hydrogen peroxide solution was dropped. Moreover, about one milliliter of phase transfer catalyst tetrabutylammonium hydroxide (40 wt.% solution in water) was dropped. The resulting solution was stirred vigorously for 5 days at room temperature. After the completion of reaction time, toluene was decanted, solid portion was filtered and washed with ethanol to remove excess TBAH and any other reagent.[39]

1.3.3 Synthesis of activated fullerol (3)

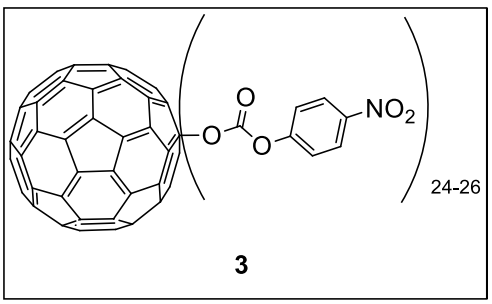

3

The suspension of fullerenol (60 mg) in dry dimethylformamide (10 mL) was sonicated for 1 h to form a homogeneous one. Then, *p*-nitrophenyl chloroformate (400 mg), anhydrous pyridine (2 mL), and catalytic *N*, *N*-dimethyl aminopyridine (30.0 mol%, 1.9 mg) were added at 0 °C. The solution was stirred for 48 h under nitrogen atmosphere. During the reaction, it was exposed to 1 h sonication once every 8 h approximately. The brown solid was precipitated out by the addition of diethyl ether and washed repeatedly with ether, dichloromethane, and isopropyl alcohol, respectively. Aromatic doublets at 6.9 and 8.2 ppm in ^{1}H NMR spectrum confers the expected product.[39]

1.3.4 Synthesis of F-His (4)

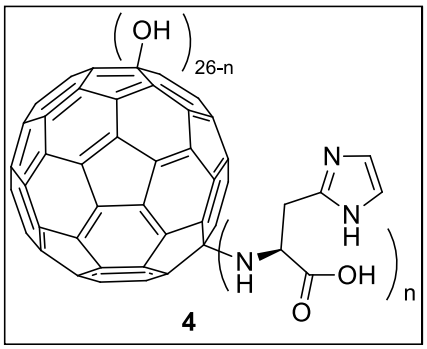

4

Activated fullerenol (5.0 mg) and histidine (60 equivalent, 8.5 mg) were dissolved in dry DMF (5 mL) and the solution was sonicated under nitrogen for 30 min. The solution was stirred at room temperature under nitrogen for 30 h along with 1 h sonication every 8 h. A brown solid was precipitated out by the addition of diethyl ether. The solid was washed twice with 1-2 drops of methanol in dichloromethane.4[39]

^{1}H NMR (400 MHz, D_2O) δ 7.65 (s, 1H), 6.89 (s, 1H), 3.81 (dd, *J* = 7.4, 5.1 Hz, 1H), 3.11 – 3.00 (m, 1H), 2.95 (dd, *J* = 15.3, 7.7 Hz, 1H).

1.3.5 Synthesis of F-Arg (5)

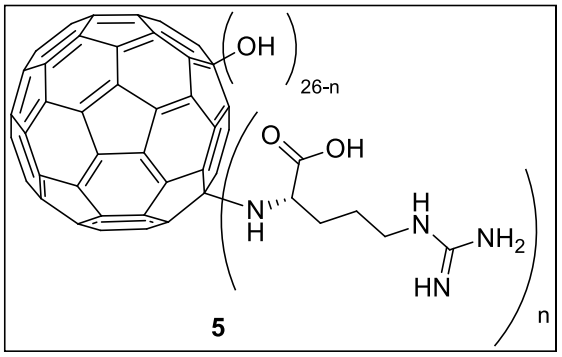

5

Activated fullerenol (5 mg) and arginine (60 equivalent, 9.6 mg) were dissolved in dry DMF (5 mL) and the solution was sonicated under nitrogen for 30 min. The solution was allowed to stir at room temperature under nitrogen for 30 h along with 1 h sonication every 8 h. A brown solid was precipitated out by the addition of diethyl ether. The solid was washed twice with 1-2 drops of methanol in dichloromethane.[39]

^{1}H NMR (400 MHz, D_2O) δ 3.19 (d, *J* = 6.1 Hz, 1H), 3.03 (d, *J* = 6.7 Hz, 2H), 1.57-1.36 (m, 4H)

1.3.6 Synthesis of F-Ser (6)

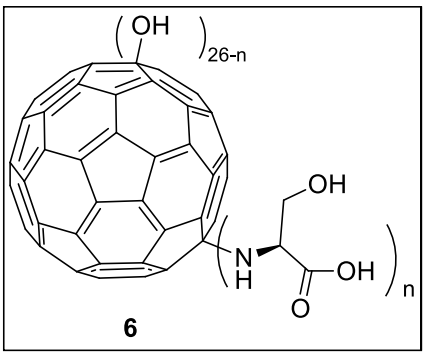

6

Activated fullerenol (20 mg) and serine (60 equivalent, 23.1 mg) were dissolved in dry DMF (10 mL) and the solution was sonicated under nitrogen for 30 minutes, then the solution was stirred at room temperature under nitrogen for 30 h along with 1 h sonication every 8 h. A brown solid was precipitated out by the addition of diethyl ether. The solid was washed twice with 1-2 drops of methanol in dichloromethane.[39]

^{1}H NMR (400 MHz, D_2O) δ 3.85 – 3.74 (m, 2H), 3.68 (t, J = 4.5 Hz, 1H).

1.3.7 Synthesis of F-Asp (7)

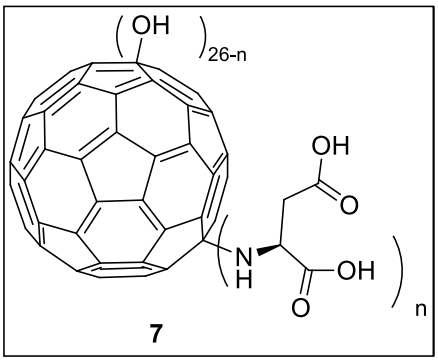

7

Activated fullerenol (20 mg) and aspartic acid (60 equivalent, 29.3 mg) were dissolved in dry DMF (10 mL) and the solution was sonicated under nitrogen for 30 min. The solution was stirred at room temperature under nitrogen for 30 h along with 1 h sonication every 8 h. A brown solid was precipitated out by the addition of diethyl ether. The solid was washed twice with 1-2 drops of methanol in dichloromethane.[39]

^{1}H NMR (400 MHz, D_2O) δ 3.98 – 3.84 (m, 1H), 2.97 – 2.73 (m, 2H).

1.3.8 Synthesis of F-Lys (8)

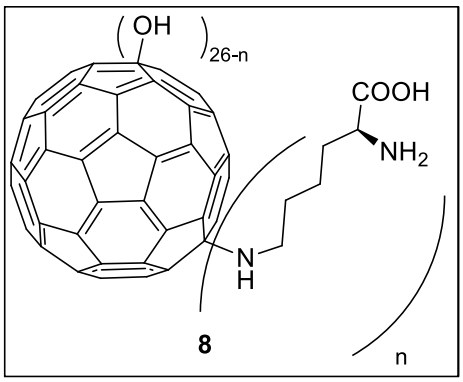

Activated fullerenol (20 mg) and lysine (60 equivalent, 32.2 mg) were dissolved in anhydrous DMF (10 mL) and the solution was sonicated under nitrogen for 30 min. The solution was allowed to stir at room temperature under nitrogen for 30 h along with 1 h sonication every 8 h. A brown solid was precipitated out by the addition of diethyl ether. The solid was washed twice with 1-2 drops of methanol in dichloromethane.[39]

^{1}H NMR (400 MHz, D_2O) δ 3.43 (t, *J* = 5.9 Hz, 1H), 2.90 – 2.76 (m, 2H), 1.69-1.59 (m, 3H), 1.58 – 1.42 (m, 3H), 1.36-1.14 (m, 3H).

1.3.9 Synthesis of F-Glu (9)

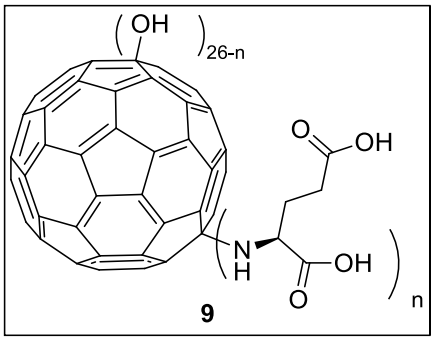

Activated fullerenol (20 mg) and glutamic acid (60 equivalent, 32.4 mg) were dissolved in dry DMF (10 mL) and the solution was sonicated under nitrogen for 30 minutes, then the solution was stirred at room temperature under nitrogen for 30 h along with 1 h sonication every 8 h. A brown solid was precipitated out by the addition of diethyl ether. The solid was washed twice with 1-2 drops of methanol in dichloromethane.[39]

^{1}H NMR (400 MHz, D_2O) δ 3.68 (t, *J* = 6.2 Hz, 1H), 2.52 – 2.30 (m, 2H), 2.10 – 1.87 (m, 2H).

1.3.10 Synthesis of F-Cystine (10)

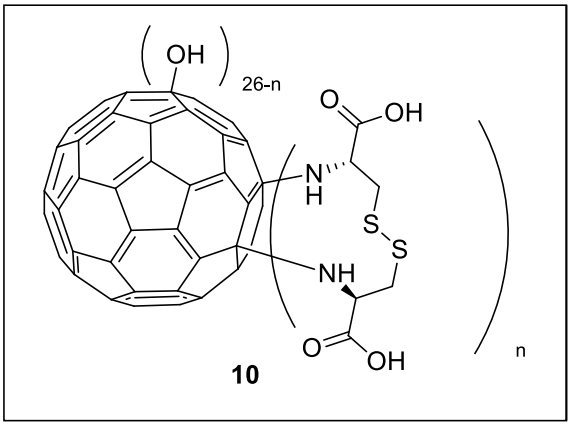

10

Activated fullerenol (60 mg) and cystine (60 equivalent, 79.3 mg) were dissolved in dry DMF (20 mL) and the solution was sonicated under nitrogen for 30 min. The solution was stirred at room temperature under nitrogen for 30 h along with 1 h sonication every 8 h. A brown solid was precipitated out by the addition of diethyl ether. The solid was washed twice with 1-2 drops of methanol in dichloromethane. [39]

^{1}H NMR (400 MHz, D_2O) δ 3.92 (t, *J* = 4.8 Hz, 1H), 2.99 (dd, *J* = 14.8, 4.9, 2H)

1.3.11 Synthesis of 1-benzyl-3-carbamoylpyridinium bromide (NAD^+ analog) (12)

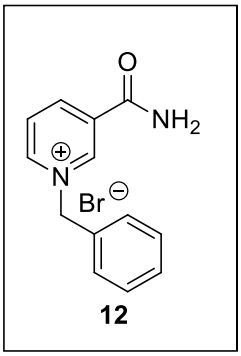

12

1.1 equivalents of benzyl bromide and 1M of nicotinamide in acetone was mixed and refluxed overnight. After cooling, diethyl ether was added and sonicated. The white precipitate was filtered and washed with diethyl ether. The product 1-benzyl-3-carbamoylpyridinium bromide was obtained with 82% yield.[43,44]

^{1}H NMR (400 MHz, DMSO) δ 9.63 (s, 1H), 9.30 (d, *J* = 6.1 Hz, 1H), 8.96 (d, *J* = 8.1 Hz, 1H), 8.60 (s, 1H), 8.35 – 8.25 (m, 1H), 8.20 (s, 1H), 7.66 – 7.51 (m, 3H), 7.45 (d, *J* = 6.0 Hz, 3H), 5.92 (s, 2H).

1.3.12 Synthesis of N-benzyl-1, 4-dihydronicotinamide (NADH analog) (13)

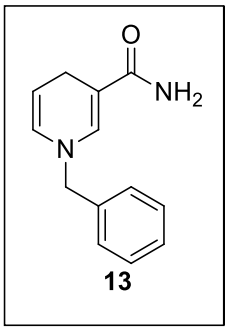

13

Sodium carbonate (1.45 g, 13.6 mmol, 4 equiv.) and sodium dithionite (2.26 g, 12.9 mmol, 3.80 equiv.) was added into the solution of **12** (1.0 g, 3.4 mmol) in H_2O (15 mL) at room temperature. The resulting solution was stirred in darkness for 3 h. Then, three times extraction with dichloromethane was performed. Organic phases were collected, dried with Na_2SO_4, filtered and evaporated under reduced pressure. The obtained product mixture was further purified with column chromatography with 95% DCM-5% methanol to obtain pure **13**.[44] ^{1}H NMR of crude **13** was given in Appendix A.

1.3.13 Synthesis of p-nitrophenyl acetamide (17)

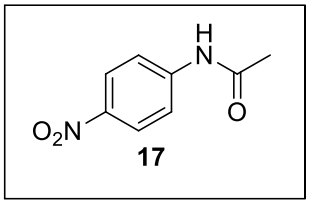

17

Acetic anhydride (1.2 mol, 1.2 equivalent) was added dropwise with into the solution of 4-nitroaniline (1 mmol) in 10 mL dichloromethane. The reaction mixture was stirred for 16 hours. The solvent was removed under reduced pressure, then the crude product was neutralized by 1M HCI solution by maintaining stirring for 30 minutes. The solid product was collected on filter paper. Moreover, it was purified by recrystallization using aqueous ethanol (60%) to obtain pure 4-nitroacetamide which is pale yellow solid. The yield was 88%.[45]

^{1}H NMR (400 MHz, $CDCl_3$) δ 8.15 (d, J = 9.1 Hz, 2H), 7.63 (d, J = 9.1 Hz, 2H), 7.36 (s, 1H), 2.18 (s, 3H).

1.3.14 Synthesis of L-Alanine anilide (20)

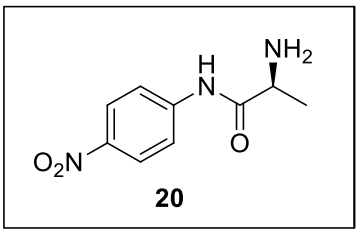

20

The alanine amino acid (2 mmol) and phosphorous pentachloride (2 mmol) were mixed in 10 mL dry dichloromethane on ice–water bath. After 3 h, it was evaporated under reduced pressure. Then, the p-nitroaniline (2 mmol) dissolved with 5 mL dry tetrahydrofuran was added. The mixture was heated to boiling, it was cooled and mixed 1 h at room temperature. Then, the solvent was removed under reduced pressure. Moreover, water (20 mL) was added to the remaining solid portion and stirred for 30 minutes. After 30 minutes, it was filtered. The pH of filtrate portion was adjusted to 8-9 with saturated sodium bicarbonate. Then, filtrate portion was extracted with ethyl acetate, washed with brine. It was dried over sodium sulfate, filtered. Solvent was removed under vacuum. The product was obtained with 19% yield.[46]

^{1}H NMR (400 MHz, $CDCl_3$) δ 9.94 (s, 1H), 8.30 – 8.05 (m, 2H), 7.83 – 7.66 (m, 2H), 3.60 (q, 7.0 Hz, 1H), 1.47 – 1.33 (d, 7.0 Hz, 3H).

CHAPTER 2

SYNTHESIS EFFORT OF TETRA ARYL PYRANONE

2.1 Introduction

2.1.1 Luminescence

Light is a basic phenomenon people want to learn more about. Accordingly, luminescence took interest in the course of the human history. People observed aurora borealis, glow worms and luminous stones such as barite ($BaSO_4$) since ancient times. Luminescence as a word is originated from 'lumen' which means light in Latin.[47] Luminescence is regarded as "cold light" which is different than incandescence. Incandescence occurs for all known materials if these materials are heated to a high temperature, which is called basically blackbody radiation.[47,48]

General mechanism of luminescence is the emission of light due to the absorption of one of the forms of energy. Excitation energy can arise from intake of UV-Vis light, mechanical energy, heat, chemical energy, ions and particles. Figure 2.1 indicates the luminescence process.

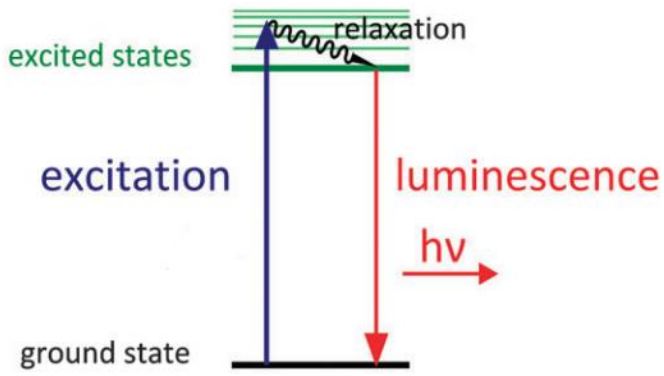

Figure 2.1 Luminescence process.[50]

2.1.2 Luminescence Classification

Luminescence as a term was first utilized by German physicist Eilhardt Wiedemann in 1888.He categorized this phenomenon into six types based on the excitation source. These are photoluminescence, thermoluminescence, electroluminescence, crystalloluminescence, triboluminescence, and chemiluminescence.[51] Although, different forms of luminescence was examined since then, this classification remains as basis. Figure 2.2 indicates the enhanced categorization of the luminescence.[48]

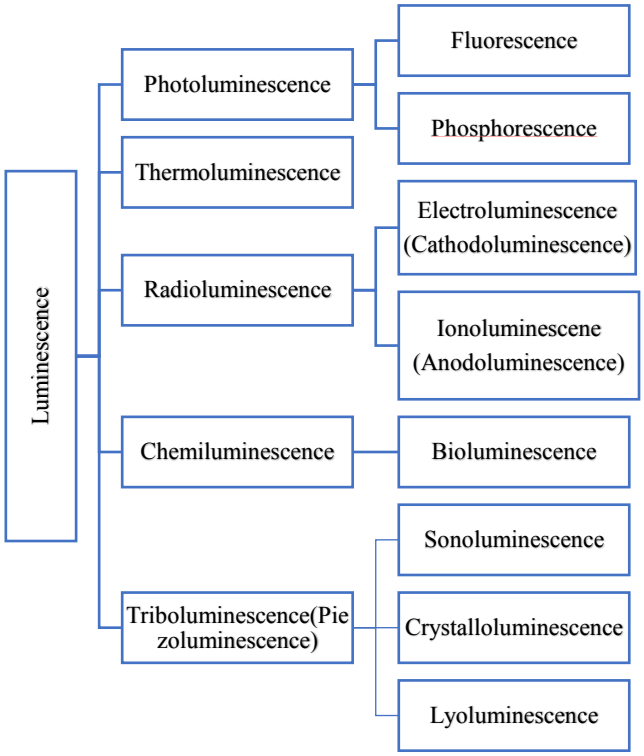

Figure 2.2 Classification of luminescence.

In photoluminescence, the excitation occurs due to absorption of UV-Vis radiation. Since the wavelength of emitted light is longer than exciting radiation, the emitted light is in UV-Vis or near Infrared(IR) region.[52] It is divided into two which are fluorescence and phosphorescence. Fluorescence is the result of light emission as long as the incoming radiation is provided. Light emission stops, when the irradiation is removed. Phosphorescence process is the same as fluorescence, but emission of light goes on to some extent, after the removal of irradiation. To clarify, the

relaxation time is longer in phosphorescence process than fluorescence process. The reason can be predicted by examining the Jablonski diagram provided in Figure 2.3.[48] An intersystem crossing should take place for phosphorescence to realize. Intersystem crossing is a transition which occurs between electronic states with distinct multiplicities without light emission. It is common in molecular photochemistry.[53] Total electronic-spin quantum number S determines electronic states in molecules and spin multiplicity is calculated via 2S+1 formula. Electronic spin quantum number is +1/2 for up state spin and -1/2 for the down state spin. Highest occupied molecular orbitals can have paired or unpaired electrons, so singlet or triplet electronic states are the result of spin multiplicity computed with 2S+1. Based on maximum multiplicity of Hund's rule, triplet energy states are lower than singlet states. As a result of excitation, ground state electrons can go to excited singlet state or it can occupy a triplet state, which is normally forbidden with the selection rules which stem from quantum mechanical calculations, but the probability of occurrence of such transition increases with significant spin-orbit coupling which is the interaction between spin of an electron and orbit around the nucleus.[54] Hence, all these processes need longer time to take place than fluorescence process.

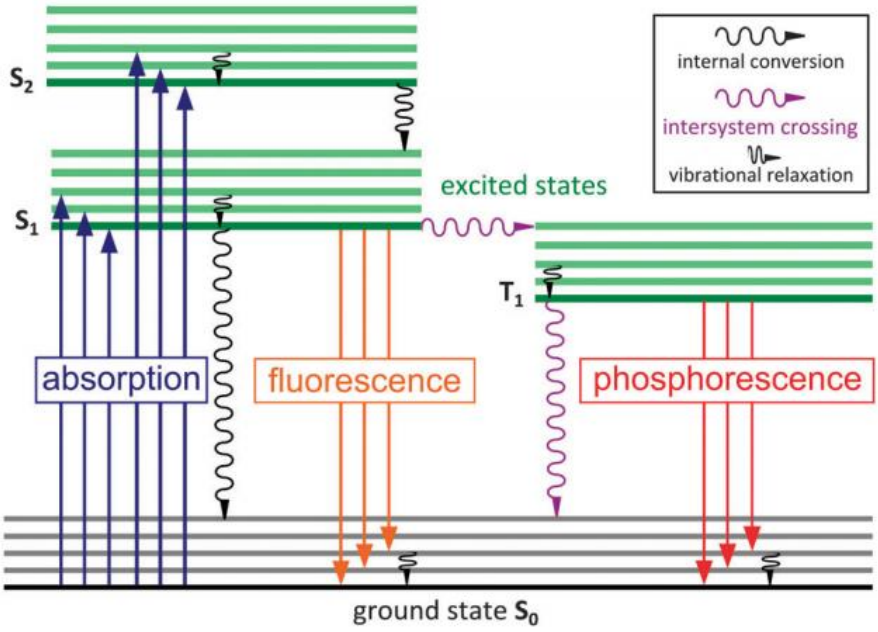

Figure 2.3 Photoluminescence processes in Jablonski diagram.[50]

Thermoluminescence is observed when the emission occurs by heating the substance. However, the temperature must be well below the incandescence point. Incandescence occurs at high temperatures and the light emission is called blackbody radiation. In 18th century, some materials were noticed for showing thermoluminescence property. Aluminum oxide, zirconium silicate, and aluminum fluorosilicate are the examples for that materials.[48] In order to explain better, blackbody is a hypothetical object which absorb or emit perfectly. The best approximation for such an object is an empty object with a small pinhole. In that case, any escape of radiation from this pinhole is absorbed or reemitted for many times that the object reaches thermal equilibrium. However, the term blackbody radiation is used for the radiation from an object due to heat content of the object.[55]

Radioluminescence was defined for the emission of light due to the excitation with different types of light. These different types can be the stream of particles like electrons and ionizing radiation portion of the electromagnetic spectrum such as X-rays and gamma rays. Radioluminescence due to the streams of particles generated in anode or cathode was realized first 1858. In today's terminology,

electroluminescence term is employed if the particles are electrons and ionoluminescence term is preferred when the exciting particles are ions. Radioluminescence studies increased after the discovery of X-rays in 1895 by Wilhelm Konrad Roentgen. It enhanced further with the discovery of uranium and radium. Their discovery also indicated the existence of gamma rays. Electroluminescence is observed when the flow of current realizes in the evacuated tubes of gases, which can be neon, argon, and nitrogen and mercury vapor. Actually, electroluminescence is noticed since ancient times, but there was no information about the reason of the phenomenon. These phenomena are polar lights which are Aurora borealis in the North Pole and Aurora Australis in the south. They are the result of collisions of charged particles coming from Sun and gaseous particles which are present in atmosphere of Earth. The reason for this light in poles is the weaker magnetic field in the poles. Generation of different colors is due to identity of gas molecules. Also, anodoluminescence or ionoluminescence is observed when stream of positively charged ions excite the substance in question. Positive rays or stream of ions are identified by Eugen Goldstein in 1886.To illustrate ionoluminescence, lithium chloride emits red color when it is exposed to the streams of positively charged ions.[48]

Chemiluminescence takes place if the light emission is triggered by a chemical reaction which may be in liquid and gas phase. Luminescence of luminol in the presence of an oxidant such as hydrogen peroxide in basic medium can be one example to the chemiluminescence.[56] Another example can be luminescence coming from white phosphorus and oxygen reaction.[57] When chemiluminescence occurs in living organisms, it is called as bioluminescence. Green fluorescent protein (GFP) which was first noticed in jellyfish *Aequorea* species can be an illustration to bioluminescence. Oxidative cyclization of three amino acid residues (glycine, serine, tyrosine) in GFP's primary structure promotes to the luminescence.[58]

Triboluminescence is the emission of light when the material is rubbed. Also, tribo means to rub in Greek. Although piezoluminescence takes place as a result of pressing, triboluminescence and piezoluminescence terms are used interchangeably.

Also, piezo is to press in Greek. Moreover, all kinds of luminescence due to mechanical stress or fracture are considered under triboluminescence class. In the generation of triboluminescence, various kinds of mechanical excitations can be employed such as grinding, crushing, compressing, and use of ultrasound or infrared laser pulse.[59]

Triboluminescence can be generated by frictional electricity forming a potential difference which is then released in air or by exposure of unstable molecules i.e. electron traps to the light previously, or by unbalanced charges on the different faces of separated crystal planes. Triboluminescence can be divided into three which are sonoluminescence, crystalloluminescence and lyoluminescence. Light emission occurs due to the absorption of energy from sound waves in sonoluminescence. Also, if the luminescence is observed, when the fracture of crystals takes place while crystals are formed, it is called crystalloluminescence. This phenomenon can be observed, if the crystals of potassium sulfate is disturbed during the crystal growth. The reason for such luminescence is attributed to the formation of potassium sulfate from dissociated ions. Moreover, light emission can be observed in the solution of crystals and this type of luminescence is called lyoluminescence.[48]

Triboluminescence is quite common. Based on the literature guess, 36% of inorganics, 19% of organics, 37% of aromatic compounds, 70% of alkaloids and almost 50% of all crystalline materials are triboluminescent.[60] Moreover, study of triboluminescence sheds light on the spectroscopic, structural, electrical and mechanical properties of the solids.[61]

However, there is no consistence in triboluminescence observations. This is because triboluminescence of some materials are seen when they contain some impurities or triboluminescence property is lost after some time at which crystals are formed.[48]

2.1.3 Fluorescence

In general, a functional group contributing or bringing about luminescence is defined as luminophore. As subclass of photoluminescence, fluorescence was introduced in previous section. Molecules indicated fluorescence property is called fluorophore. Luminophores and fluorophores can be organic or inorganic.

2.1.3.1 Aggregation Caused Quenching (ACQ)

Plenty of organic fluorophores were synthesized. When their fluorescence spectra are considered, the fluorescence intensity in the spectra decreased as the concentration of solutions goes up or in solid state. The reason for that tendency is that most of the conventional organic fluorophores are planar and have strong intermolecular interactions. One of these interactions is the π-π stacking which triggers ACQ, and resulting in loss of luminescence or weakening the luminescence intensity in aggregate state.[62] Figure 2.4 indicates the some molecules which indicate ACQ.[62–64]

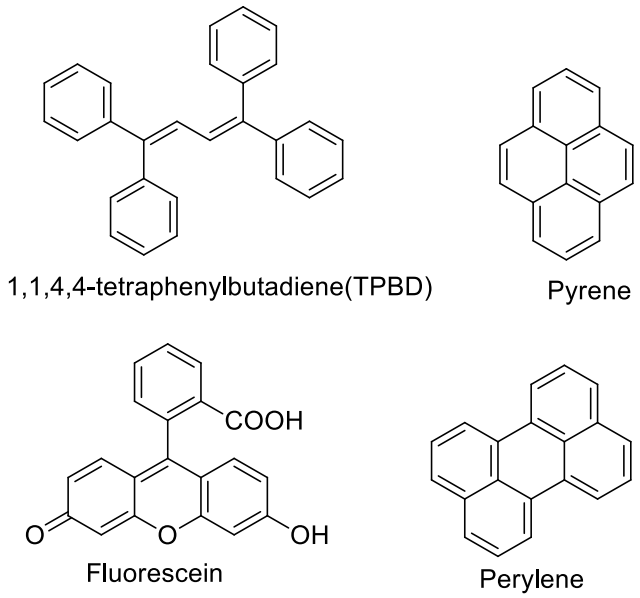

Figure 2.4 Molecules with ACQ property.

2.1.3.2 Aggregation Induced Emission (AIE)

Tang et al. synthesized 1-methyl-1,2,3,4,5-pentaphenylsilole (MPPS) and observed that it has no luminescence in solution state, but luminescence increased in aggregate state. They employed water-ethanol solvent system, as the water percentage increases, MPPS aggregates.[65] After that, they proposed "aggregation induced emission" concept. Figure 2.5 indicates the molecules synthesized in the literature with AIE property since 2001.[64,66,67] As seen in the Figure 2.5, they can contain hydrogen and carbon only, or heteroatoms with polar functional groups. Also, by different functional groups, their properties can be tuned.[67]

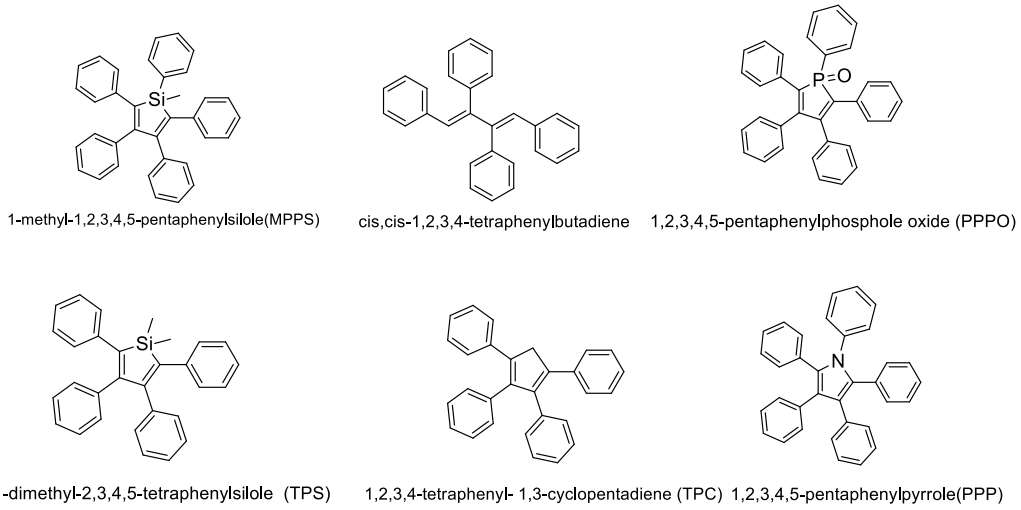

Figure 2.5 Synthesized molecules in the literature with AIE property.

The reason for AIE phenomenon was claimed to be the combined result of the restriction of intramolecular motions (RIM) which are Restriction of Intramolecular Rotation (RIR) and Restriction of Intramolecular Vibration (RIV).[67] As it is seen in Figure 2.5, they are propeller shape and composed of olefinic and aromatic stators with multiple phenyl rotors. Moreover, the phenyl groups can rotate freely around the single bond, which was predicted that free rotation in solution is the way for non-radiative relaxation. However, when these molecules aggregates, they cannot rotate freely due to RIM mechanism and thus it gives fluorescence to relax when they are

excited. Moreover, the shape of these molecules prevent π-π stacking which is the main reason for ACQ.[62]

2.1.4 Motivation of the Study

Previously, 2,3,5,6-tetraphenyl-1,4-dioxine was synthesized and fluorometric study of this molecule was performed to investigate whether it has ACQ or AIE property with water-THF solvent system. It was observed that 2,3,5,6-tetraphenyl-1,4-dioxine indicates ACQ. As the water percentage increases, its fluorescence quenches. Its core has eight electrons. Although, it is supposedly to be anti-aromatic, it was seen that the core is planar based on XRD data.

In this part of the study, synthesis of 2,3,5,6-tetrapheny-4H-pyran-4-one via a new route was aimed as the kind of counterpart of 2,3,5,6-tetraphenyl-1,4-dioxine with aromatic core to examine whether it shows ACQ/AIE property and to investigate the effect of aromaticity of the core.

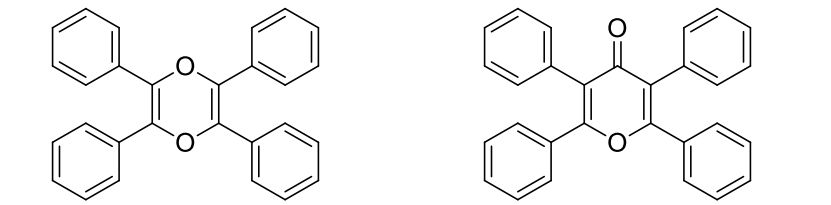

2,3,5,6-tetraphenyl-1,4-dioxine 2,3,5,6-tetraphenyl-4*H*-pyran-4-one

Figure 2.6 Previously synthesized dioxin derivative (left) and the molecule aimed to be synthesized in this study (right).

2.2 Results and Discussion

2.2.1 Effort to synthesize 2, 3, 4, 5-tetraphenyl-4H-pyran-4-one

As a first try, Lithium diisopropylamide (LDA) as base was employed. Except last step in Scheme 2.1, the same reaction scheme was described with 3-pentanone as ketone in the literature.[68] In this procedure, it was expected that starting material , 3-diphenylacetone would undergo tandem aldol reaction. Then, product **26** would be oxidized by Swern oxidation to form **26**. However, molecule **26** was not obtained when the Scheme 2.1 was followed. There are two possible reasons for that result. First one is the bulky structure of LDA and the steric effect of LDA can prevent to extract the acidic hydrogens of the ketone. The second possible explanation is that benzylic anion formed after the removal of the acidic hydrogen is stabilized by resonance, which impedes the reaction to proceed with the attack to the electrophilic reagent which is benzaldehyde in that case.

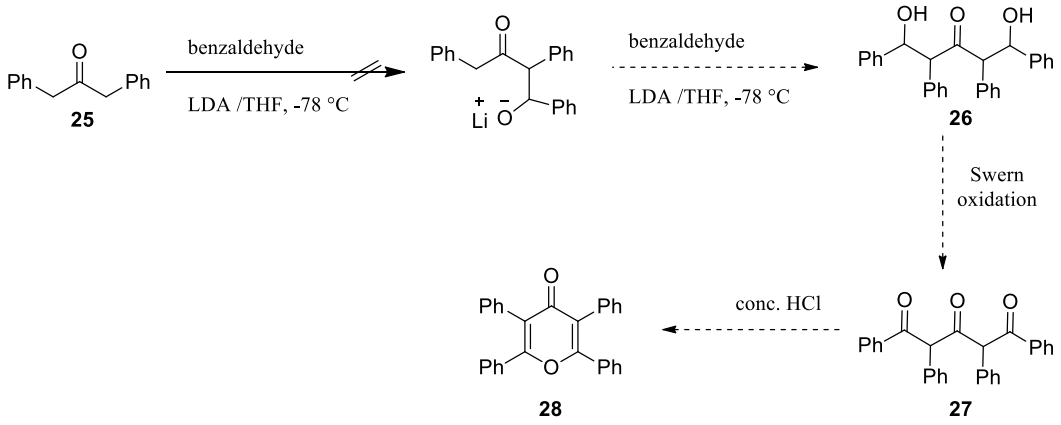

Scheme 2.1 First synthesis attempts for the synthesis of 2,3,4,5-tetraphenyl-4H-pyran-4-one.

Although, there was no similar reaction with benzoyl chloride in the literature, Scheme 2.2 was followed with the freshly prepared benzoyl chloride, but the reaction

did not take place. The reasons for that can be the resonance stabilization of benzylic anion or the reaction between strong bulky base LDA and the benzoyl chloride. Benzoyl chloride is one of the most reactive carbonyl compounds in organic chemistry. Although, LDA is a strong base, it is also a nucleophile and thus it can attack to the carbonyl of benzoyl chloride.

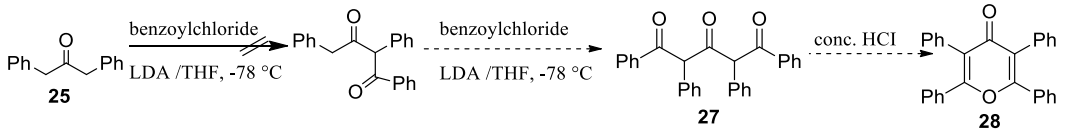

Scheme 2.2 Second synthesis attempt for the synthesis of 2, 3, 4, 5-tetraphenyl-4H-pyran-4-one.

As a third pathway, the reaction sequence in Scheme 2.3 was pursued. There was no exact reaction in the literature, but the below pathway was inspired by the following articles.[69,70] Although, the reaction conditions by playing the parameters were varied. The aimed product **27** could not be synthesized. Reaction time was extended, up to 3 days, two different electrophilic carbonyl compounds were employed, but the result was the same for all. The first reason can be thought easily as the loss of NaH activity. With time, NaH absorbs water in humid air and converts into NaOH along with H_2 gas release. However, this explanation for the negative result is eliminated, because NaH was fresh. The second reason is the unusual stability of benzylic anion after the extraction of acidic hydrogen in 1,3-diphenylacetone. Moreover, it is the best explanation which can be done for this result.

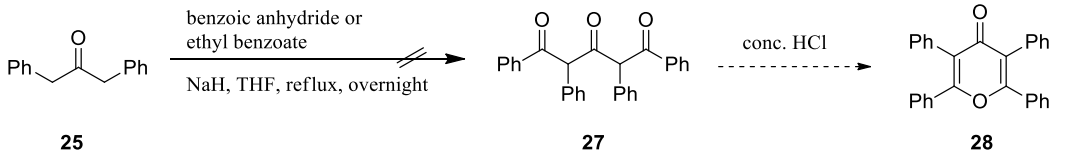

Scheme 2.3 Third synthesis attempt for the synthesis of 2,3,4,5-tetraphenyl-4H-pyran-4-one.

After above effort, Scheme 2.4 was followed as a start of fourth attempt. This pathway was inspired by the following article.[71] In this article, Singh & Bhardwaj extracted acidic hydrogen of deoxybenzoin with sodium hydroxide and could achieve aldol reaction with benzaldehyde in ethanol: water (1:2) solvent system. A similar reaction condition was established to obtain **26**. However, since the ketone is different and bis-aldol reaction is required to get **26**, reaction time and equivalency of the reactant aldehyde were increased. The product was obtained, but it has some unusual properties. **26** does not dissolve in common polar and nonpolar solvents such as in water, methanol, and DCM. Actually, work-up procedure was performed by washing the solid precipitate on filter paper by cold DCM. This lower solubility can be attributed to intramolecular H-bonding.

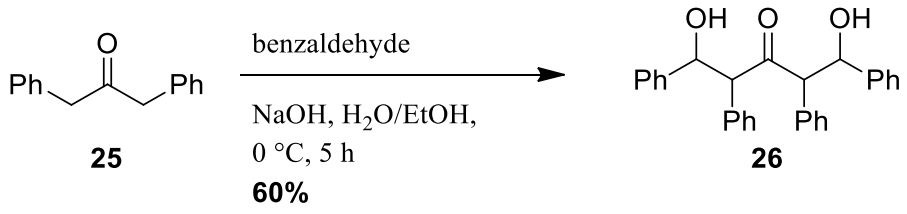

Scheme 2.4 Synthesis of 26.

The characterization of **26** was done with ^{1}H NMR, ^{13}C NMR, IR and HRMS. Figure 2.7 indicates the ^{1}H NMR spectrum of **26**. Except the peak at 7.34 ppm, the other peaks are as expected. The additional peak can be due to the intramolecular H bonding.

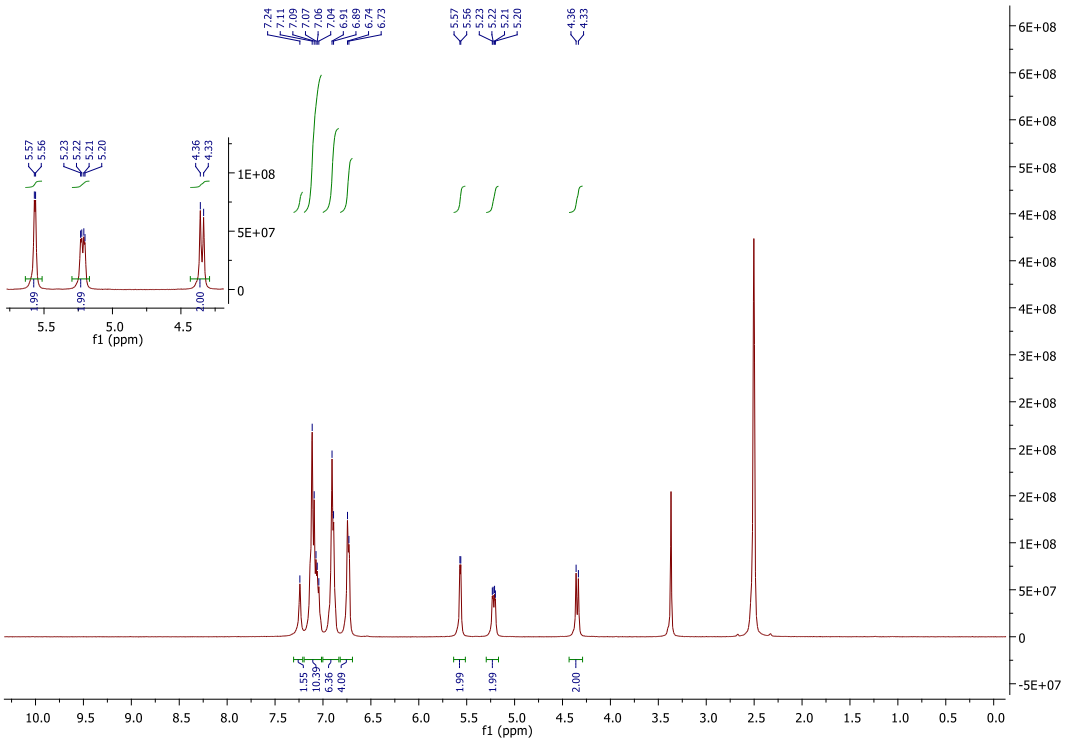

Figure 2.7 ^{1}H NMR spectrum of 26.

To prove that additional peak at 7.34 ppm is due to intermolecular H bonding and peak around 5.57 ppm belongs to hydroxyl groups, ^{1}H NMR analysis of the substance in deuterated methanol was performed, these peaks were cleared away as expected. The Figure 2.8 indicates this spectrum.

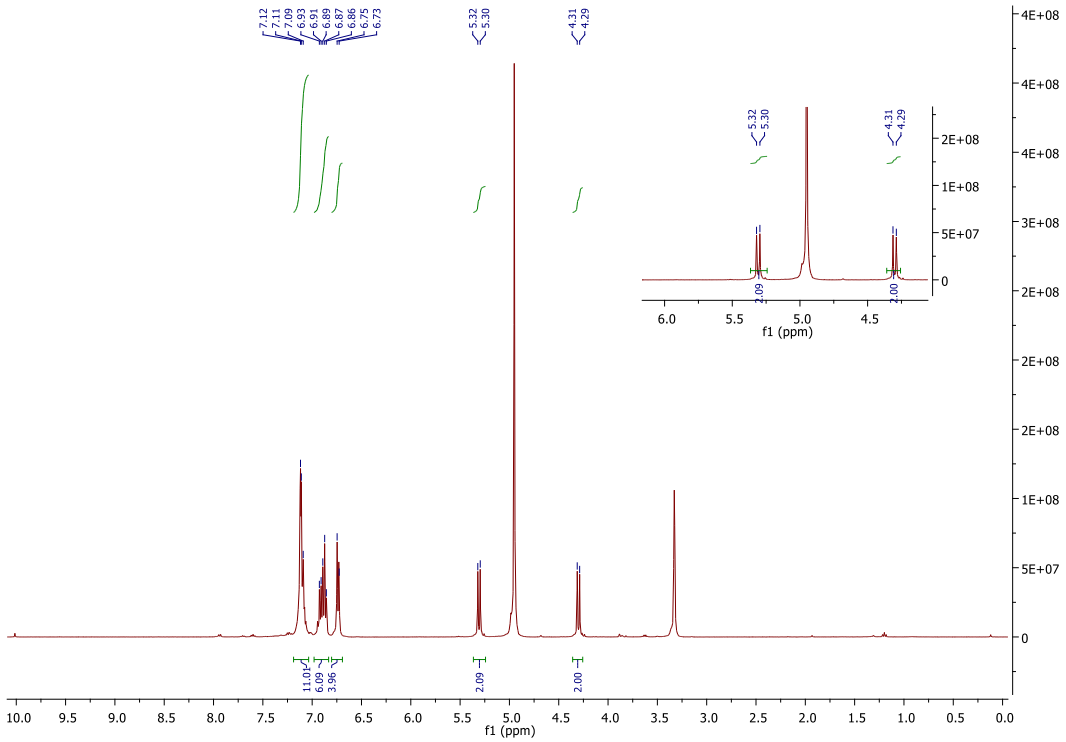

Figure 2.8 ^{1}H NMR spectrum of 26 in deuterated methanol.

Figure 2.9 indicates ^{13}C NMR spectrum of **26**, and it is as expected. In order to confirm the existence of hydroxyl group and carbonyl group, IR measurement was performed, and Figure 2.10 shows the IR spectrum of molecule **26**. Broad peak around 3300 wavenumber and peak around 1700 wavenumber prove the presence of hydroxyl group and carbonyl group, respectively. Moreover, there are two peaks around 2900 and 2800 wavenumbers, and these peaks are due to benzylic C-H stretching.

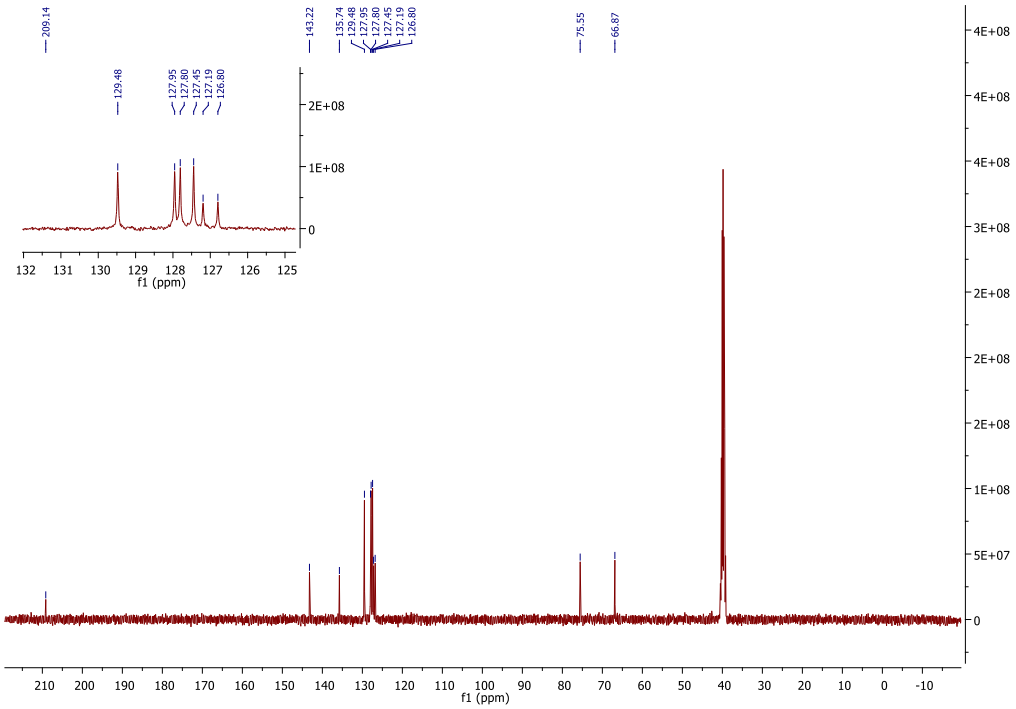

Figure 2.9 ^{13}C NMR spectrum of 26.

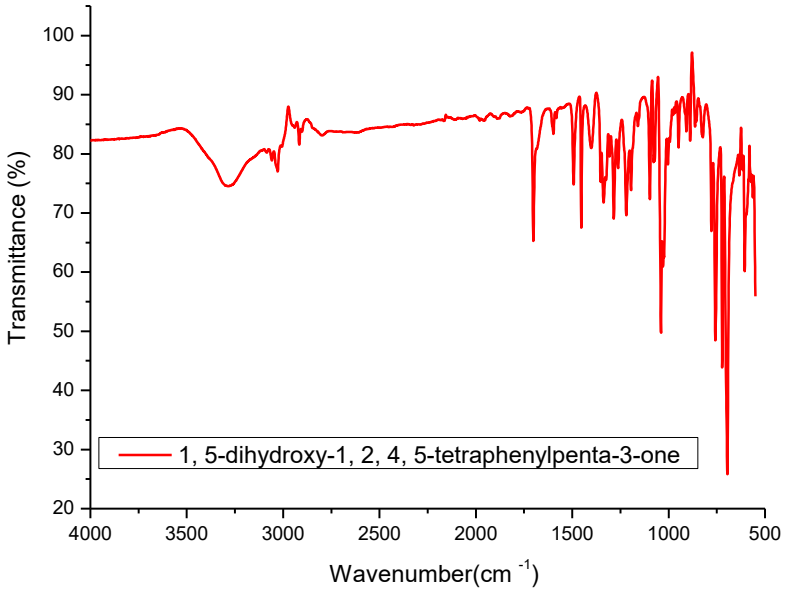

Figure 2.10 IR spectrum of 26.

However, HRMS result presented in Figure 2.11 does not show the expected molecular ion peak. The molecular weight of **26** is 422.51 g per mol. Its molecular ion peak was expected to be 423.51, but the closest peak observed in the spectrum is 419.27 which is four protons less than expected. There is no explanation for that. Although, ^{1}H NMR, ^{13}C NMR and IR results are as guessed, HRMS result does not support the expected result.

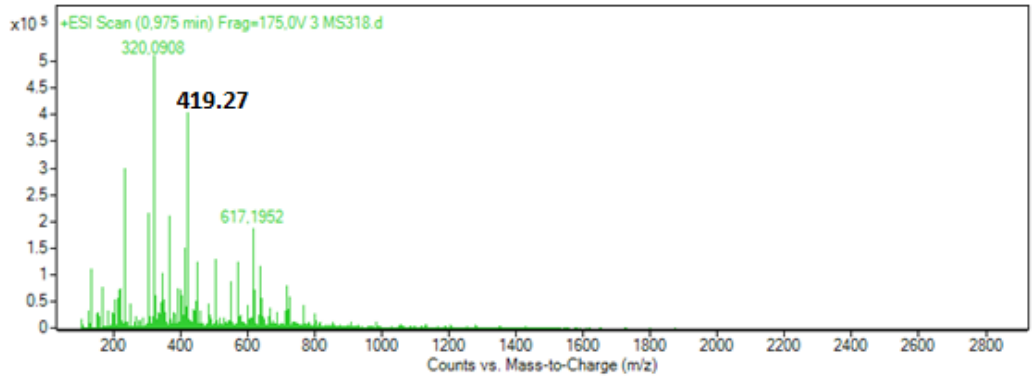

Figure 2.11 HRMS spectrum of 26.

Meanwhile, 1,3-diphenylacetone derivatives as shown in Figure 2.12 were synthesized based on the literature.[72–74] The aim was to synthesize the derivatives of 2,3,4,5-tetraphenyl-4H-pyran-4-one and explore the functional group effect on the spectroscopic properties of 2,3,4,5-tetraphenyl-4H-pyran-4-one molecule.

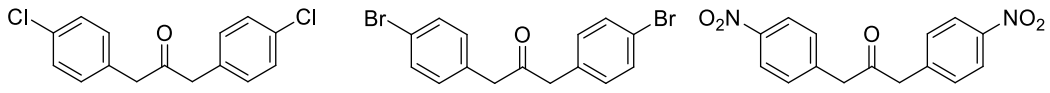

29 **30** **31**

Figure 2.12 Synthesized 1, 3-diphenylacetone derivatives.

Since ^{1}H NMR, ^{13}C NMR and IR spectrums satisfy the expectance. Various oxidation methods were employed to oxidize molecule **26** to the molecule **27** as presented in Scheme 2.5. Although, trichloroisocyanuric/TEMPO oxidation[75–77] and oxidation with activated manganese dioxide,[78–80] copper chloride,[81] pyridinium dichromate (PDC) and pyridinium chlorochromate (PCC)[82] were performed, the oxidation of molecule **26** to **27** was not achieved.

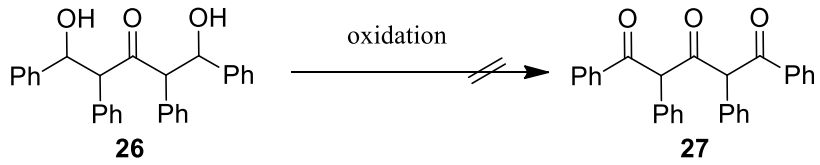

26 **27**

Scheme 2.5 Oxidation of 26 to 27.

As a final alternative, Jones reagent was used as a stronger oxidizer to oxidize **26** to **27**. It was observed that **27** was obtained based on IR, ^{1}H and ^{13}C NMR spectrums. Then, cyclization of **27** was achieved with concentrated H_2SO_4.[83,84] Molecule **28** was also characterized via IR, ^{1}H and ^{13}C NMR. Scheme 2.6 indicates the total synthesis of **28**.

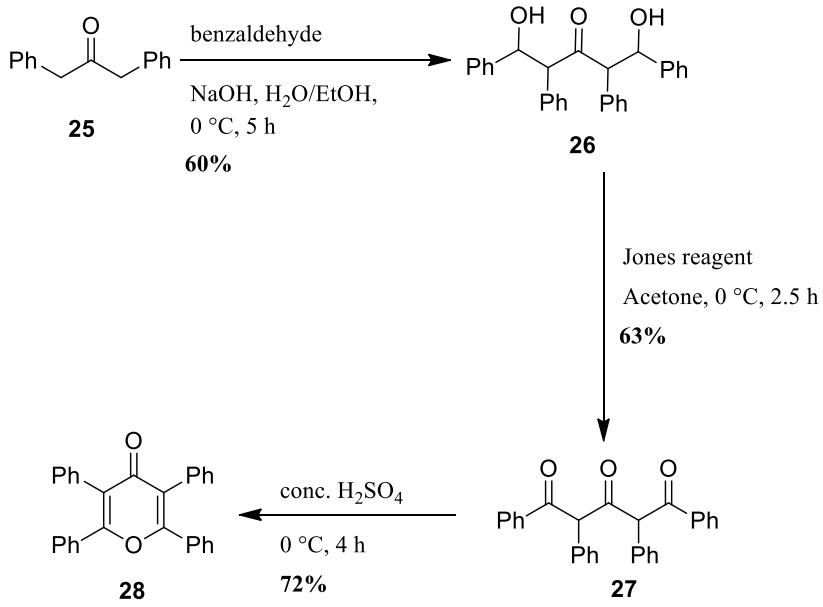

25 **26** **28** **27**

Scheme 2.6 Fourth synthesis attempt for the synthesis of 2, 3, 4, 5-tetraphenyl-4H-pyran-4-one.

Figure 2.13 indicates ^{1}H spectrum of **27**. The singlet peak at 6.0 ppm confers the benzylic hydrogens on **27** and the rest of the peaks belong to the phenylic hydrogens.

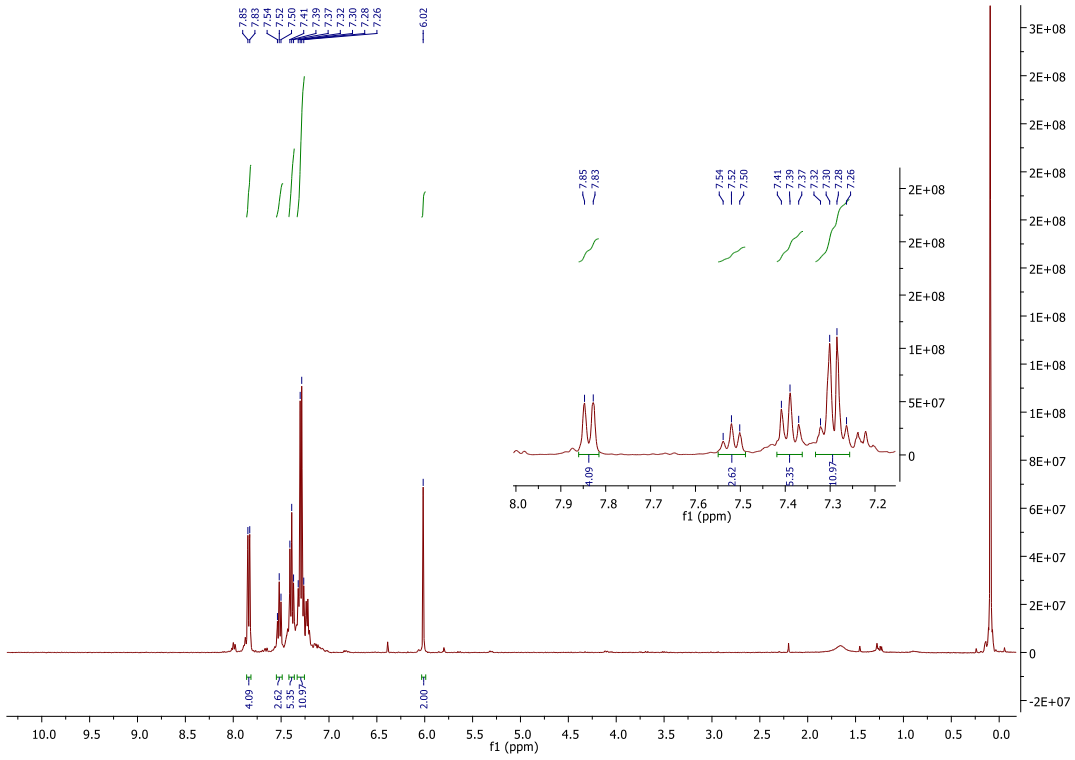

Figure 2.13 ^{1}H NMR spectrum of 27.

Also, ^{13}C NMR spectrum of **27** was presented in Figure 2.14, and it shows the existence of two different carbonyl carbons, which is crucial for the characterization of the molecule.

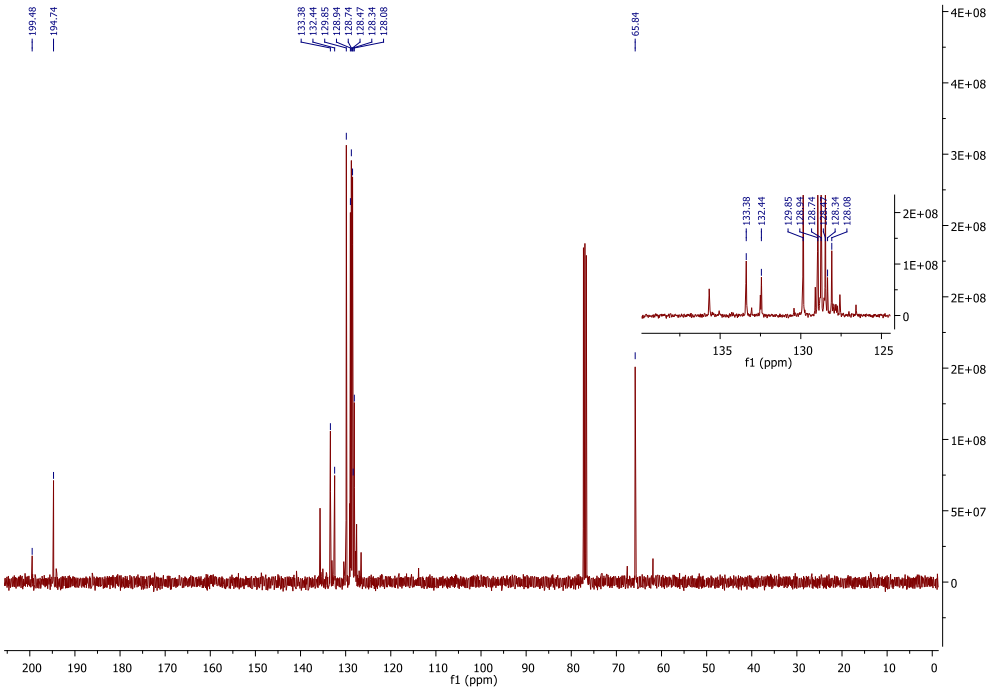

Figure 2.14 ^{13}C NMR spectrum of 27.

^{1}H NMR spectrum of **28** presented in Figure 2.15 does not give critical information about the molecule, but presence of all peaks in aromatic region and clearance of peak at 6.0 ppm imply that cyclization of **27** took place.

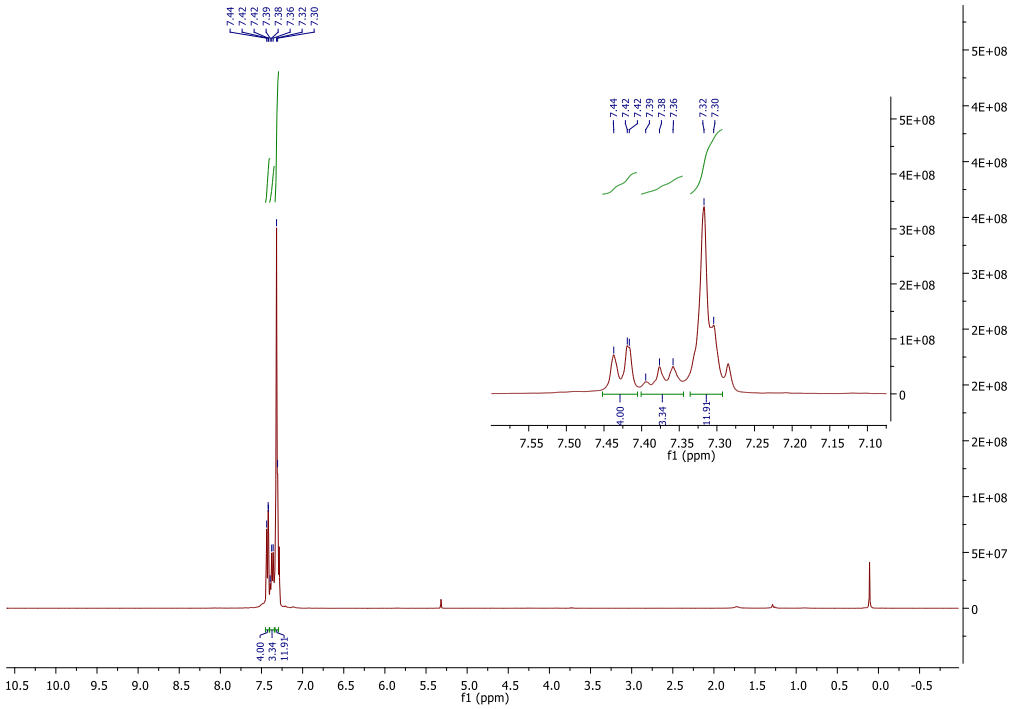

Figure 2.15 ^{1}H NMR spectrum of 28.

^{13}C NMR spectrum of **28** is significant to confirm the structure. Figure 2.16 indicates ^{13}C NMR spectrum of **28**. The peak around 180 ppm indicates the carbonyl carbon in the structure. In the literature, the peak around 160 ppm for another pyranone derivative was assigned for core carbon attached to oxygen atom. Thus, it was also observed in ^{13}C NMR of **28** as in the literature.[84] Hence, ^{13}C NMR of **28** was as expected and shows the formation of **28**.

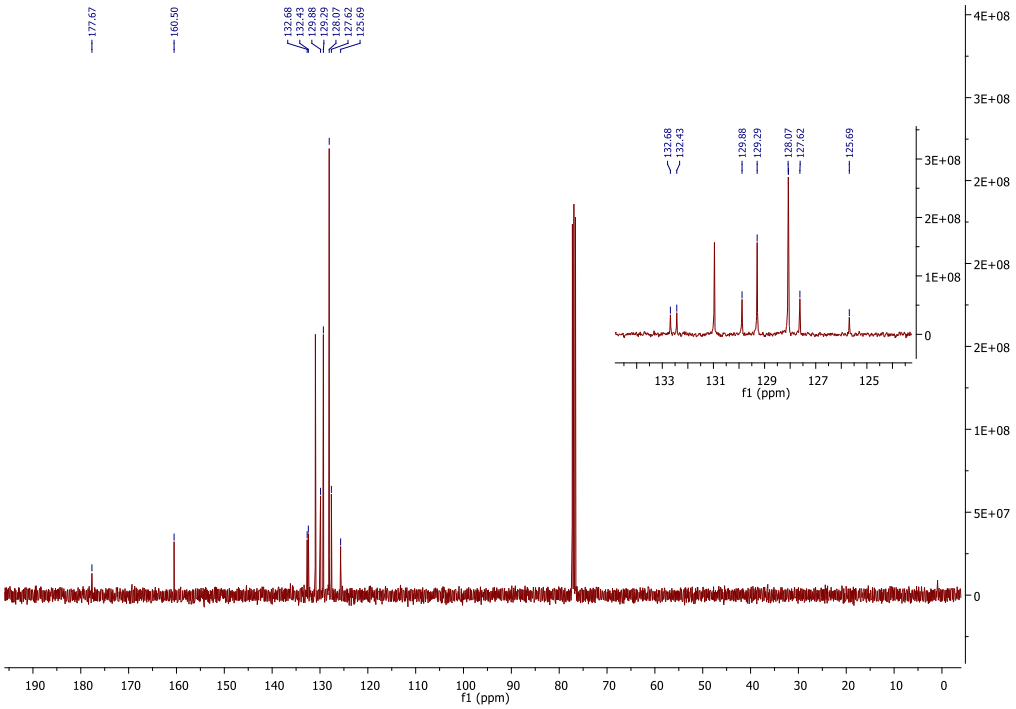

Figure 2.16 ^{13}C NMR spectrum of 28.

2.2.1.1 Fluorescence spectrum of 2, 3, 4, 5-tetraphenyl-4H-pyran-4-one (28)

After the synthesis of **28**, its fluorescence spectrum was obtained to determine whether it shows ACQ or AIE property. Absorption maximum of **28** is 260 nm in THF based on UV spectrum presented in Appendix C. Emission maximum is 307 nm in THF, although it is shifted as water percentage increases. Moreover, the concentration of all solutions is 10 μM. Fluorescence spectra were collected with 5 nm excitation and emission slit with at 800 V for all samples. Figure 2.17 indicates the fluorescence spectrum with varying water: THF fractions.

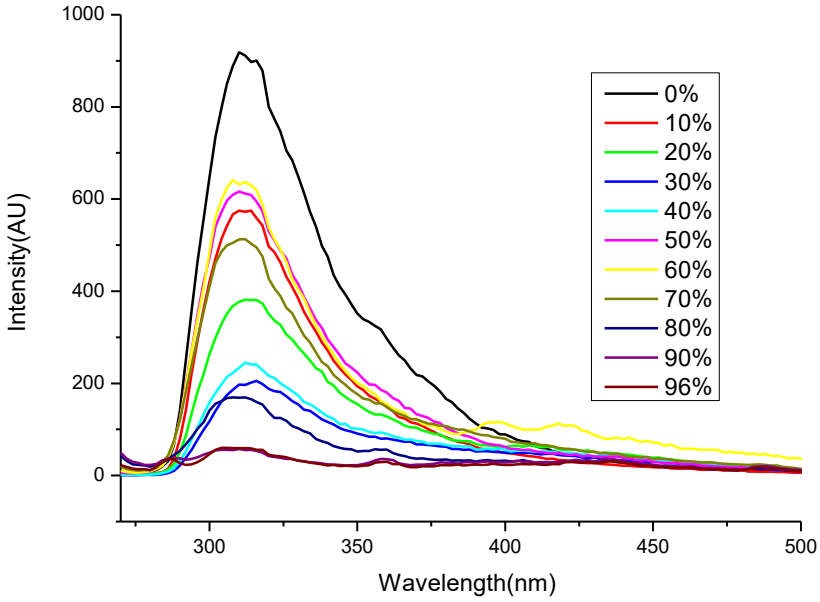

Figure 2.17 Fluorescence spectrum of 28 with varying water %.

As it can be seen in Figure 2.17, signal of solutions with 0-30% water decreases regularly, then signal of solutions with 40%, 50% and 60% water fraction increases, fluorescence intensity decreases again in the rest of the solutions. Normally, it was expected that signal of solutions would decrease or increase regularly depending on ACQ or AIE property. However, this is not the case in above figure. The reason for that can be the pipetting error in the preparation of solutions.

2.2.2 Synthesis of 2, 3, 4, 5-tetraphenyl-4H-pyran-4-one in the literature

2,3,4,5-tetraphenyl-4H-pyran-4-one(**28**) was synthesized in the literature as seen in Scheme 2.7.[85] The product was obtained with 8.5% yield and it was purified with repetitive recrystallization of the crude product by using ethanol:DCM solvent system (0.95:0.05).In the article, it was stated that the substance did not dissolve in hot ethanol:DCM solvent system (0.95:0.05). Moreover, the product was characterized with IR, elemental analysis and melting point determination methods. Based on the article, the product has melting point of 284-286 °C.

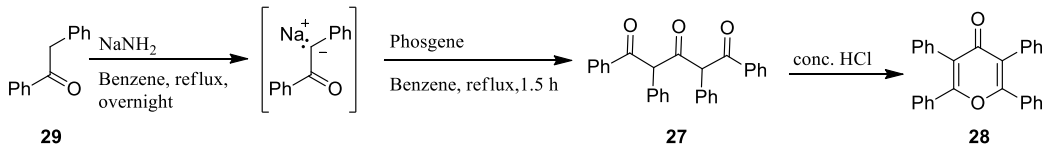

29 27 28

Scheme 2.7 The synthesis of 2, 3, 4, 5-tetraphenyl-4H-pyran-4-one in the literature.

In this study, a similar path as shown in Scheme 2.8 was followed as a last try. Moreover, a white product was obtained after column chromatography (EtOAc:Hex (1:3)) as described in the literature. However, IR spectrum and ^{13}C NMR do not confer the existence of ketone group on the structure. There are two options in that case. Although, the reaction scheme is quite plausible, the characterization methods are poor and thus the product could not be obtained as in the article. Also, several different products can be produced in this reaction and they could obtain one of these, and thus they interpreted the results erroneously. Moreover, the scale of the reaction in the article is 10 g, and the yield is quite low (8.5%). Therefore, it is possible that the product was formed, but it was too low to detect in this case.

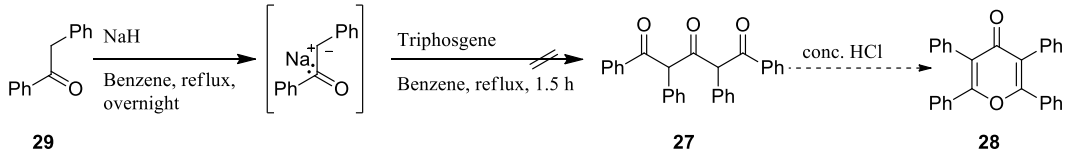

29 27 28

Scheme 2.8 The synthesis of 2,3,4,5-tetraphenyl-4H-pyran-4-one in this study.

2.2.3 Conclusion

In this part of the study, various attempts to propose an alternative synthesis pathway to the literature for 2,3,4,5-tetraphenyl-4H-pyran-4-one (**28**) were performed. The fourth attempt includes the conversion of **25** to **26**, oxidation of **26** to **27** and cyclization of **27** to obtain **28**. Based on ^{1}H NMR, ^{13}C NMR and IR results, it seems that **26**, **27** and **28** were synthesized successfully. Since the plan presented in Scheme

2.6 proceeded successfully, the fluorometric study was also performed. It was observed that 2,3,4,5-tetraphenyl-4H-pyran-4-one (**28**) indicates ACQ property. Moreover, the new synthesis pathway enables to synthesize derivatives of 2,3,4,5-tetraphenyl-4H-pyran-4-one (**28**). For this purpose, derivatives of 1,3-diphenylacetone (**25**) were synthesized. These derivatives are **29**, **30** and **31** and they would undergo bis aldol reaction with various benzaldehyde derivatives to synthesize derivatives of **28**. Therefore, as a future work, the derivatives of 2,3,4,5-tetraphenyl-4H-pyran-4-one would be synthesized by chasing the reaction path presented in Scheme 2.6. Additionally, XRD data would be obtained for **28**.

2.3 Experimental

2.3.1 Materials and Methods

Commercial amino acids were supplied from Chem-Impex International Inc. Common used solvents such as DCM, MeCN, THF, Et_2O, DMF, ethanol and methanol were obtained from Merck. Solvents such as EtOAC, hexane and DCM employed to perform column chromatography were technical grade and they were dried with calcium chloride in distillation system.

Starting materials were obtained from commercial sources and they were used without further purification.

Deuterated solvents were provided by Merck.

Column chromatography purifications were performed with Merck Silica gel 60 (0.063-0.20 mm)

Nuclear Magnetic Spectrum of molecules obtained on Bruker Spectrospin Advance DPX 400 spectrometer. Chemical shifts were presented in parts per million (ppm) and TMS was utilized as internal standard.

The progress of the reactions was traced with TLC plates which were purchased from Merck. TLC plates were coated with silica gel and contain F254 fluorescent indicator which enables the visualization at 254 nm.

HRMS data were collected with Agilent 6224.

FT-IR measurements were done in Thermo Scientific Nicolet is10 instrument.

UV spectrum was collected via Agilent Technologies Cary 8454 UV-Vis spectrometer.

Fluorescence spectrum was obtained by using Agilent Technologies Cary Eclipse Fluorescence Spectrophotometer.

2.3.2 Synthesis of 1, 5-dihydroxy-1, 2, 4, 5-tetraphenylpenta-3-one (26)

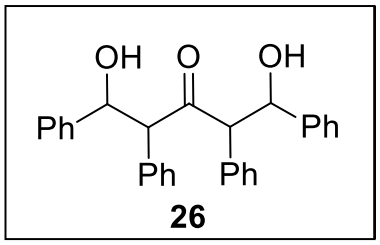

26

NaOH (8 equivalent, 38.0 mmol, and 1.52 g) in 7.5 mL ethanol-water (1:2) was cooled in ice bath. Then, 1,3-diphenylacetone (1.00 g, 4.75 mmol) was added. 3 minutes later, benzaldehyde (5 equivalent, 23.8 mmol) was added. The reaction mixture was stirred for 5 h. Then, the product was filtered and washed with excess, cold DCM. The product was obtained with 60% yield.[71]

^{1}H NMR (400 MHz, DMSO) δ 7.08 (m, 10H), 6.98 – 6.85 (m, 6H), 6.74 (d, J = 7.5 Hz, 4H), 5.57 (d, J = 3.6 Hz, 2H), 5.22 (dd, J = 9.4, 3.4 Hz, 2H), 4.35 (d, J = 9.6 Hz, 2H).

^{13}C NMR (101 MHz, DMSO) δ 209.1, 143.2, 135.7, 129.5, 128.0, 127.8, 127.5, 127.2, 126.8, 75.6, 66.9.

2.3.3 Synthesis of 1,2,4,5-tetraphenylpentane-1,3,5-trione (27)

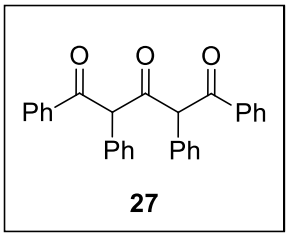

27

2.67 M Jones reagent was prepared as follows. 2.67 g CrO_3 was dissolved in 3.0 mL water, 2.3 mL concentrated H_2SO_4 was added to this solution and solution was diluted to 10 mL to obtain 2.67 M Jones reagent. 1,5-dihydroxy-1,2,4,5-tetraphenylpentan-3-one (**26**) (200.0 mg, 0.4730 mmol) was dissolved in 5 mL acetone and cooled to 0 °C in ice bath. Jones reagent (2.88 equivalent) was added dropwise in 30 minutes. Reaction was maintained for additional 2 h at 0 °C. At the end of the reaction, 10 mL of isopropyl alcohol was added to deactivate Jones reagent. Then, ether extraction was performed twice, then

organic fractions were collected and washed with water and $NaHSO_4$, respectively. Organic phase was dried over Na_2SO_4 and evaporated under reduced pressure. The product was recrystallized with EtOH:DCM (90:10) solvent system. White colored **27** was obtained with 63% yield.

^{1}H NMR (400 MHz, $CDCl_3$) δ 7.88-7.81 (m, 4H), 7.56-7.49 (m, 2H), 7.42-7.35 (m, 5H), 7.33-7.24 (m, 9H), 6.02 (s, 2H).

^{13}C NMR (101 MHz, $CDCl_3$) δ 199.5, 194.7, 133.4, 132.4, 129.9, 128.9, 128.7, 128.5, 128.3, 128.1, 65.8.

2.3.4 Synthesis of 2,3,5,6-tetraphenyl-4H-pyran-4-one (28)

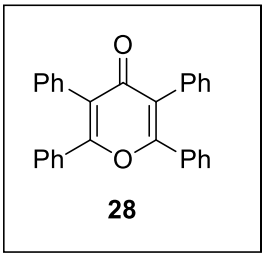

28

1,2,4,5-tetraphenylpentane-1,3,5-trione (**27**) (80.0 mg, 0.190 mmol) was added to a reaction vessel and put into ice bath. Ice cooled concentrated H_2SO_4 (300 µL) was added. Reaction mixture was stirred for 4 h at 0 °C. After 4 h, ice cooled water (3.5 mL) was added and then saturated $NaHCO_3$ was added slowly to neutralize H_2SO_4.Then, extraction with DCM was performed, organic fractions were collected, dried with Na_2SO_4 and DCM was removed under vacuum. The product was recrystallized with EtOH: DCM (90:10) solvent system. White colored 28 was obtained with 72% yield.

^{1}H NMR (400 MHz, $CDCl_3$) δ 7.45 – 7.40 (m, 4H), 7.40 – 7.34 (m, 4H), 7.31 (d, *J* = 5.1 Hz, 12H).

^{13}C NMR (101 MHz, $CDCl_3$) δ 177.7, 160.5, 132.7, 132.4, 131.0, 129.9, 129.3, 128.1, 127.6, 125.7.

2.3.5 Synthesis of 1, 3-Bis (4-chlorophenyl) propan-2-one (29)

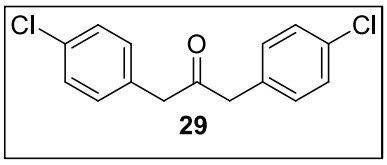

29

4-chlorophenylacetic acid (2.00 g, 14.7 mmol) in dry DCM (80 mL) was added slowly to a solution of DCC (2.80 g, 14.7 mmol) and DMAP (0.45 g, 3.6 mmol) in dry DCM, the reaction mixture was stirred for 4 h at room temperature. After the completion of reaction time, the urea portion was filtered on celite and solvent was removed under reduced pressure. The product was purified via column chromatography with DCM only. The product obtained with 62% yield.[72]

^{1}H NMR (400 MHz, $CDCl_3$) δ 7.34 – 7.30 (m, 4H), 7.10 (d, *J* = 8.4 Hz, 4H), 3.72 (s, 4H).

^{13}C NMR (101 MHz, $CDCl_3$) δ 204.3, 133.1, 132.0, 130.7, 128.8, 48.3.

2.3.6 Synthesis of 1, 3-Bis (4-bromophenyl) propan-2-one (30)

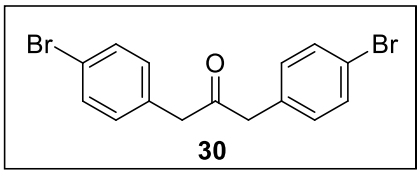

30

DCC (2.28 g, 11.0 mmol), DMAP (369 mg, 3.00 mmol) and dry dichloromethane (21 mL) was dissolved. 4-bromophenyl acetic acid (2.15 g, 10.0 mmol) was dissolved in dry dichloromethane (9 mL), then added dropwise to the previously formed reaction mixture at room temperature. The reaction was stirred overnight, and the urea precipitate was filtered on celite. The filtrate was evaporated under reduced pressure. The crude product was purified via column chromatography with DCM as only eluent.[73]

^{1}H NMR (400 MHz, $CDCl_3$) δ 7.48 – 7.44 (m, 4H), 7.05 – 7.01 (m, 4H), 3.72 – 3.68 (m, 4H).

^{13}C NMR (101 MHz, $CDCl_3$) δ 204.2, 132.6, 131.7, 131.1, 121.1, 48.3.

2.3.7 Synthesis of 1, 3-bis (4-nitrophenyl) propan-2-one (31)

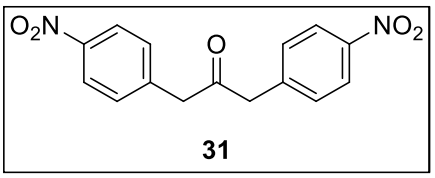

31

Firstly, DCC (1.14 g, 5.50 mmol) and DMAP (0.168 g, 1.38 mmol) was dissolved in dry DCM. To this solution, 1.0 g (5.5 mmol) of 4-nitrophenylacetic acid in dry DCM was added dropwise. The reaction mixture was stirred for 24 h at room temperature. The urea precipitate was filtered on celite. The filtrate was evaporated under vacuum. The crude product was purified via column chromatography with DCM only. The pure yellow product was obtained with 50% yield.[74]

^{1}H NMR (400 MHz, $CDCl_3$) δ 8.23 (d, J = 8.6 Hz, 4H), 7.37 (d, J = 8.6 Hz, 4H), 3.96 (s, 4H)

REFERENCES

1. Carbon | Facts, Uses, & Properties. *Encyclopedia Britannica* https://www.britannica.com/science/carbon-chemical-element.
2. Becker, W. M., Kleinsmith, L. J. & Hardin. *The World of the Cell*. (Pearson Benjamin Cummings, 2006).
3. Falcao, E. H. & Wudl, F. Carbon allotropes: beyond graphite and diamond. *J. Chem. Technol. Biotechnol.* **82**, 524–531 (2007).
4. Karfunkel, H. R. & Dressler, T. New hypothetical carbon allotropes of remarkable stability estimated by MNDO solid-state SCF computations. *J. Am. Chem. Soc.* **114**, 2285–2288 (1992).
5. Karthik, P. S., Himaja, A. L. & Singh, S. P. Carbon-allotropes: synthesis methods, applications and future perspectives. *Carbon Lett.* **15**, 219–237 (2014).
6. He, H., Sekine, T. & Kobayashi, T. Direct transformation of cubic diamond to hexagonal diamond. *Appl. Phys. Lett.* **81**, 610–612 (2002).
7. Vaughan, D. J. Graphite to Graphene: From a Mineral to an Advanced Technological Material. *Elements* **15**, 215–216 (2019).
8. Li, Z. Q., Lu, C. J., Xia, Z. P., Zhou, Y. & Luo, Z. X-ray diffraction patterns of graphite and turbostratic carbon. *Carbon* **45**, 1686–1695 (2007).
9. Henning, T. & Salama, F. Carbon in the Universe. *Science* **282**, 2204–2210 (1998).

10. Tiwari, S. K. *et al.* Magical Allotropes of Carbon: Prospects and Applications. *Crit. Rev. Solid State Mater.* **41**, 257–317 (2016).
11. Iijima, S. Helical microtubules of graphitic carbon. *Nature* **354**, 56–58 (1991).
12. Kramer, C. N. *Fullerene Research Advances*. (Nova Publishers, 2007).
13. Kokubo, K., Shirakawa, S., Kobayashi, N., Aoshima, H. & Oshima, T. Facile and scalable synthesis of a highly hydroxylated water-soluble fullerenol as a single nanoparticle. *Nano Res.* **4**, 204–215 (2011).
14. He, H., Zheng, L., Jin, P. & Yang, M. The structural stability of polyhydroxylated C60(OH)24: Density functional theory characterizations. *Comput. Theor. Chem.* **974**, 16–20 (2011).
15. Semenov, K. N., Charykov, N. A. & Keskinov, V. N. Fullerenol Synthesis and Identification. Properties of the Fullerenol Water Solutions. *J. Chem. Eng. Data* **56**, 230–239 (2011).
16. Voet, D., Voet, J. G. & Pratt, C. W. *Fundamentals of Biochemistry: Life at the Molecular Level*. (Wiley, 2008).
17. Breslow, R. *Artificial Enzymes*. (John Wiley & Sons, Ltd, 2005). doi:10.1002/3527606645.
18. Manea, F., Houillon, F. B., Pasquato, L. & Scrimin, P. Nanozymes: Gold-Nanoparticle-Based Transphosphorylation Catalysts. *Angew. Chem.* **116**, 6291–6295 (2004).
19. Huang, Y., Ren, J. & Qu, X. Nanozymes: Classification, Catalytic Mechanisms, Activity Regulation, and Applications. *Chem. Rev.* **119**, 4357–4412 (2019).

20. Wu, J. *et al.* Nanomaterials with enzyme-like characteristics (nanozymes): next-generation artificial enzymes (II). *Chem. Soc. Rev.* **48**, 1004–1076 (2019).
21. Lin, Y., Ren, J. & Qu, X. Catalytically Active Nanomaterials: A Promising Candidate for Artificial Enzymes. *Acc. Chem. Res.* **47**, 1097–1105 (2014).
22. Zhang, Q. *et al.* Artificial hydrolase based on carbon nanotubes conjugated with peptides. *Nanoscale* **8**, 16851–16856 (2016).
23. Song, Y., Qu, K., Zhao, C., Ren, J. & Qu, X. Graphene Oxide: Intrinsic Peroxidase Catalytic Activity and Its Application to Glucose Detection. *Adv. Mater.* **22**, 2206–2210 (2010).
24. T, L. *et al.* Graphite-like carbon nitrides as peroxidase mimetics and their applications to glucose detection. *Biosens Bioelectron* **59**, 89–93 (2014).
25. Hu, Z. *et al.* Photodynamic anticancer activities of water-soluble C(60) derivatives and their biological consequences in a HeLa cell line. *Chem. Biol. Interact.* **195**, 86–94 (2012).
26. Liang, M. & Yan, X. Nanozymes: From New Concepts, Mechanisms, and Standards to Applications. *Acc. Chem. Res.* **52**, 2190–2200 (2019).
27. Liu, B., Sun, Z., Huang, P.-J. J. & Liu, J. Hydrogen Peroxide Displacing DNA from Nanoceria: Mechanism and Detection of Glucose in Serum. *J. Am. Chem. Soc.* **137**, 1290–1295 (2015).
28. Cheng, H. *et al.* Monitoring of Heparin Activity in Live Rats Using Metal–Organic Framework Nanosheets as Peroxidase Mimics. *Anal. Chem.* **89**, 11552–11559 (2017).

29. Vanderlinde, R. E. Measurement of total lactate dehydrogenase activity. *Ann. Clin. Lab. Sci.* **15**, 13–31 (1985).
30. Everse, J. & Kaplan, N. O. Lactate Dehydrogenases: Structure and Function. in *Advances in Enzymology - and Related Areas of Molecular Biology* (ed. Meister, A.) 61–133 (John Wiley & Sons, Inc., 2006).
31. Masterson, J. E. The enzymatic reaction catalyzed by lactate dehydrogenase exhibits one dominant reaction path. *Chem. Phys.* 5 (2014).
32. Di Cera, E. Serine proteases. *IUBMB Life* **61**, 510–515 (2009).
33. Hedstrom, L. Serine Protease Mechanism and Specificity. *Chem. Rev.* **102**, 4501–4524 (2002).
34. Fremout, W. Tryptic cleavage of proteinaceous paint : a high--performance protein binder analytical technique. (Ghent University, 2014).
35. O'Reilly, C. & Turner, P. D. The nitrilase family of CN hydrolysing enzymes - a comparative study. *J. Appl. Microbiol.* **95**, 1161–1174 (2003).
36. Gong, J.-S. *et al.* Nitrilases in nitrile biocatalysis: recent progress and forthcoming research. *Microb. Cell Fact.* **11**, 142 (2012).
37. Howden, A. J. M. & Preston, G. M. Nitrilase enzymes and their role in plant-microbe interactions: Nitrilase enzymes and plant-microbe interactions. *Microb. Biotechnol.* **2**, 441–451 (2009).
38. Biocatalytic hydrolysis of nitriles | SpringerLink. https://link.springer.com/article/10.1134/S2079978011030010.

39. Chaudhuri, P., Paraskar, A., Soni, S., Mashelkar, R. A. & Sengupta, S. Fullerenol−Cytotoxic Conjugates for Cancer Chemotherapy. *ACS Nano* **3**, 2505–2514 (2009).

40. Sakakura, A., Kawajiri, K., Ohkubo, T., Kosugi, Y. & Ishihara, K. Widely Useful DMAP-Catalyzed Esterification under Auxiliary Base- and Solvent-Free Conditions. *J. Am. Chem. Soc.* **129**, 14775–14779 (2007).

41. Wei, W. *et al.* Improved dissolution of cellulose in quaternary ammonium hydroxide by adjusting temperature. *RSC Adv.* **5**, 39080–39083 (2015).

42. Jaramillo, P., Pérez, P. & Fuentealba, P. Relationship between basicity and nucleophilicity. *J. Phys. Org. Chem.* **20**, 1050–1057 (2007).

43. van Schie, M. M. C. H., Paul, C. E., Arends, I. W. C. E. & Hollmann, F. Photoenzymatic epoxidation of styrenes. *Chem. Commun.* **55**, 1790–1792 (2019).

44. Ismail, M. *et al.* Straightforward Regeneration of Reduced Flavin Adenine Dinucleotide Required for Enzymatic Tryptophan Halogenation. *ACS Catal.* **9**, 1389–1395 (2019).

45. Vedpathak, S. G., Momle, R. G., Kakade, G. K. & Ingle, V. S. An Improved and Convenient Route for the Synthesis of 5-methyl-1H-Tetrazol-1-yl Substituted Benzamines. *WJPR* **5**, 10.

46. Tishinov, K., Bayryamov, S., Nedkov, P., Stambolieva, N. & Galunsky, B. A highly enantioselective aminopeptidase from sunflower seed—Kinetic studies, substrate mapping and application to biocatalytic transformations. *J. Mol. Catal., B Enzym.* **59**, 106–110 (2009).

47. Murthy, K. V. R. & Virk, H. S. Luminescence Phenomena: An Introduction. *DDF* **347**, 1–34 (2013).
48. Harvey, E. N. *A History of Luminescence from the Earliest Times Until 1900*. (American Philosophical Society, 1957).
49. Incandescent lamp | lighting. *Encyclopedia Britannica* https://www.britannica.com/technology/incandescent-lamp.
50. Heine, J. & Müller-Buschbaum, K. Engineering metal-based luminescence in coordination polymers and metal–organic frameworks. *Chem. Soc. Rev.* **42**, 9232 (2013).
51. *Luminescence Basic Concepts, Applications and Instrumentation*. (Trans Tech Publications Ltd, 2014).
52. Valeur, B. Molecular Fluorescence Principles and Applications. *Molecular Fluorescence* 399 (2001).
53. Bañares, L. Unexpected intersystem crossing. *Nature Chem.* **11**, 103–104 (2019).
54. *Solid State Luminescence: Theory, materials and devices*. (Springer Netherlands, 1993). doi:10.1007/978-94-011-1522-3.
55. Atkins, P. & De Paula, J. *Atkins' Physical Chemistry*. (Oxford University Press, 2006).
56. Roda, A. *Chemiluminescence and Bioluminescence: Past, Present and Future*. (Royal Society of Chemistry, 2010).
57. Keiter, R. L., Gamage, C. P., & Paul E. Smith. Combustion of white phosphorus. *J. Chem. Educ.* **78**, 908 (2001).

58. Malikova, N. P. *et al.* Green-Fluorescent Protein from the Bioluminescent Jellyfish Clytia gregaria Is an Obligate Dimer and Does Not Form a Stable Complex with the Ca2+-Discharged Photoprotein Clytin. *Biochemistry* **50**, 4232–4241 (2011).

59. Xie, Y. & Li, Z. Triboluminescence: Recalling Interest and New Aspects. *Chem* **4**, 943–971 (2018).

60. Sweeting, L. M. Triboluminescence with and without Air. *Chem. Mater.* **13**, 854–870 (2001).

61. Zink, J. I. Triboluminescence. *Acc. Chem. Res.* **11**, 289–295 (1978).

62. Zhao, Z., Zhang, H., Lam, J. W. Y. & Tang, B. Z. Aggregation-Induced Emission: New Vistas at the Aggregate Level. *Angew. Chem. Int. Ed.* **59**, 9888–9907 (2020).

63. He, Z., Ke, C. & Tang, B. Z. Journey of Aggregation-Induced Emission Research. *ACS Omega* 11 (2018).

64. *Principles and Applications of Aggregation Induced Emission*. (Springer).

65. Luo, J. *et al.* Aggregation-induced emission of 1-methyl-1,2,3,4,5-pentaphenylsilole. *Chem. Commun.* 1740–1741 (2001)

66. Nie, H. *et al.* Tetraphenylfuran: aggregation-induced emission or aggregation-caused quenching? *Mater. Chem. Front.* **1**, 1125–1129 (2017).

67. Hong, Y., Lam, J. W. Y. & Tang, B. Z. Aggregation-induced emission: phenomenon, mechanism and applications. *Chem. Commun.* 4332 (2009)

68. Pratt, N. E., Zhao, Y., Hitchcock, S. & Albizati, K. F. Generation of Polypropionate via Tandem Aldol-Bis-Oxidation Procedure. *Synlett* (1991).

69. Nandurkar, N. S., Bhanushali, M. J., Patil, D. S. & Bhanage, B. M. Synthesis of Sterically Hindered 1,3-Diketones. *Synth. Commun.* **37**, 4111–4115 (2007).

70. Zeng, L., Chen, R., Zhang, C., Xie, H. & Cui, S. Iridium(I)-catalyzed hydration/esterification of 2-alkynylphenols and carboxylic acids. *Chem. Commun.* **56**, 3093–3096 (2020).

71. Singh, P. & Bhardwaj, A. Mono-, Di-, and Triaryl Substituted Tetrahydropyrans as Cyclooxygenase-2 and Tumor Growth Inhibitors. Synthesis and Biological Evaluation. *J. Med. Chem.* **53**, 3707–3717 (2010).

72. Hu, C., Gao, Y. & Du, W. Design, Synthesis, and Biological Evaluation of Pyrazole Derivatives. *Chem. Biol. Drug Des.* **87**, 673–679 (2016).

73. New photo- and electroluminescent conjugated copolyfluorenes with 7,8,10-triarylfluoranthene units in the backbone | SpringerLink. https://link.springer.com/article/10.1134/S1560090412050016.

74. Pal, R., Mukherjee, S., Chandrasekhar, S. & Guru Row, T. N. Exploring Cyclopentadienone Antiaromaticity: Charge Density Studies of Various Tetracyclones. *J. Phys. Chem. A* **118**, 3479–3489 (2014).

75. De Luca, L., Giacomelli, G., Masala, S. & Porcheddu, A. Trichloroisocyanuric/TEMPO Oxidation of Alcohols under Mild Conditions: A Close Investigation. *J. Org. Chem.* **68**, 4999–5001 (2003).

76. De Luca, L., Giacomelli, G. & Porcheddu, A. A Very Mild and Chemoselective Oxidation of Alcohols to Carbonyl Compounds. *Org. Lett.* **3**, 3041–3043 (2001).

77. Dip, I., Gethers, C., Rice, T. & Straub, T. S. A rapid and convenient oxidation of secondary alcohols. *Tetrahedron Lett.* **58**, 2720–2722 (2017).

78. Firouzabadi, H., Karimi, B. & Abbassi, M. Efficient Solvent-free Oxidation of Benzylic and Aromatic Allylic Alcohols and Biaryl Acyloins by Manganese Dioxide and Barium Manganate. *J. Chem. Res. (S)* 236–237 (1999)

79. Hirano, M., Yakabe, S., Chikamori, H., Clark, J. H. & Morimoto, T. Oxidation by Chemical Manganese Dioxide. Part 1. Facile Oxidation of Benzylic Alcohols in Hexane†. *J. Chem. Res.* 308–309 (1998)

80. Hirano, M., Yakabe, S., Chikamori, H., Clark, J. H. & Morimoto, T. Oxidation by Chemical Manganese Dioxide. Part 3.1 Oxidation of Benzylic and Allylic Alcohols, Hydroxyarenes and Aminoarenes. *J. Chem. Res.* 770–771 (1998)

81. Lokhande, P. D., Waghmare, S. R., Gaikwad, H. & Hankare, P. P. Copper Catalyzed Selective Oxidation of Benzyl Alcohol to Benzaldehyde. *J. Korean Chem. Soc.* **56**, 539–541 (2012).

82. Tojo, G. & Fernández, M. Pyridinium Dichromate (PDC) in Dimethylformamide. The Method of Corey and Schmidt. in *Oxidation of Primary Alcohols to Carboxylic Acids* 33–41 (Springer New York, 2006).

83. Harding, K. E., May, L. M. & Dick, K. F. Selective oxidation of allylic alcohols with chromic acid. *J. Org. Chem.* **40**, 1664–1665 (1975).

84. Allwohn, J. *et al.* Synthese und Konformationsanalyse von Pyranophanonen und Pyrylophanium-Verbindungen mit intraannularen Substituenten. *J. Prakt. Chem.* **335**, 503–514 (1993).

85. Yates, Peter. & Weisbach, J. A. 3-Furanones. I. The Yellow Compound of Kleinfeller and Fiesselmann. *J. Am. Chem. Soc.* **85**, 2943–2950 (1963).

APPENDICES

A. NMR SPECTRA

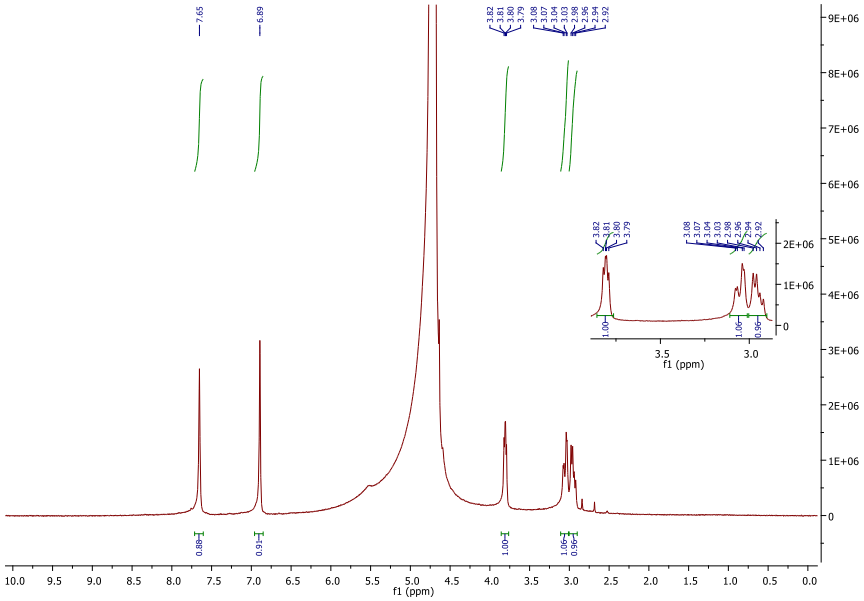

Figure A. 1 ^{1}H NMR spectrum of 4.

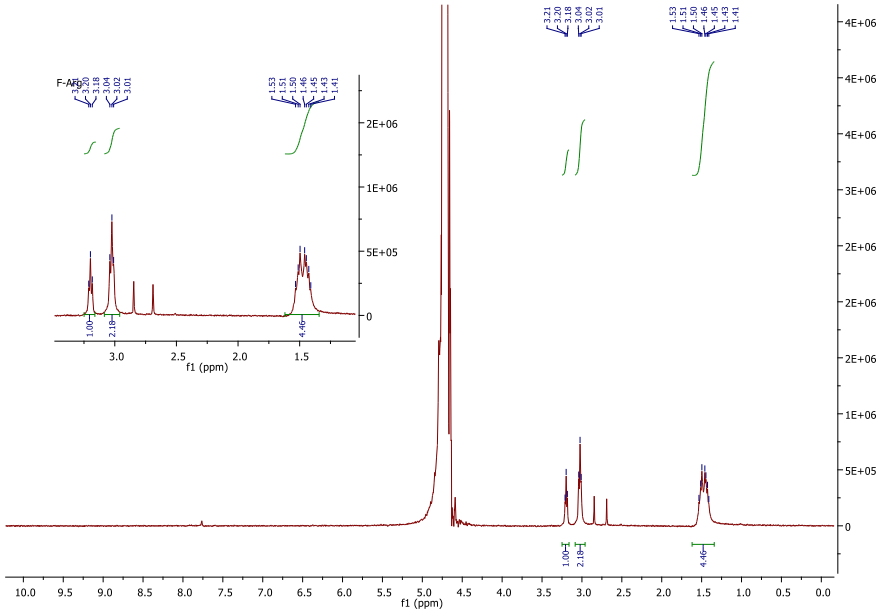

Figure A. 2 ^{1}H NMR spectrum of 5.

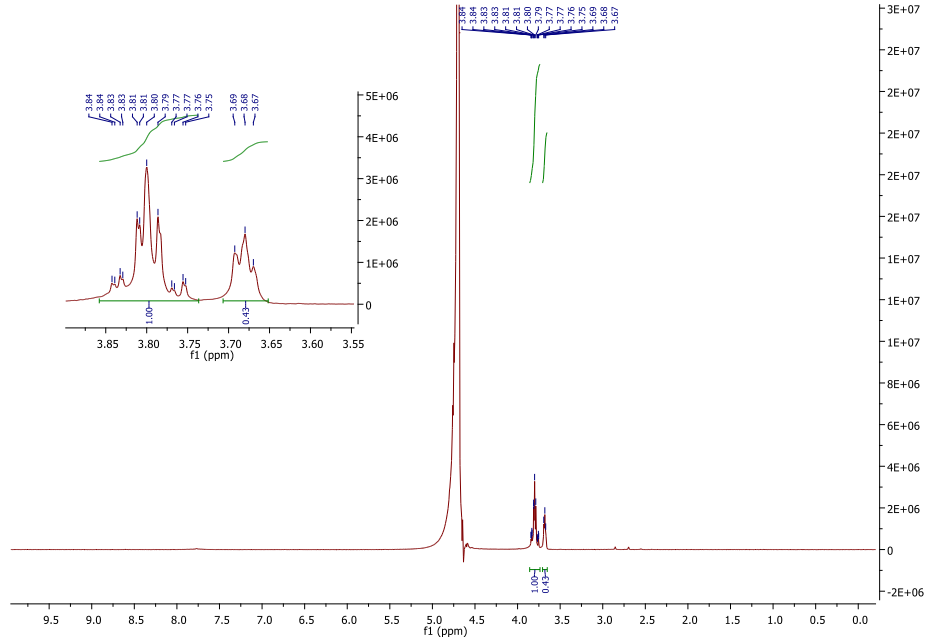

Figure A. 3 [1]H NMR spectrum of 6.

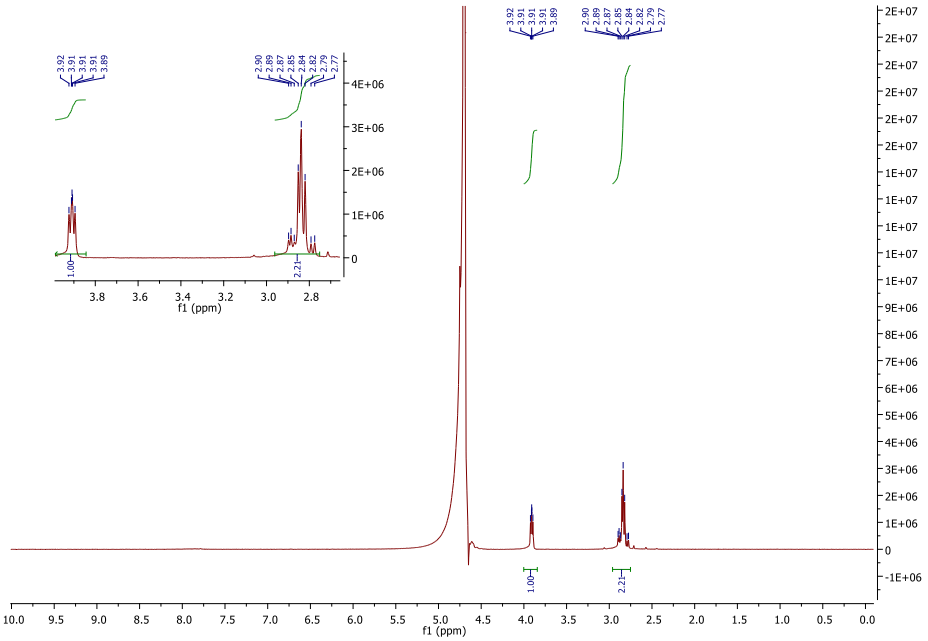

Figure A. 4 [1]H NMR spectrum of 7.

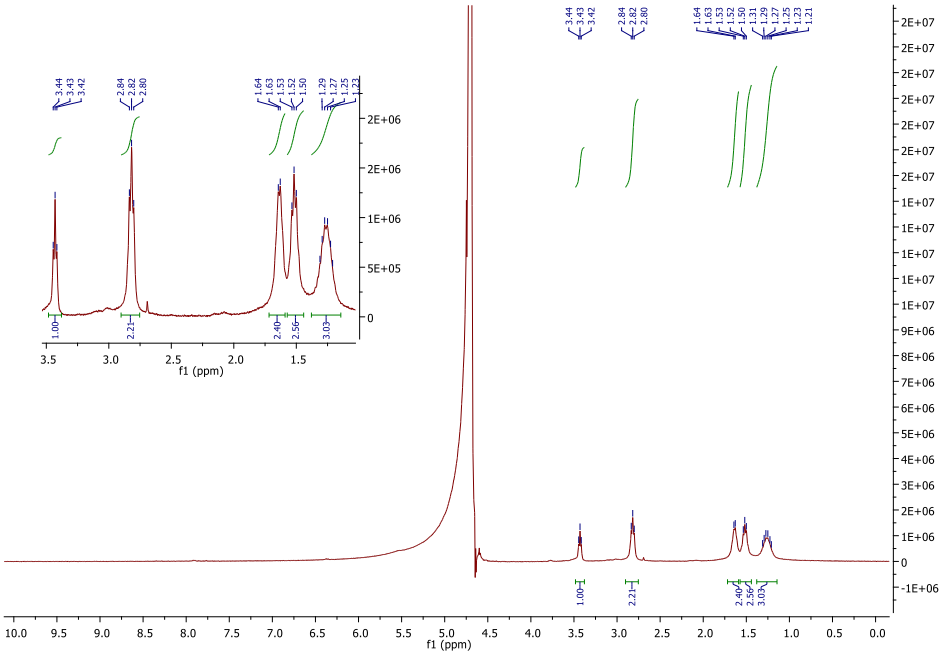

Figure A. 5 ^{1}H NMR spectrum of 8.

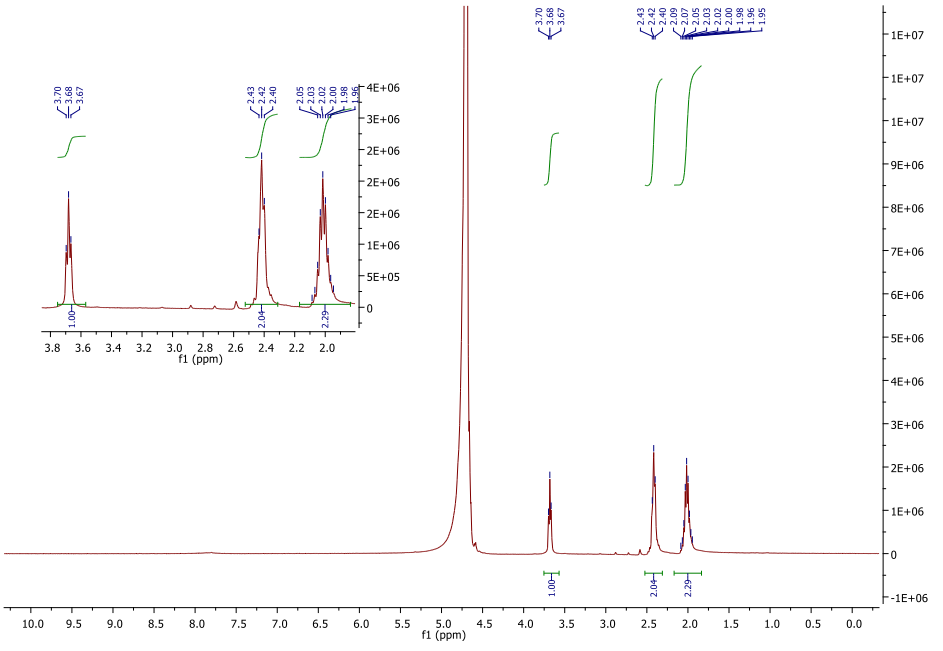

Figure A. 6 ^{1}H NMR spectrum of 9.

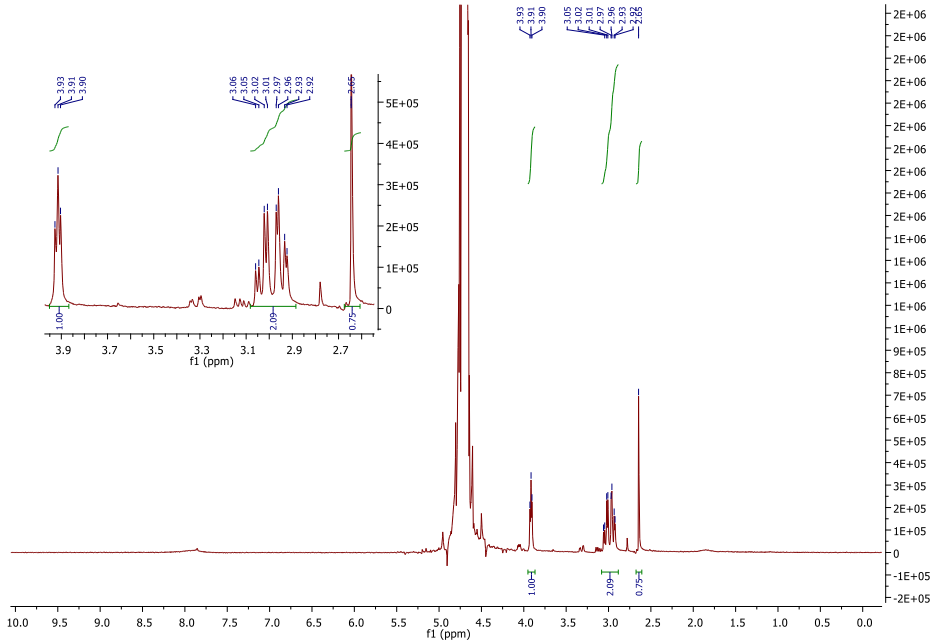

Figure A. 7 ^{1}H NMR spectrum of 10.

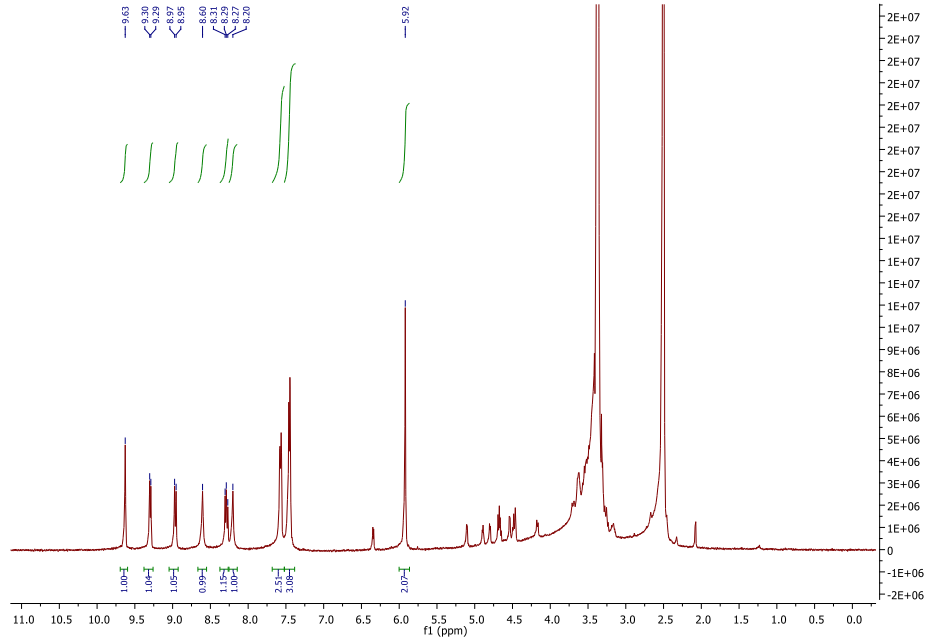

Figure A. 8 ^{1}H NMR spectrum of 12.

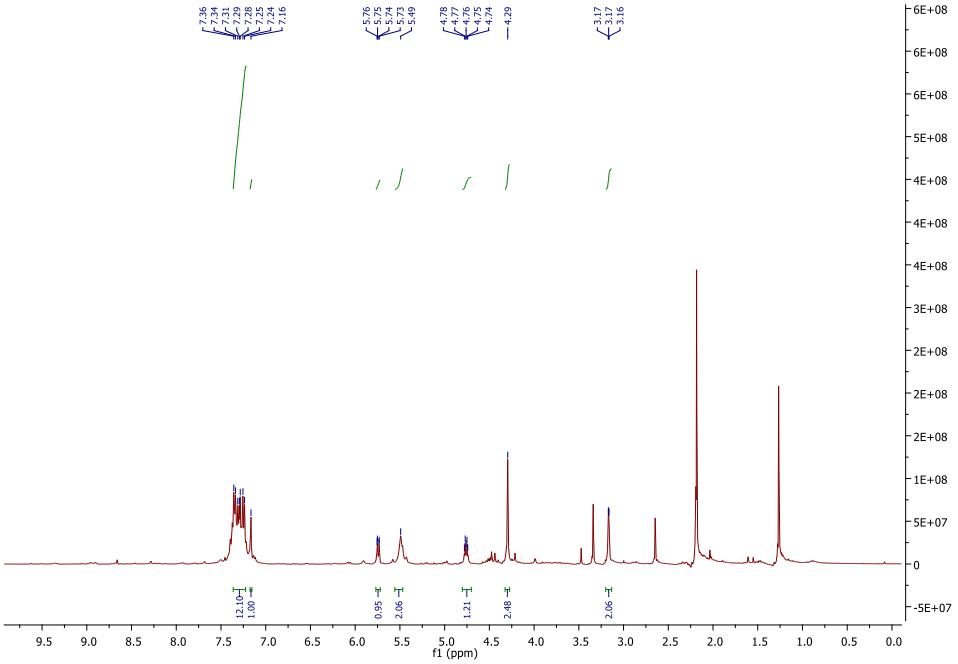

Figure A. 9 ^{1}H NMR spectrum of crude 13.

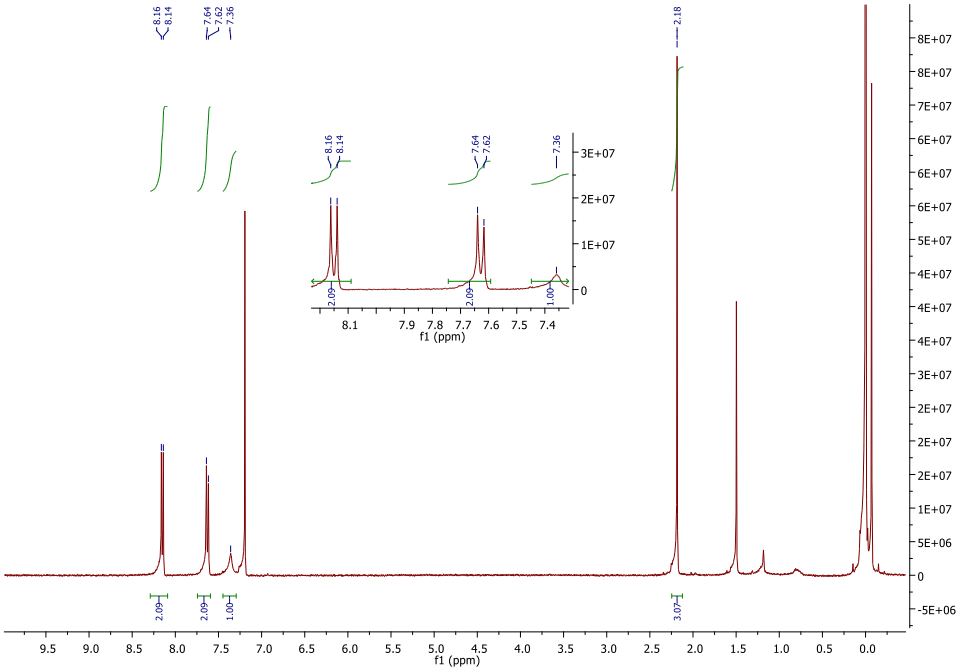

Figure A. 10 ^{1}H NMR spectrum of 17.

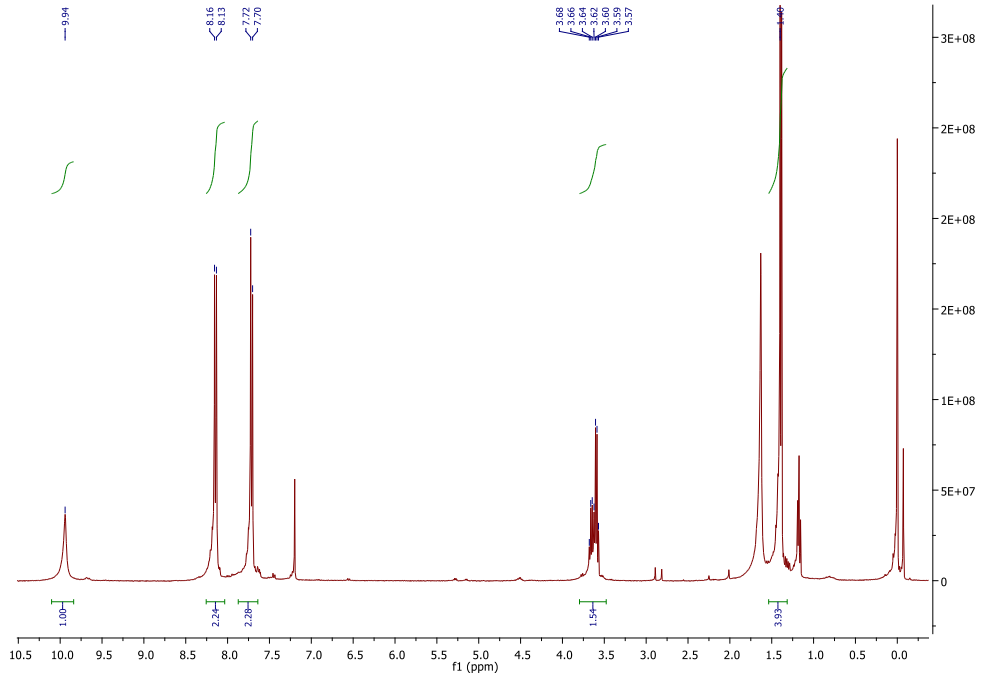

Figure A. 11 ^{1}H NMR spectrum of 20.

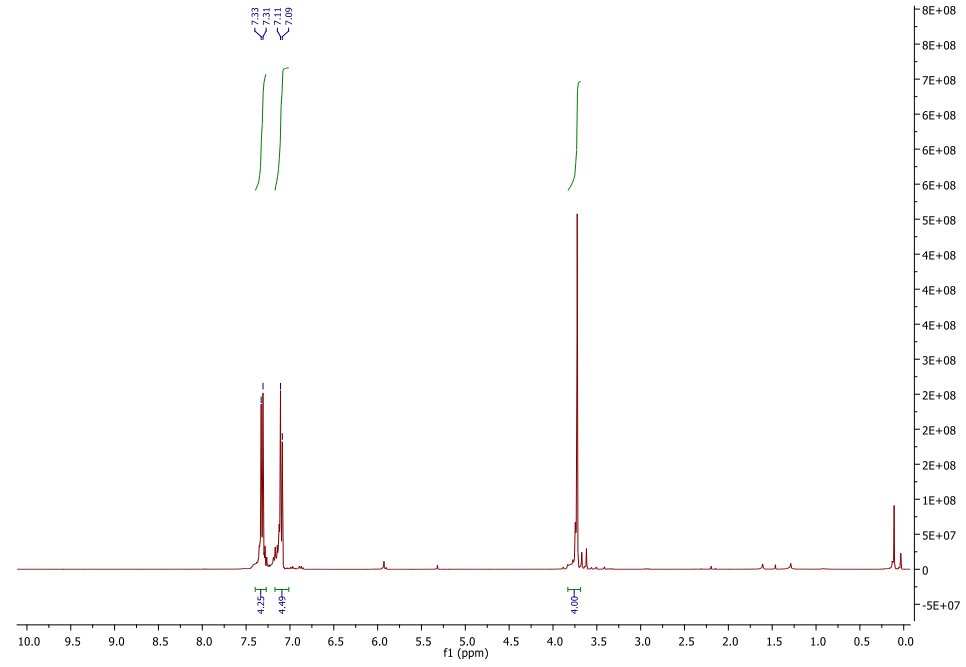

Figure A. 12 ^{1}H NMR spectrum of 29.

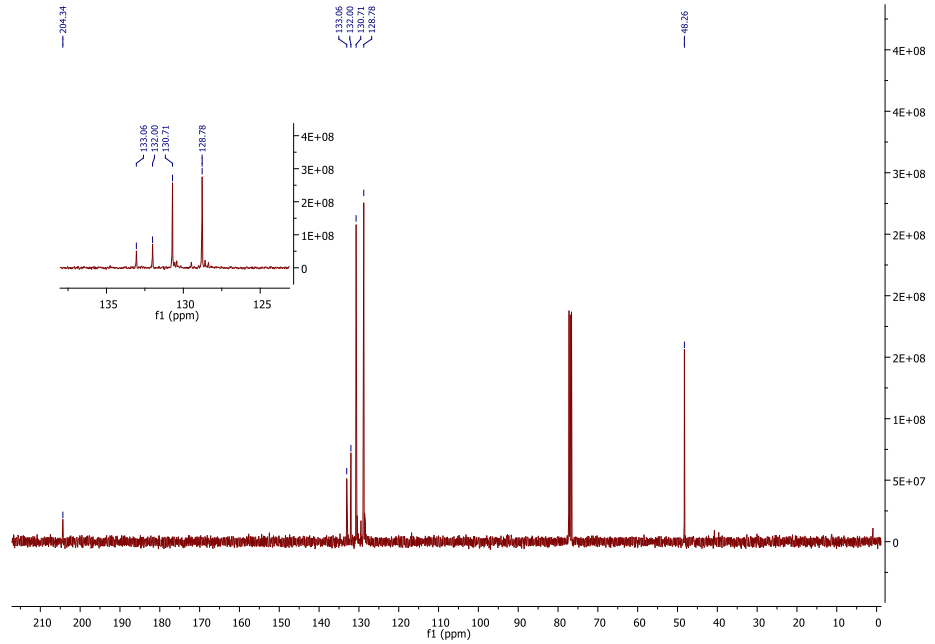

Figure A. 13 ^{13}C NMR spectrum of 29.

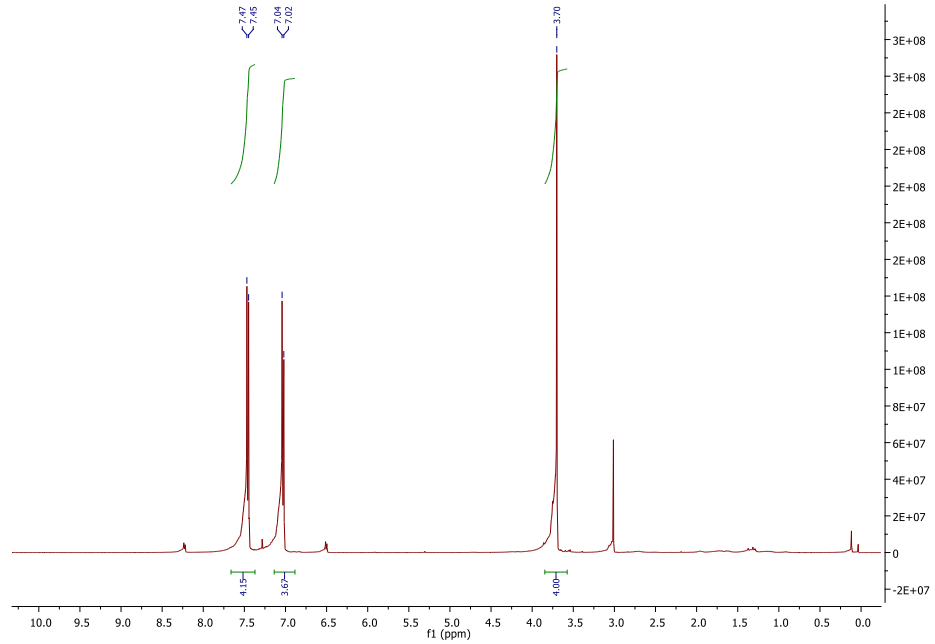

Figure A. 14 ^{1}H NMR spectrum of 30.

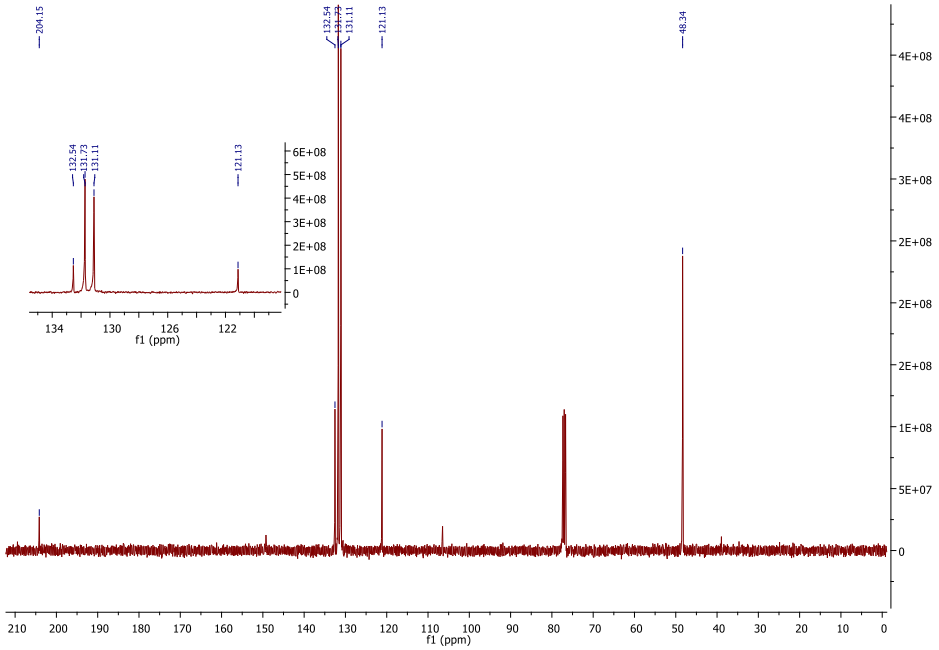

Figure A. 15 ^{13}C NMR spectrum of 30.

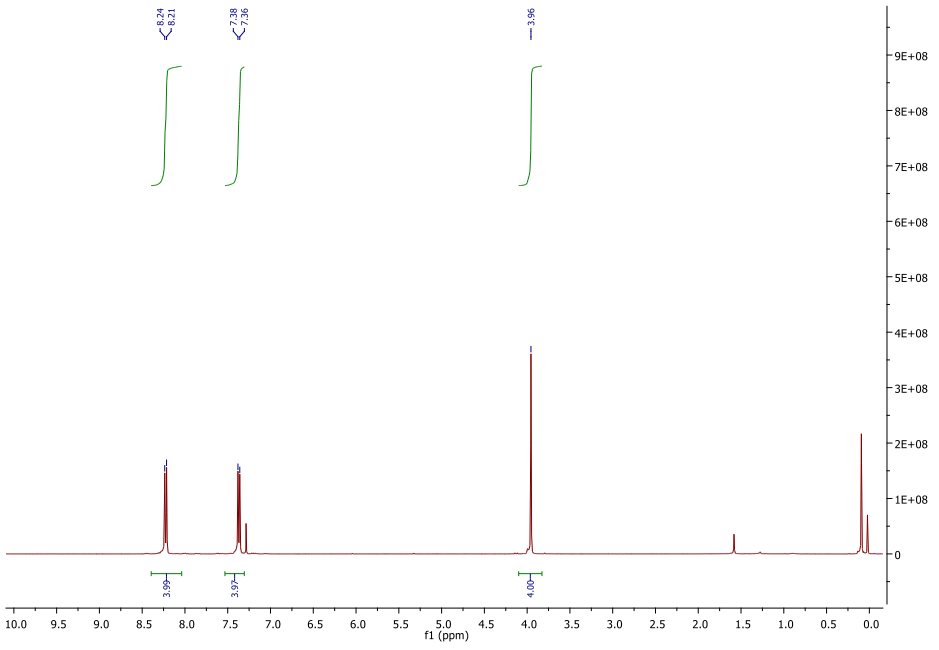

Figure A. 16 ^{1}H NMR spectrum of 31.

B. IR SPECTRA

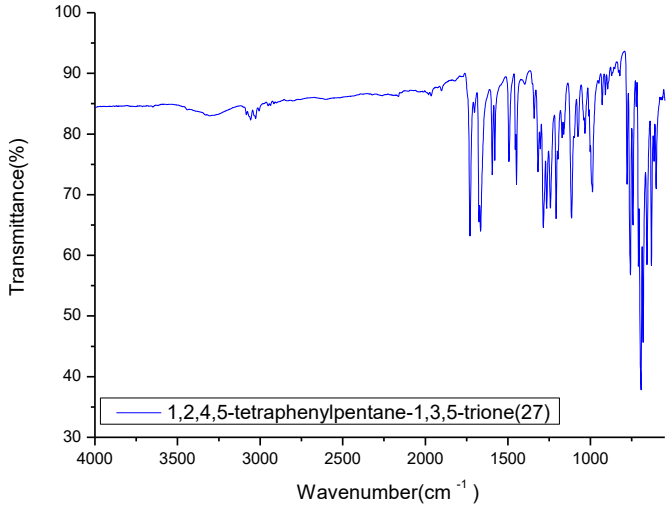

Figure B. 1 IR spectrum of 27.

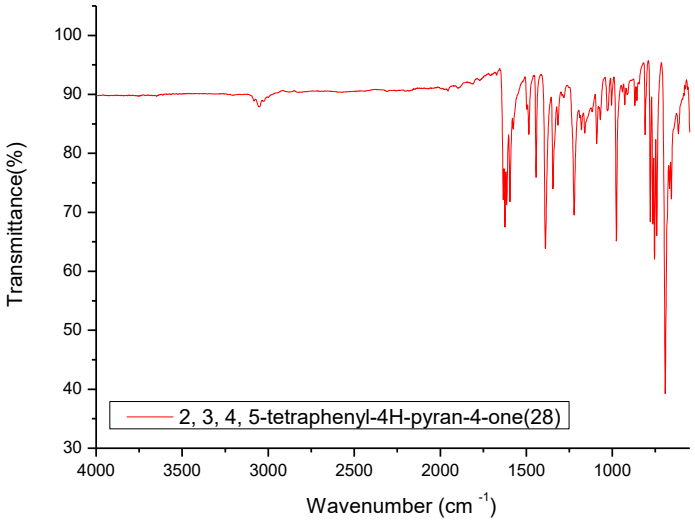

Figure B. 2 IR spectrum of 28.

C. UV SPECTRA

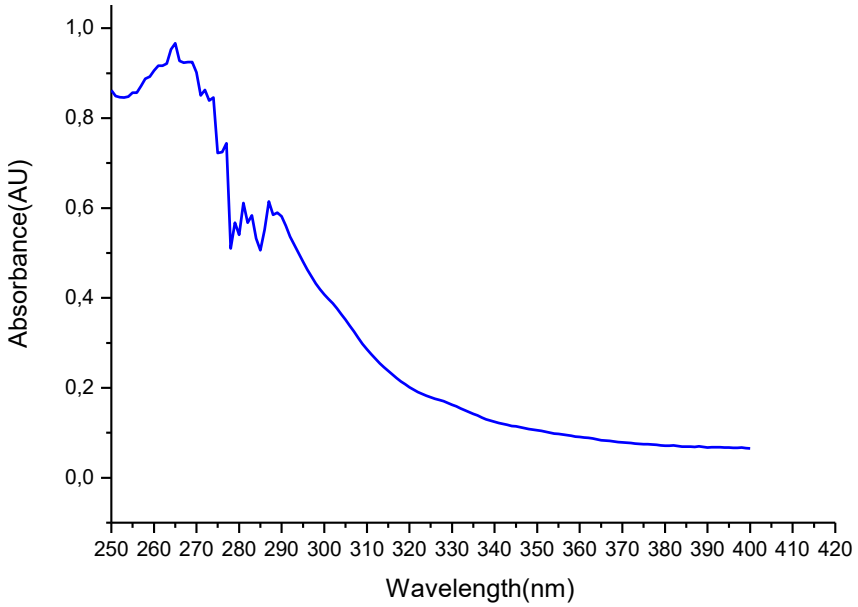

Figure C. 1 UV spectrum of 2,3,5,6-tetraphenyl-4H-pyran-4-one (28) in THF.